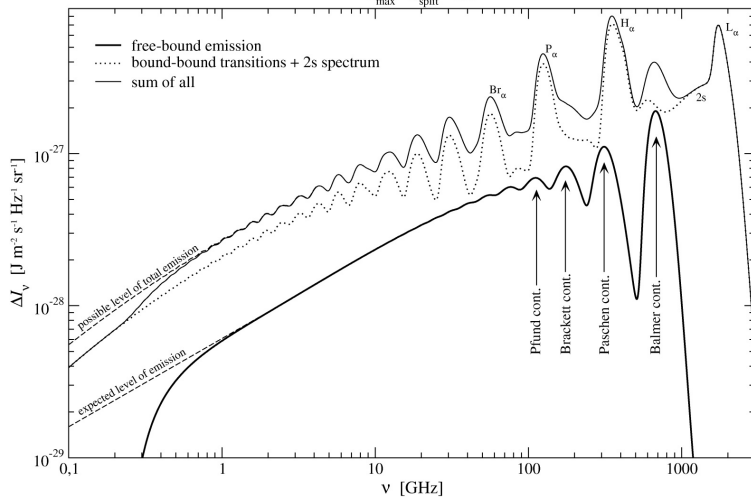


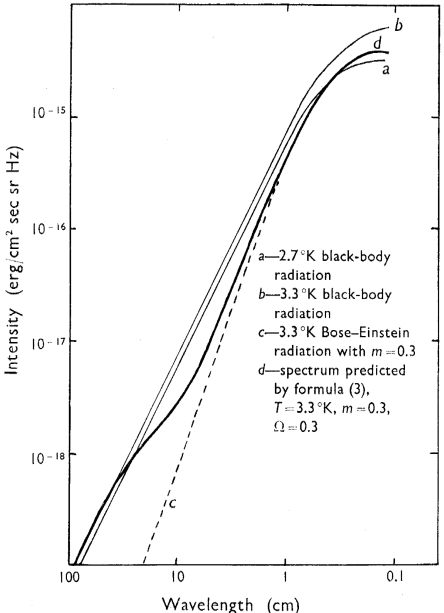
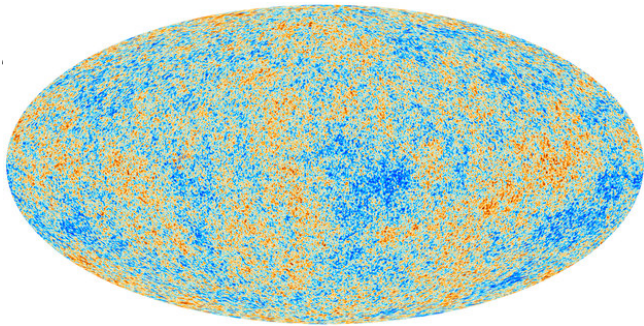
**Texas Symposium on
Relativistic Astrophysics
Geneva**

December 14, 2015



CMB spectral distortions

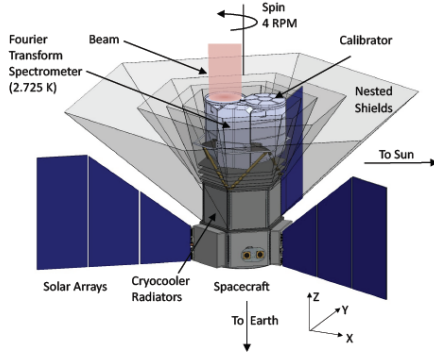
*(Two milestones in the life of the Universe
Last Scattering Surface and
Black Body Photosphere)*

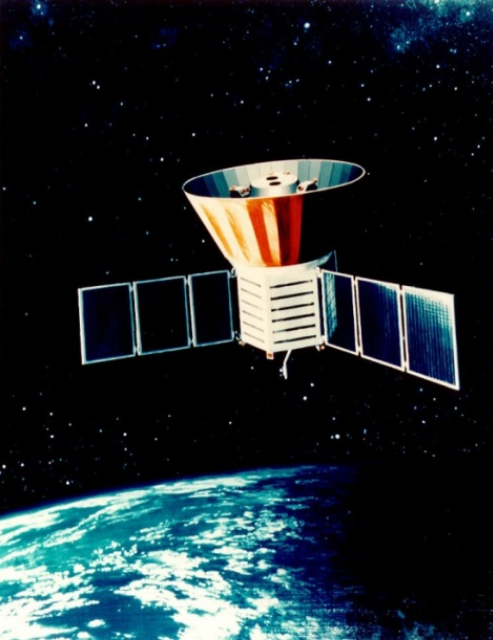


Rashid Sunyaev

*Max-Planck Institut fuer Astrophysik, Garching
Space Research Institute, RAS, Moscow*

with Rishi Khatri (Mumbai) & Jens Chluba (Cambridge)





Adiabatic expansion of the Universe preserves the blackbody spectrum established at early times (for example during electron-positron annihilation)
 (In general $x = \nu/T$ is invariant w.r.t. expansion of the Universe.)

Cosmic Microwave Background (CMB): The most precise black body known: $T = 2.725K \pm 1mK$

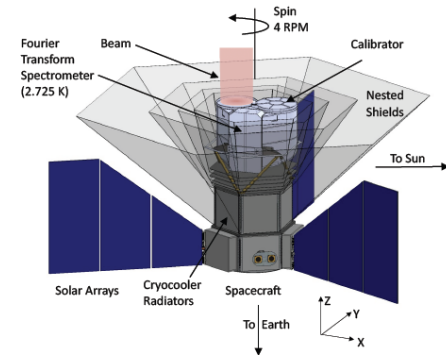
No spectral deviations are detected by COBE/FIRAS !

This was 25 years ago

Now:

Great progress in the technology of experiments and especially of detectors and cryogenics

PIXIE proposal: up to 100 or even thousand times more sensitive !



THERE ARE MANY THEORETICAL MODELS PREDICTING SIGNIFICANT ENERGY RELEASE IN THE EARLY UNIVERSE and *CMB spectral distortions*:

γ and μ
are two main types

I WILL SPEAK TODAY ONLY ABOUT UNAVOIDABLE SPECTRAL FEATURES, WHICH ARE PREDICTED WITHIN STANDARD COSMOLOGICAL MODEL



Black body photosphere of the Universe

In the spring of 1966 Yakov Zeldovich asked me to review on the group seminar the preprints of Layzer (Harvard) and Burbidges (Caltech) stating that CMB spectrum is just the stellar light thermalized by the dust.

I decided to check in addition the usual mechanism responsible for black body spectrum production inside hot stars: **the Rosseland free-free optical depth of the Universe for CMB – it was negligibly small up to the time of positron-electron annihilation.**

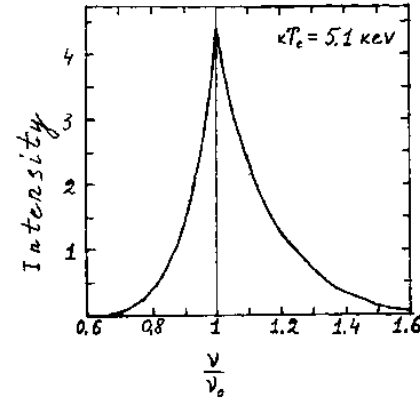
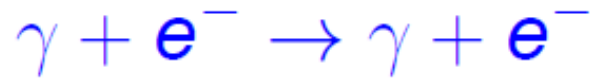
$$\begin{aligned}\tau_{\text{free-free}} &\sim \int_0^{t(z)} dt n_e^2 \sigma_{\text{TC}} \frac{\alpha_{\text{fs}}}{(24\pi^3)^{1/2}} \left(\frac{k_B T_e}{m_e c^2} \right)^{-7/2} \left(\frac{h}{m_e c x_e} \right)^3 (1 - e^{-x_e}) \\ &\sim 4 \times 10^{-5} \left(\frac{1+z}{10^8} \right)^{1/2},\end{aligned}$$

but Thomson optical depth was huge.

$$\tau_{\text{Thomson}} = \int_0^{t(z)} n_e \sigma_{\text{TC}} c dt \stackrel{z \gg z_{\text{eq}}}{\approx} 0.21(1+z) \sim 2 \cdot 10^7 (z/10^8)$$

Optical depth – probability for the photon to be absorbed or scattered

Comptonization



$$\text{Doppler} : \frac{\delta\nu}{\nu} \sim \frac{v_e}{c} \sim \left(\frac{kT_e}{m_e c^2} \right)^{1/2}$$

$$\text{2ndorderDoppler} : \left(\frac{\delta\nu}{\nu} \right)_{\text{rms}} \sim 4 \left(\frac{kT_e}{m_e c^2} \right)$$

$$\text{Recoil} : \frac{\delta\nu}{\nu} = -\frac{h\nu}{m_e c^2} (1 - \cos \theta)$$

=====

y: Amplitude of distortion

$$y = \int dt c \sigma_T n_e \frac{k_B (T_e - T_\gamma)}{m_e c^2}$$

Fokker-Planck expansion of the kinetic equation with induced scattering term yields

$$\frac{\partial n}{\partial y} = \frac{1}{x^2} \frac{\partial}{\partial x} x^4 \left(n + n^2 + \frac{\partial n}{\partial x} \right)$$

Kompaneets (1956)

$$n = c^2 I_\nu / 8\pi h\nu^3$$

- occupation number, I – radiation intensity

$$x = h\nu / kT_e$$

$$y = \frac{kT_e}{m_e c^2} \sigma_T N_e c t = \frac{kT_e}{m_e c^2} u$$

- photon frequency,

time and number of scatterings

Kompaneets equation describes interaction of **a radiation field** with free **hot maxwellian electrons** due to **Compton scattering**. **The energy exchange due to Doppler effect and recoil. Thomson cross-section limit.**

Beautiful physics behind the term $\sim n^2$ describing **induced** Compton scattering

Efficiency of energy exchange between electrons and photons

Recoil:

$$y_\gamma = \int dt c \sigma_T n_e \frac{k_B T_\gamma}{m_e c^2}, \quad T_\gamma = 2.725(1+z)$$

Doppler effect:

$$y_e = \int dt c \sigma_T n_e \frac{k_B T_e}{m_e c^2}$$

In early Universe $y_\gamma \approx y_e$

y : Amplitude of distortion

$$y = \int dt c \sigma_T n_e \frac{k_B (T_e - T_\gamma)}{m_e c^2}$$

Efficiency of energy exchange between electrons and photons

Recoil:

$$y_\gamma = \int dt c \sigma_T n_e \frac{k_B T_\gamma}{m_e c^2}, \quad T_\gamma = 2.725(1+z)$$

No. of scatterings

Doppler effect:

$$y_e = \int dt c \sigma_T n_e \frac{k_B T_e}{m_e c^2}$$

In early Universe $y_\gamma \approx y_e$

y : Amplitude of distortion

$$y = \int dt c \sigma_T n_e \frac{k_B (T_e - T_\gamma)}{m_e c^2}$$

Fokker-Planck expansion of the kinetic equation with induced scattering term yields

$$\frac{\partial n}{\partial y} = \frac{1}{x^2} \frac{\partial}{\partial x} x^4 \left(n + n^2 + \frac{\partial n}{\partial x} \right)$$

$$n = c^2 I_\nu / 8\pi h\nu^3$$

- occupation number, I – radiation intensity

$$x = h\nu/kT_e :$$

$$y = \frac{kT_e}{m_e c^2} \sigma_T N_e c t = \frac{kT_e}{m_e c^2} u$$

- photon frequency,

time and number of scatterings

Kompaneets equation describes interaction of **a radiation field** with free **hot maxwellian electrons** due to **Compton scattering**. **The energy exchange due to Doppler effect and recoil. Thomson cross-section limit.**

Beautiful physics behind the term $\sim n^2$ describing **induced** Compton scattering

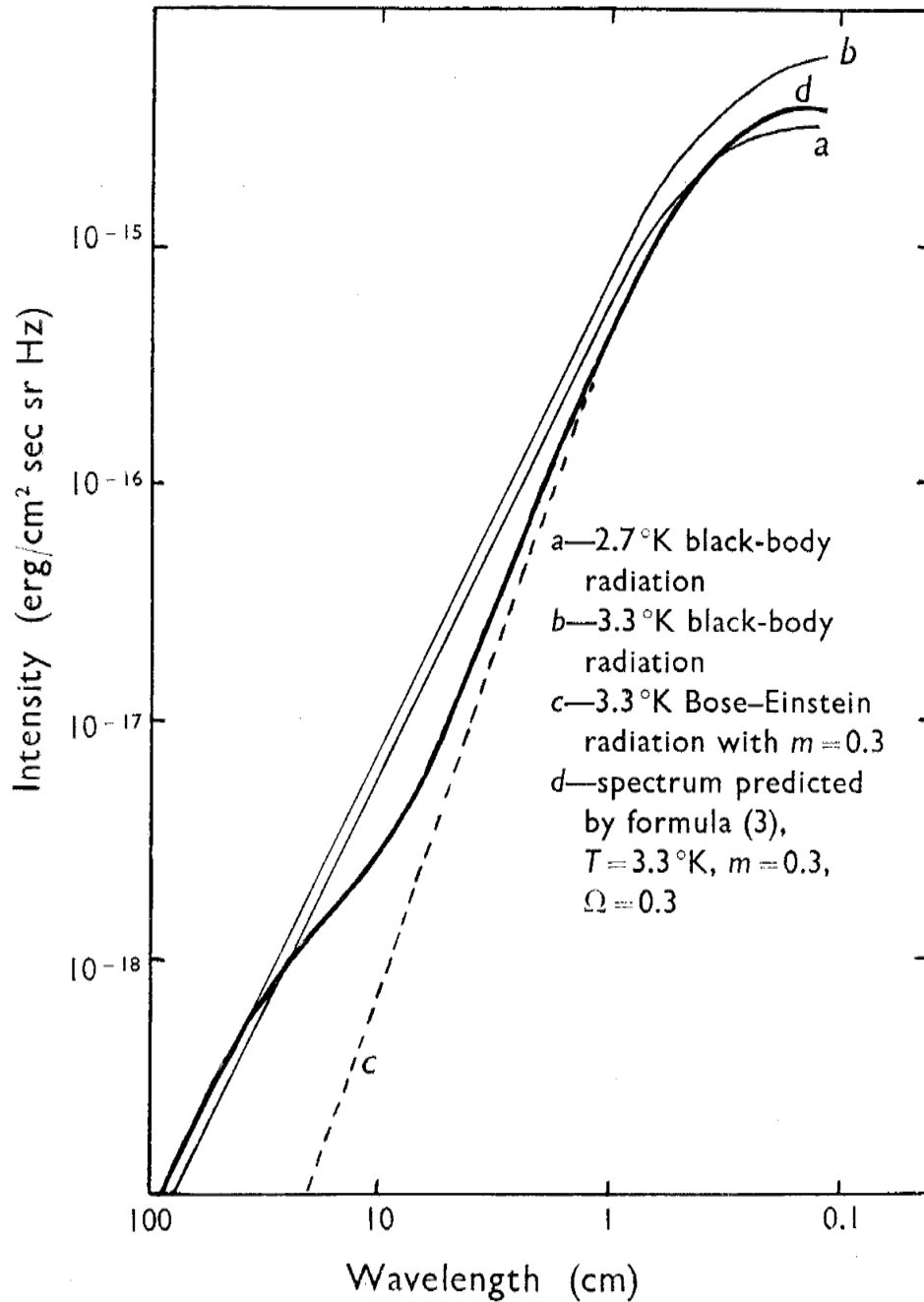
Bose-Einstein spectrum- Chemical potential (μ)

Stationary solution of Kompaneets equation at $y \gg 1$

$$n(x) = \frac{1}{e^{x+\mu} - 1}$$

Given two constraints, energy density (E) and number density (N) of photons, T, μ uniquely determined.

Thomson scattering does not change amount of photons
(*photon number conservation in Kompaneets equation*)



myu-type CMB distortions
 due to energy release in the
 early Universe $10^5 < z < 210^6$

Sunyaev, Zeldovich, 1970

Bose-Einstein spectrum

$$\begin{aligned}n_{\text{BE}} &= \frac{1}{e^{\frac{h\nu}{k_{\text{B}}T_{\text{BE}}} + \mu} - 1} \\ &= \frac{1}{e^{x-0.456\mu x + \mu} - 1} \\ &\approx n_{\text{pl}}(x) + \frac{\mu e^x}{(e^x - 1)^2} \left(\frac{x}{2.19} - 1 \right),\end{aligned}$$

We call this type of spectral distortions as a μ

distortion

At small $y \ll 1$, $\tau \ll 1$

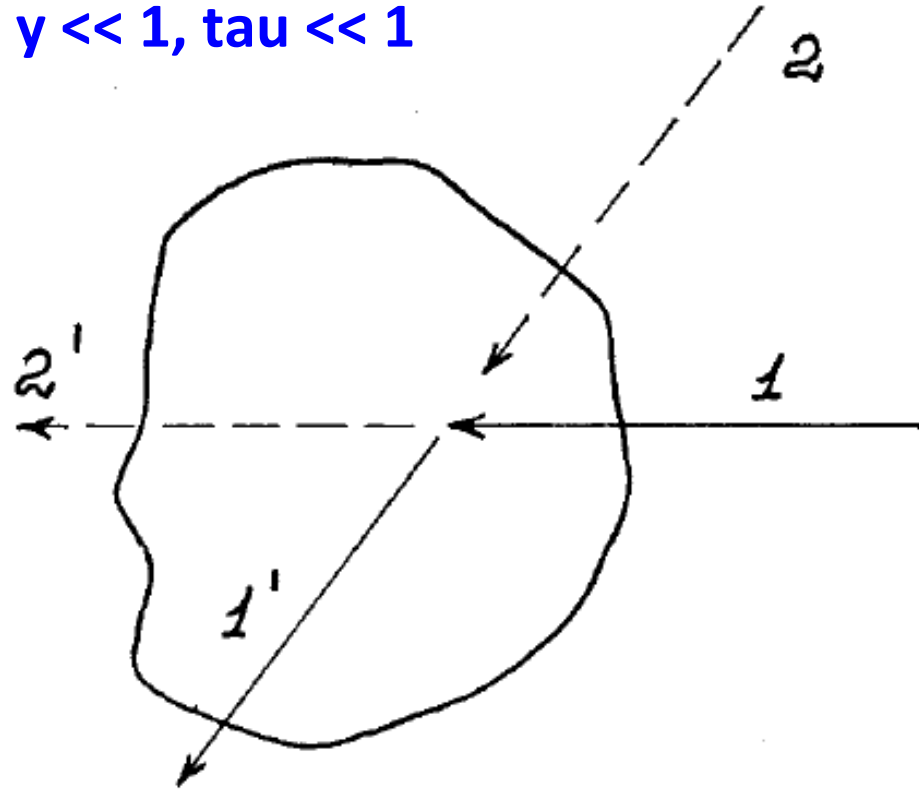
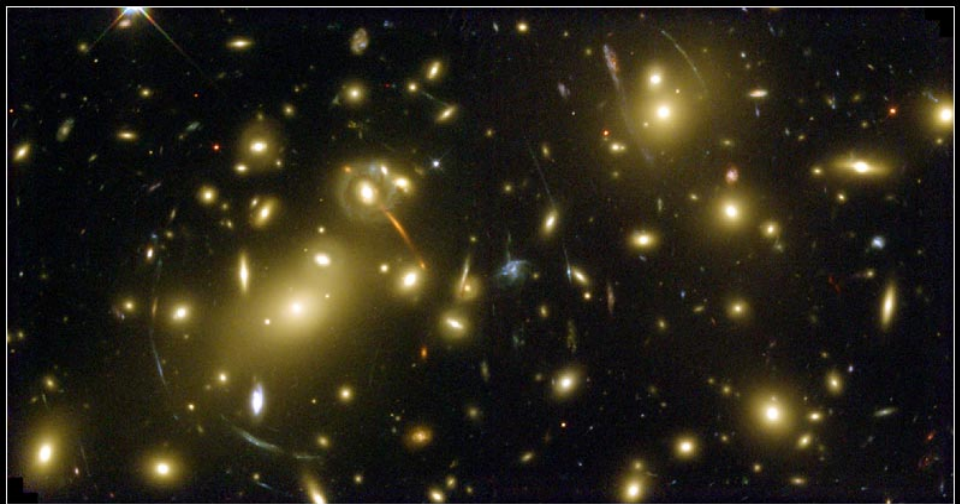


FIG. 2. The scattering of isotropic radiation field by the cloud of electrons.

Cloud is invisible in CMB radiation field



Galaxy Cluster Abell 2218 HST • WFPC2
 NASA, A. Fruchter and the ERO Team (STScI) • STScI-PRC00-08

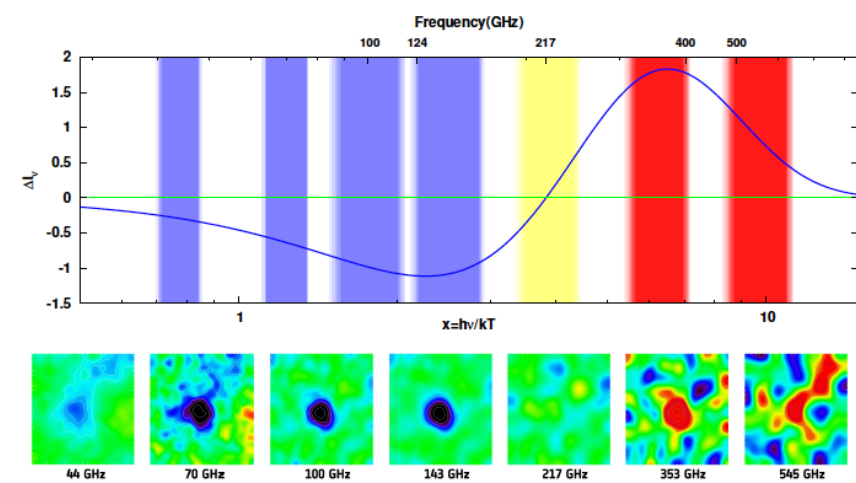


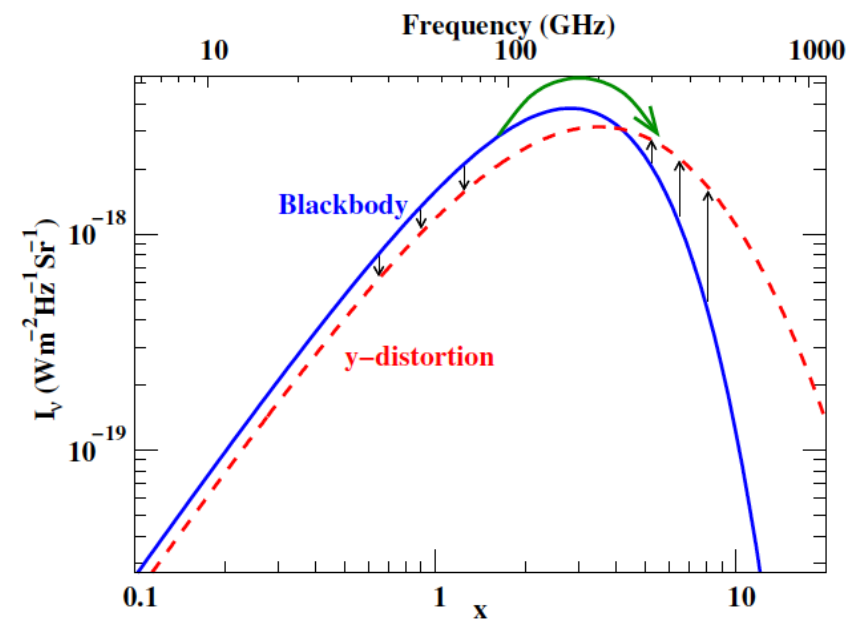
Image credit: ESA / HFI & LFI Consortia

$$n_{SZ} = y T^4 \frac{\partial}{\partial T} \frac{1}{T^2} \frac{\partial n_{PI}}{\partial T}$$

$$= y \frac{x e^x}{(e^x - 1)^2} \left(x \frac{e^x + 1}{e^x - 1} - 4 \right)$$

$$\Delta I_{SZ} = I_{SZ} - I_{planck} = \frac{2 h \nu^3}{c^2} n_{SZ}$$

(Zeldovich and Sunyaev 1969)
 COBE-FIRAS limit (95%): $y \lesssim 1.5 \times 10^{-5}$ (Fixsen et al. 1996)



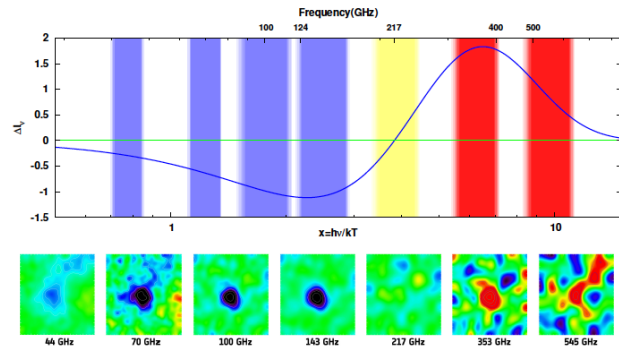
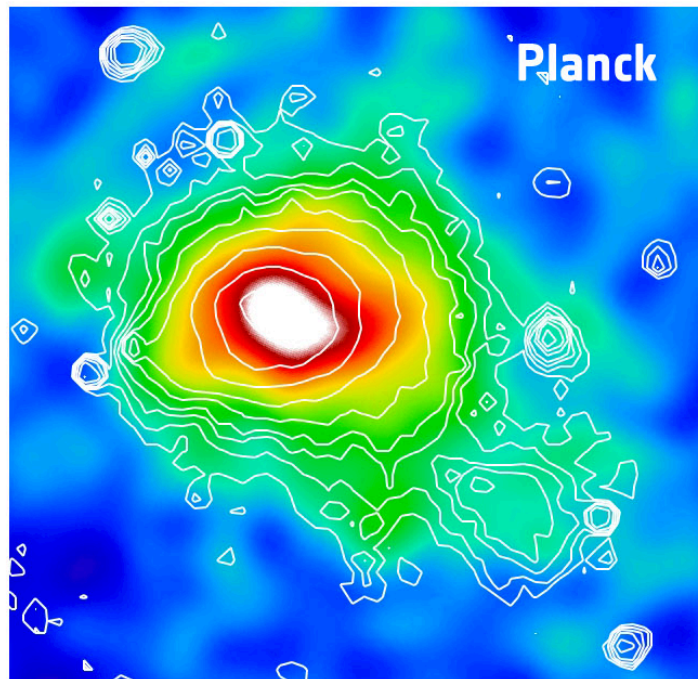


Image credit: ESA / HFI & LFI Consortia

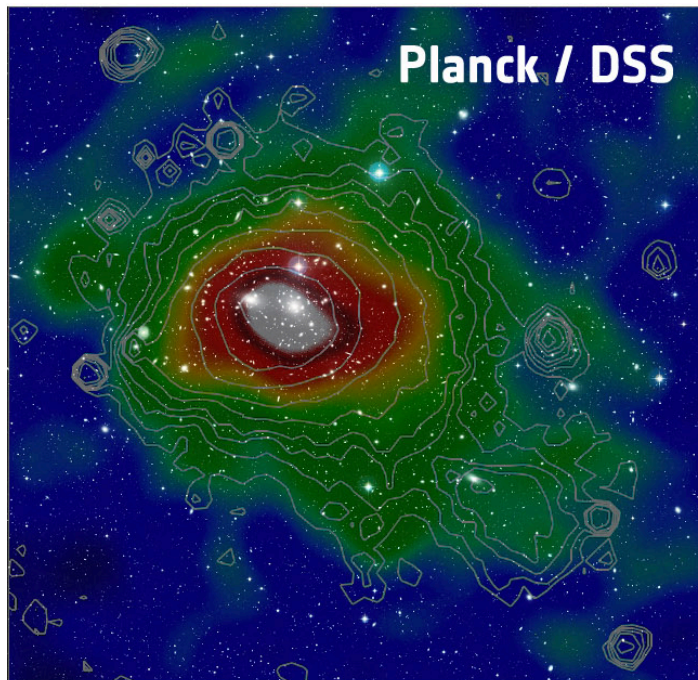
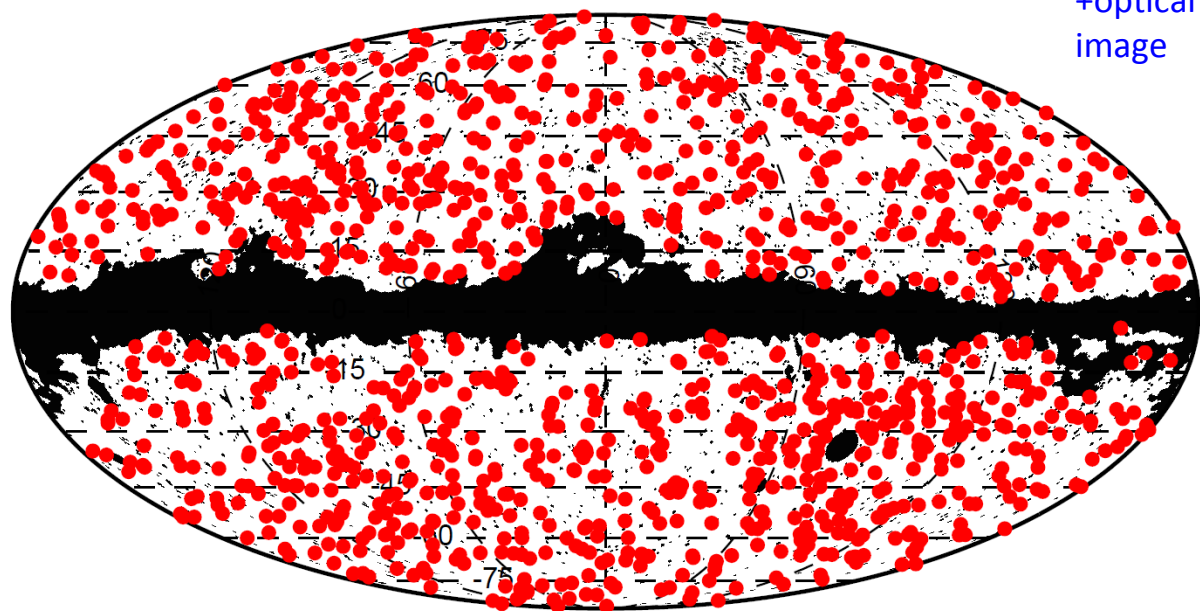
SZ shadow,
Coma cluster
of galaxies

y-parameter map,
based on
100-857 GHz data



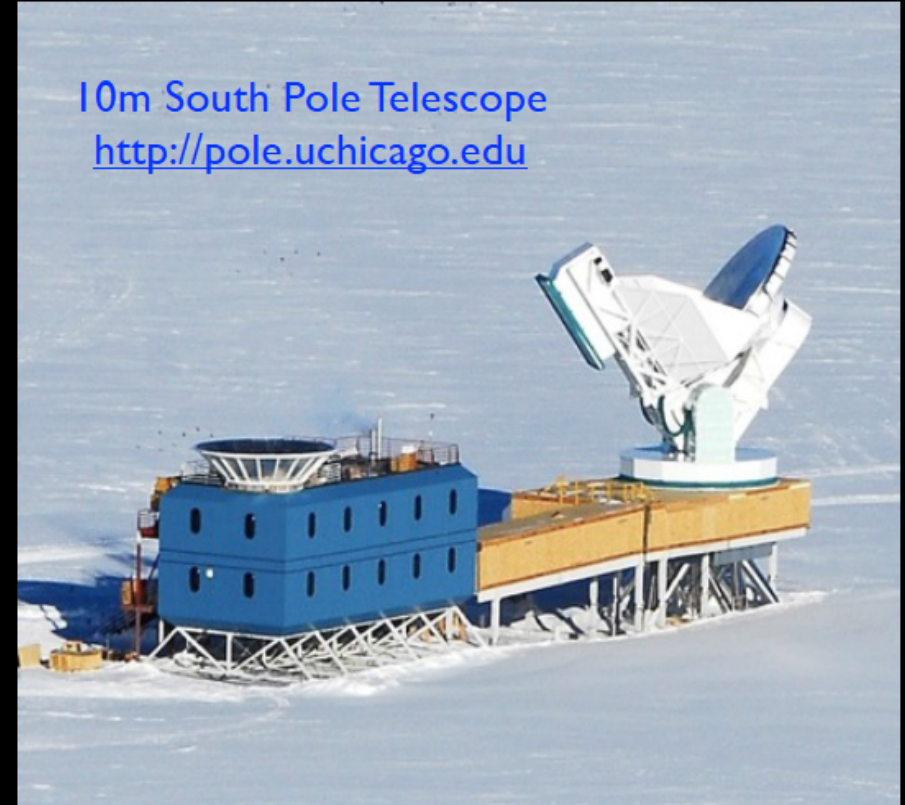
~ 900 clusters confirmed by X-Ray
or optical observations

Planck
+optical
image



ACT and SPT

Dedicated Telescopes for measurement of
CMB polarization and fine angular scale temperature anisotropy

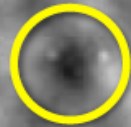
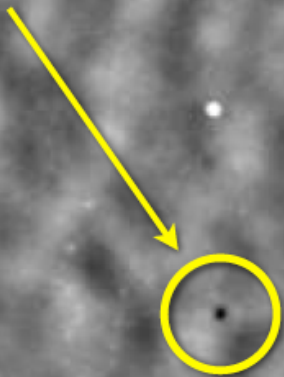
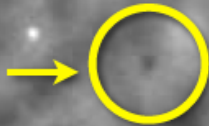


- Exceptional high and dry sites for dedicated CMB observations.
- Exploiting ongoing revolution in low-noise bolometer cameras

SPT
150 GHz.
50 deg²

Clusters of Galaxies

"Shadows" in the microwave
background from clusters of galaxies



Lower limit on $\langle y \rangle$ from Planck and SPT detected clusters

Sum the $\langle y \rangle$ from Planck clusters at $z < 0.3$ and SPT clusters at $z > 0.3$

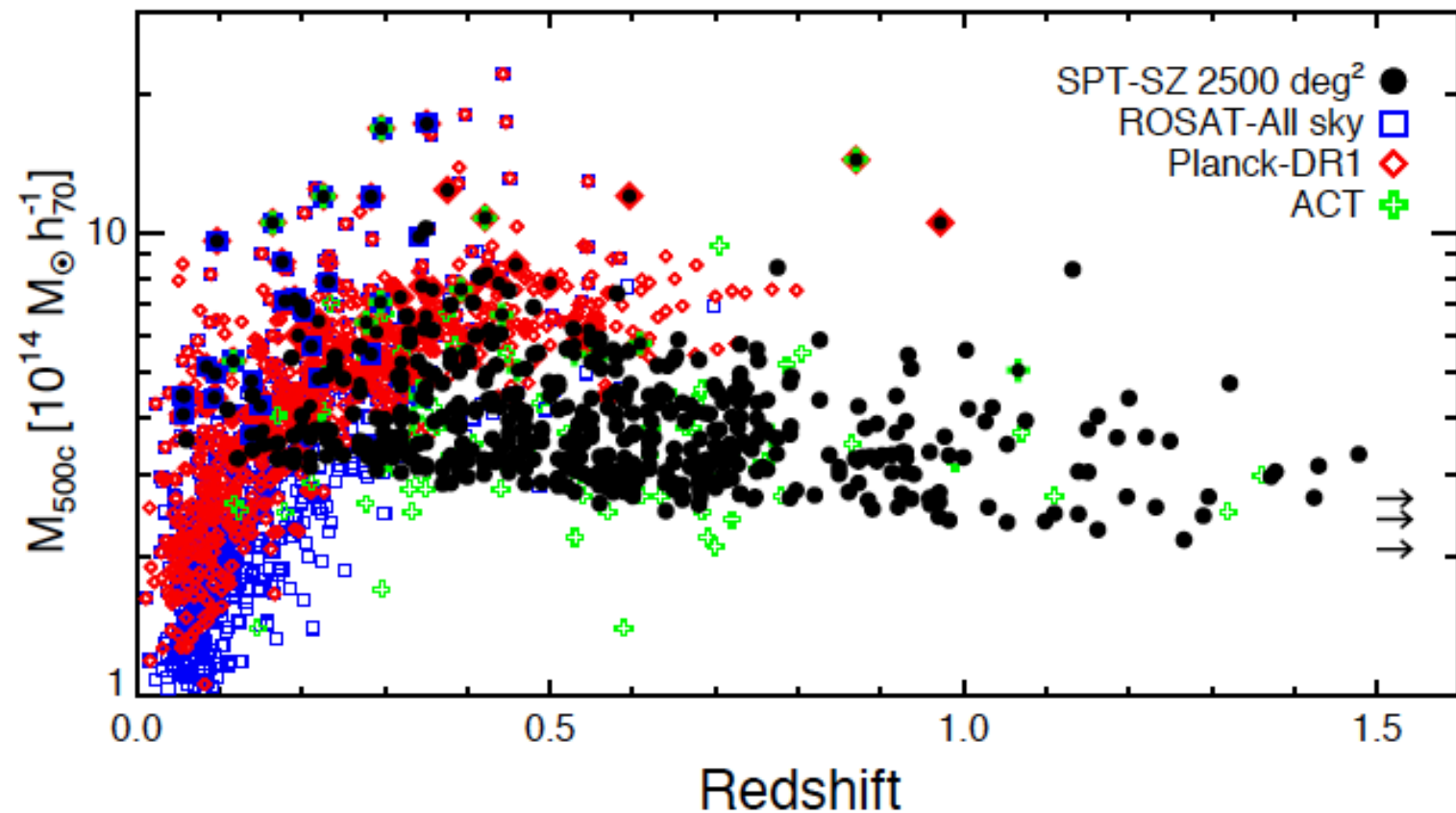


Fig. from Bleem et al. 2015 (SPT) arXiv:1409.0850

Lower limit on $\langle y \rangle$ from Planck and SPT detected clusters

Observed clusters \Rightarrow Minimum average y -distortion in the CMB
 $\langle y \rangle > 5.4 \times 10^{-8}$ (Khatri & Sunyaev 2015)

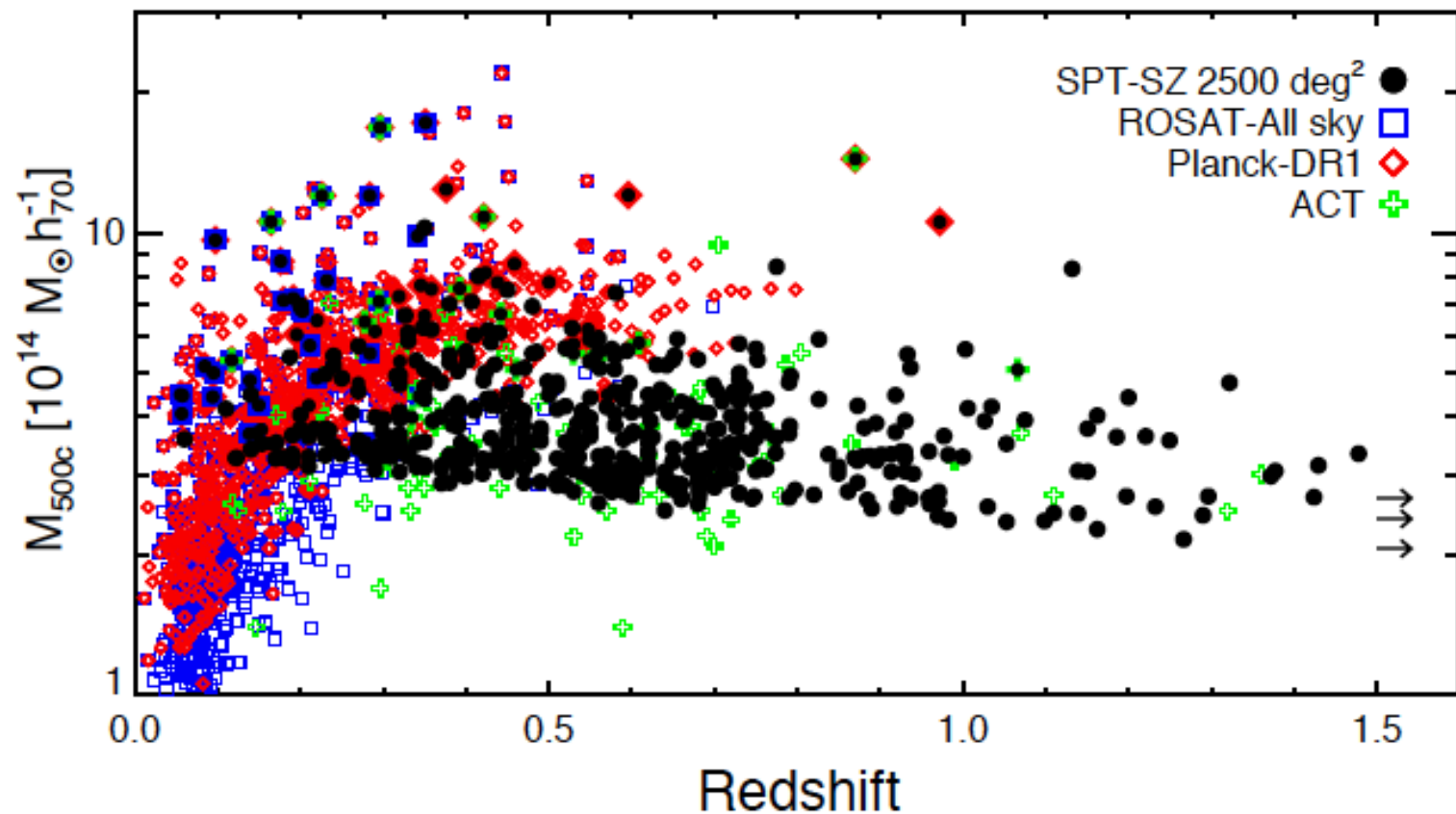


Fig. from Bleem et al. 2015 (SPT) arXiv:1409.0850

New upper limit on $\langle y \rangle$ from y -map created by combining Planck HFI channels

y -distortion map, 10 arcmin

Coma

Khatri (2015) arXiv:1505.00778

Virgo

A1651

A2142

A2029

A2219

A2147

A1644

A2256

A2255

Shapley

A754

A2319

Ophiuchus

Triangulum A

Perseus

Bullet

A3404

A3395-3391

A401

A3667

A496

A3266

A3822

A3827

A3158

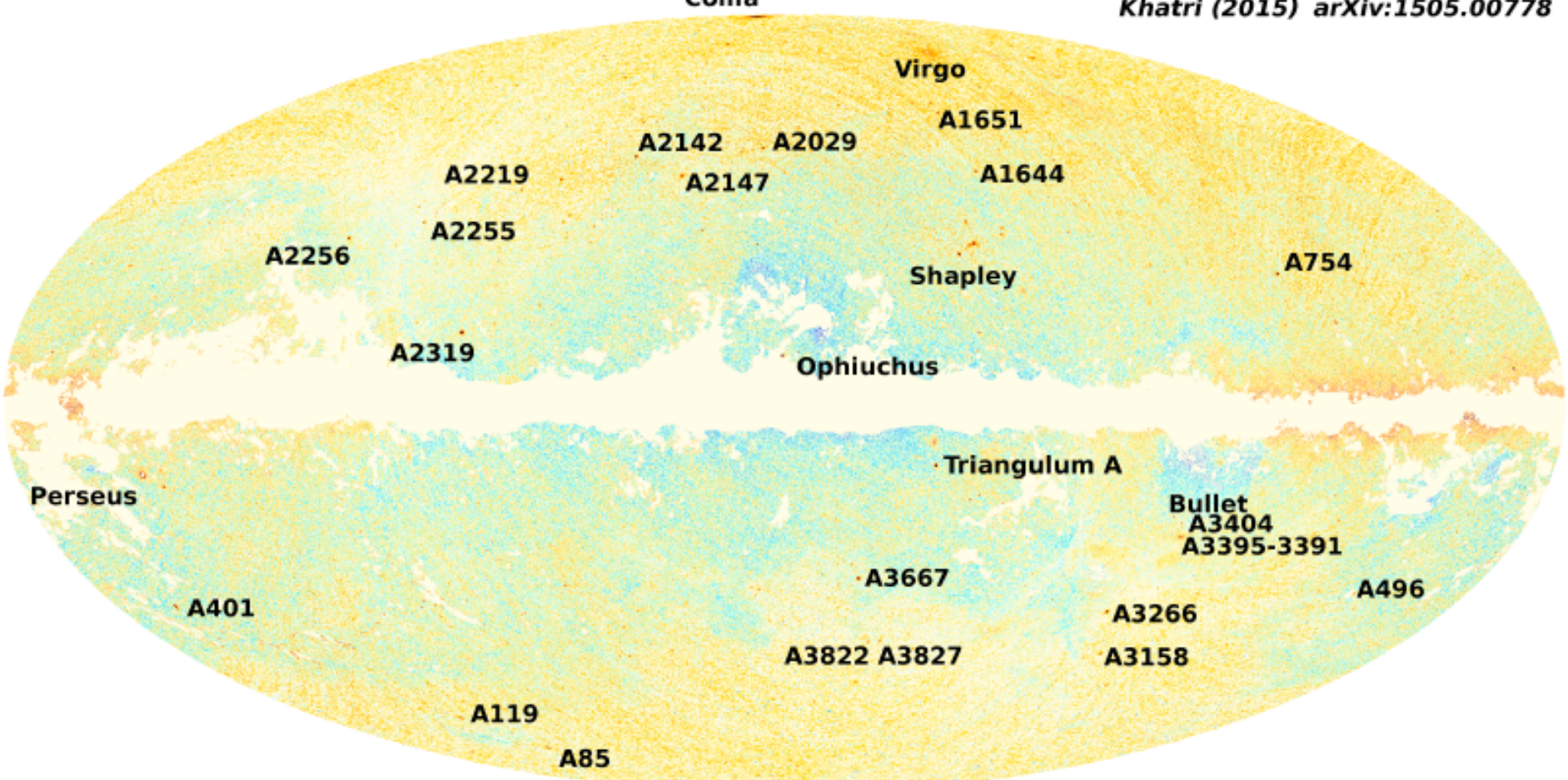
A119

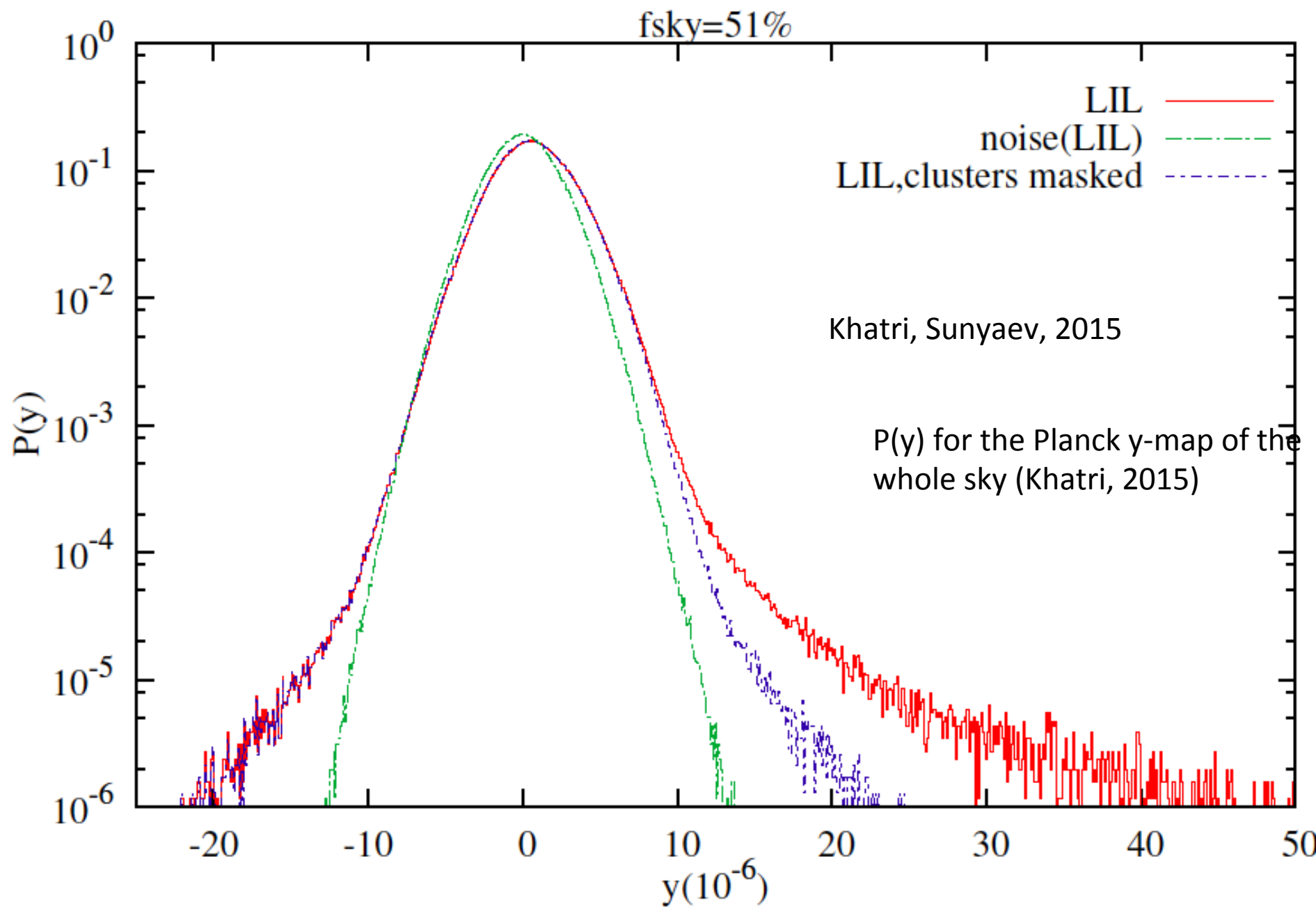
A85

-25.0



25.0 x 1e-6





New upper limit on $\langle y \rangle$ from y -map created by combining Planck HFI channels

A simple conservative approach:

- ▶ Take all the positive pixels in the map (excluding contaminated regions)
- ▶ Average the y -distortion in the pixels (All pixels have equal area)

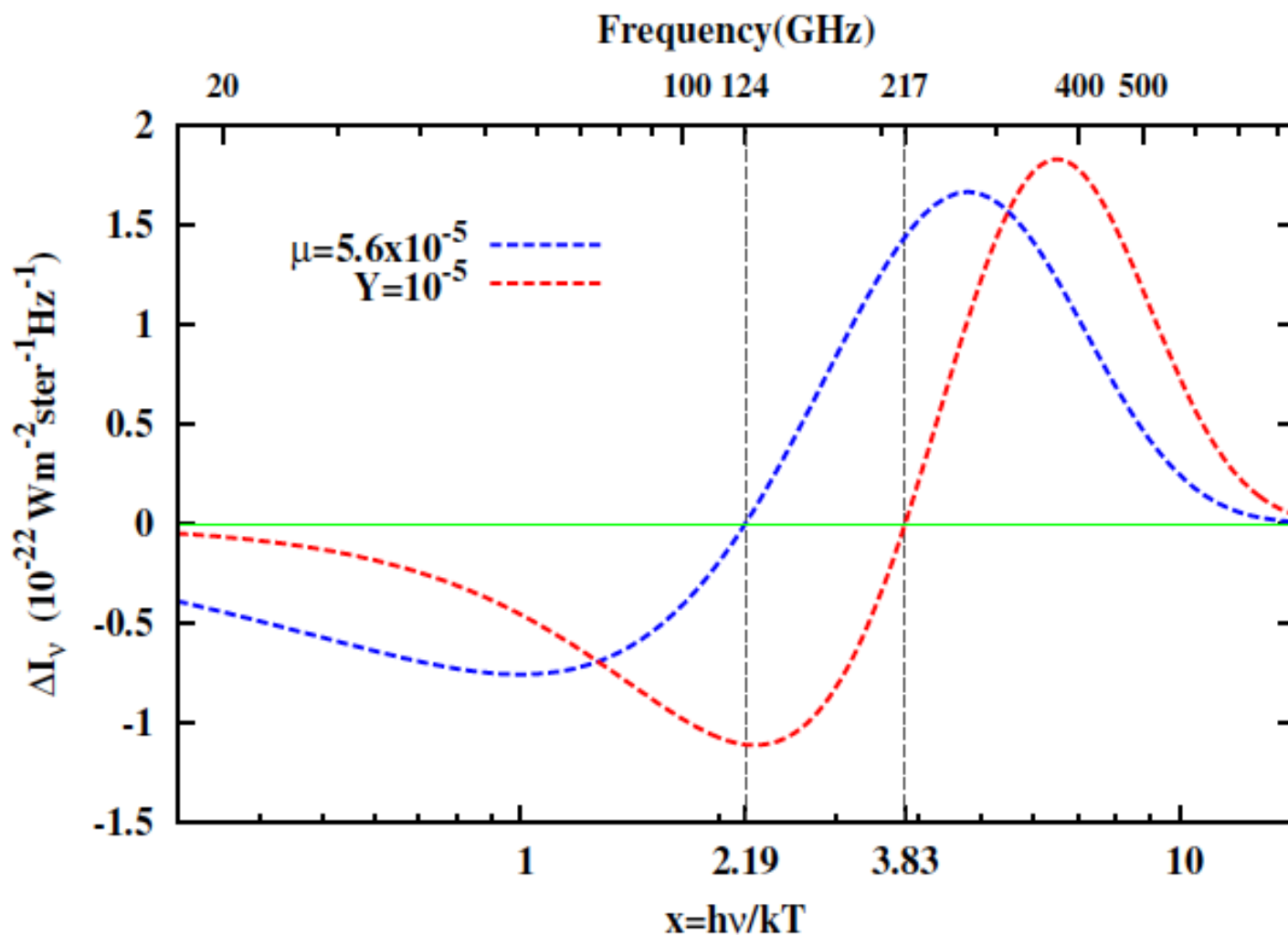
Result: $\langle y \rangle < 2.2 \times 10^{-6}$ (*Khatri & Sunyaev 2015*)

6.8 times stronger compared to the COBE-FIRAS upper limit:

$\langle y \rangle < 15 \times 10^{-6}$ (*Fixsen et al. 1996*)

μ -distortion: Bose-Einstein spectrum, $y_\gamma \gg 1$

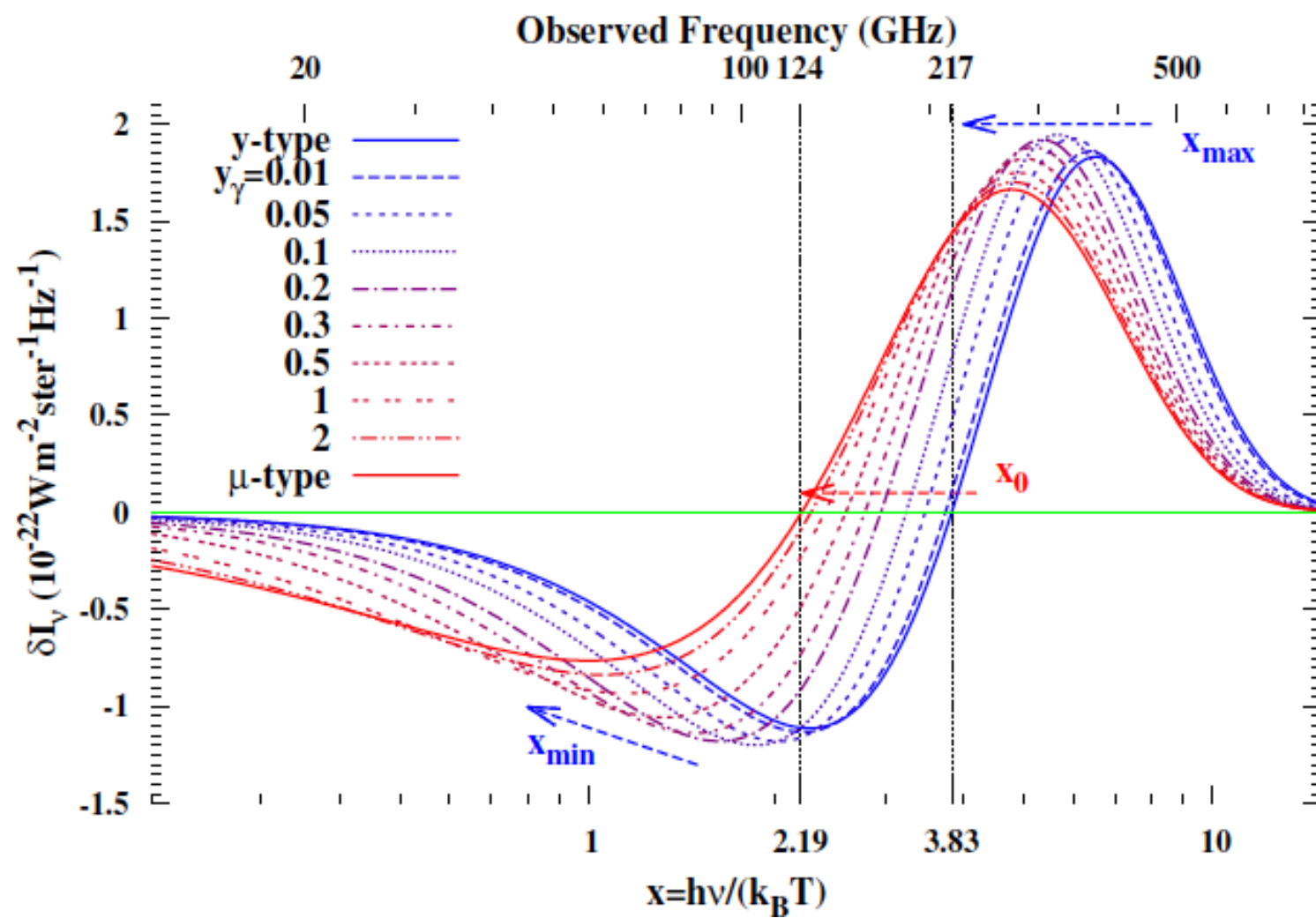
COBE-FIRAS limit (95%): $\mu \lesssim 9 \times 10^{-5}$ (Fixsen et al. 1996)



Intermediate-type distortions *(Khatri and Sunyaev 2012b)*

Solve Kompaneets equation with initial condition of y -type solution.

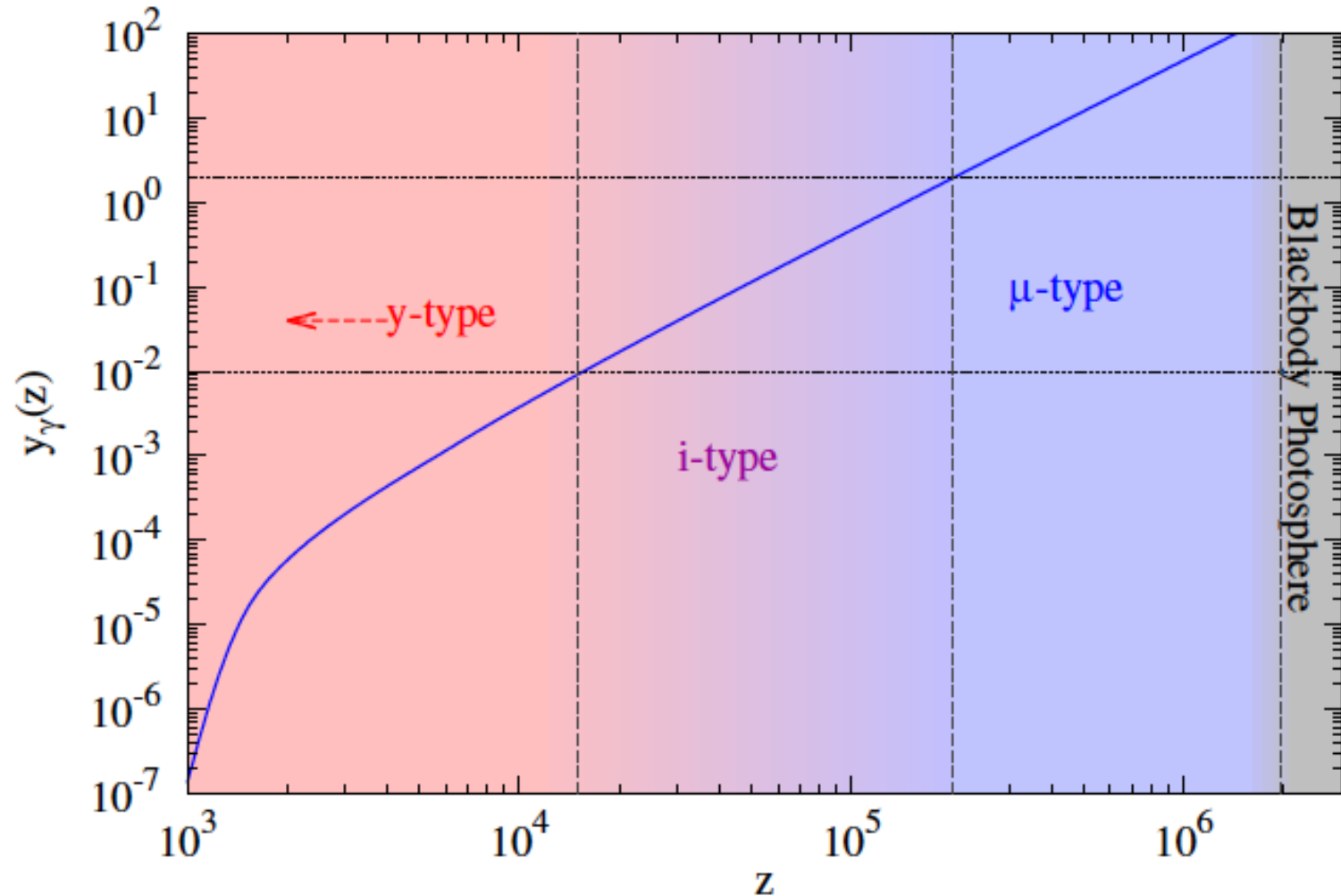
$$\frac{\partial n}{\partial y_\gamma} = \frac{1}{x^2} \frac{\partial}{\partial x} x^4 \left(n + n^2 + \frac{T_e}{T} \frac{\partial n}{\partial x} \right), \quad \frac{T_e}{T} = \frac{\int (n + n^2) x^4 dx}{4 \int n x^3 dx}$$



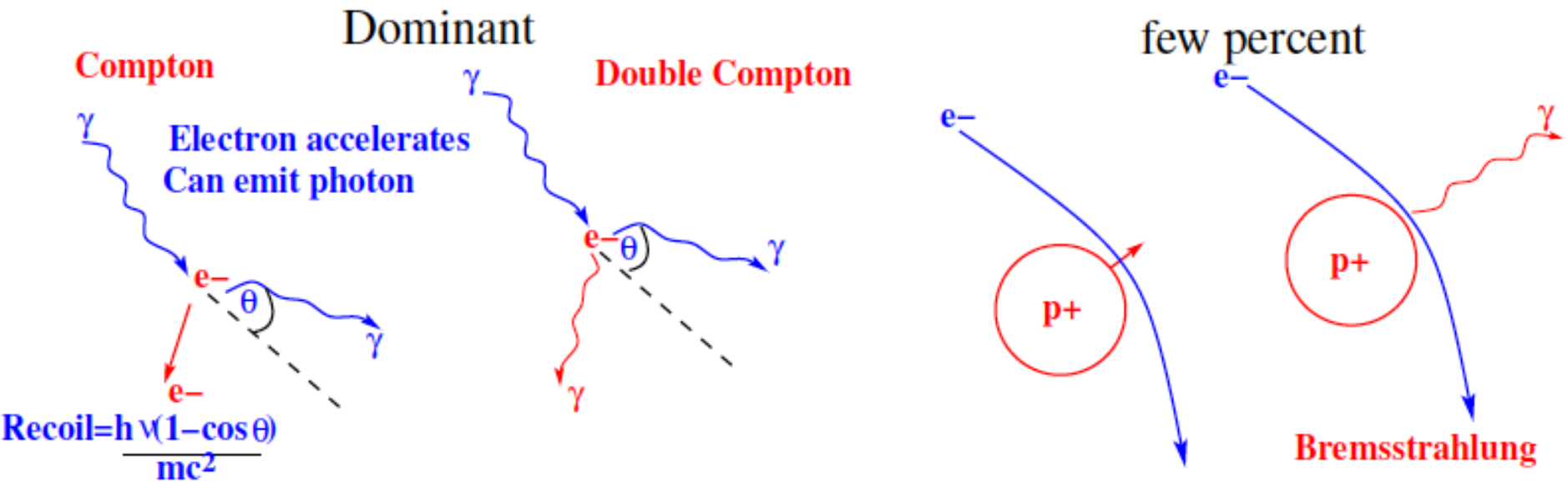
For $y_\gamma \gg 1$ equilibrium is established.

T_e and T_γ converge to common value

The photon spectrum relaxes to equilibrium Bose-Einstein distribution

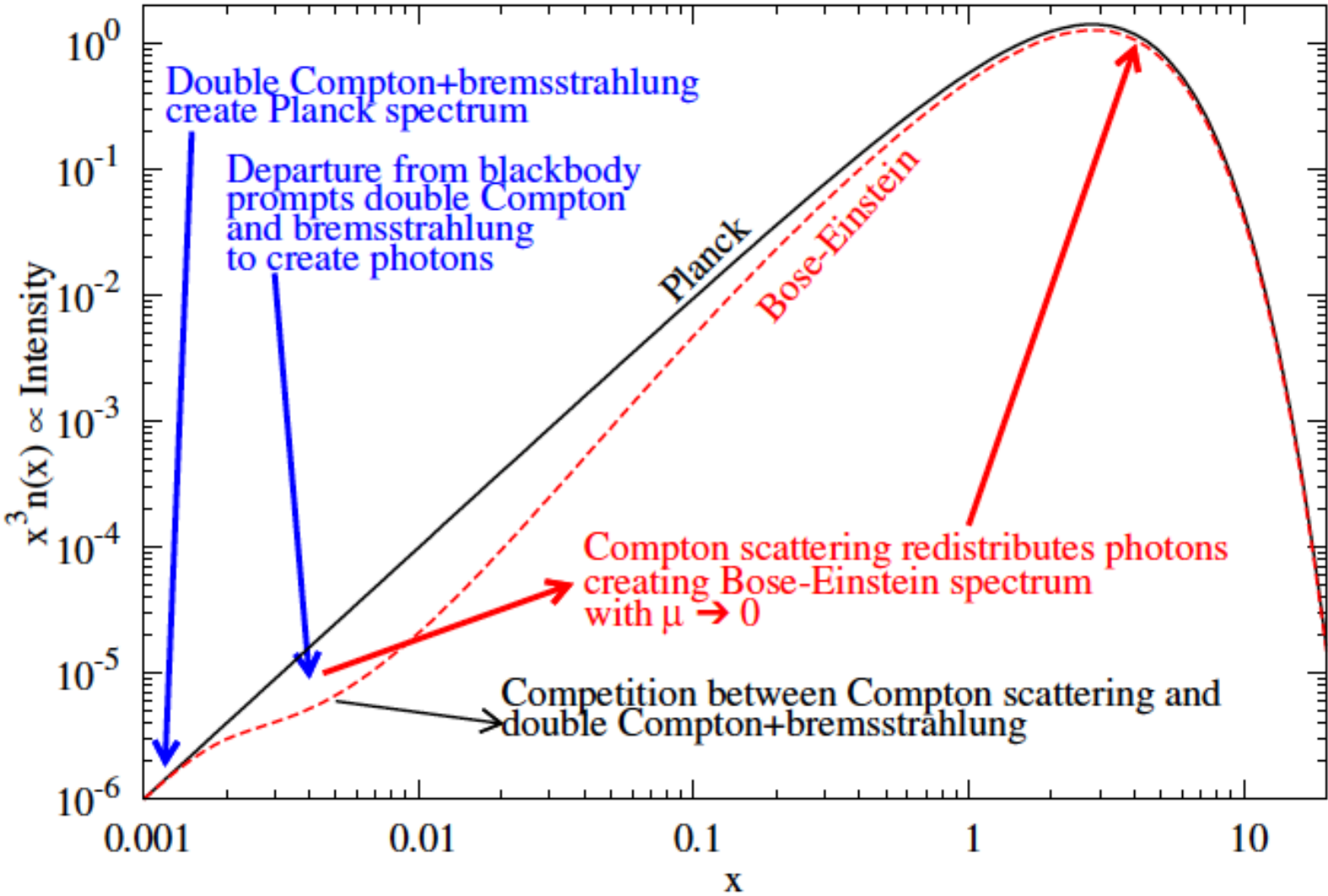


Processes responsible for creation of CMB spectrum



- ▶ Double Compton and bremsstrahlung create/absorb photons ($\propto 1/x^2$)
- ▶ Compton scattering distributes them over the whole spectrum

Creation of CMB Planck spectrum



Analytical solution (Sunyaev, Zeldovich, 1970)

$$\mu = \mu(t_0) e^{-2 \sqrt{ak} (t - t_0)}$$

Where a and k are scattering (Comptonisation) and real absorption coefficients correspondently

In the case of Double Compton (emission of second photon during scattering) spectral deviations decrease with time

$$\frac{\mu^{\text{final}}}{\mu^{\text{initial}}} \approx e^{-(z_i/z_{\text{dc}})^{5/2}}$$

Danese, de Zotti, 1984

Bose-Einstein spectrum- Chemical potential (μ)

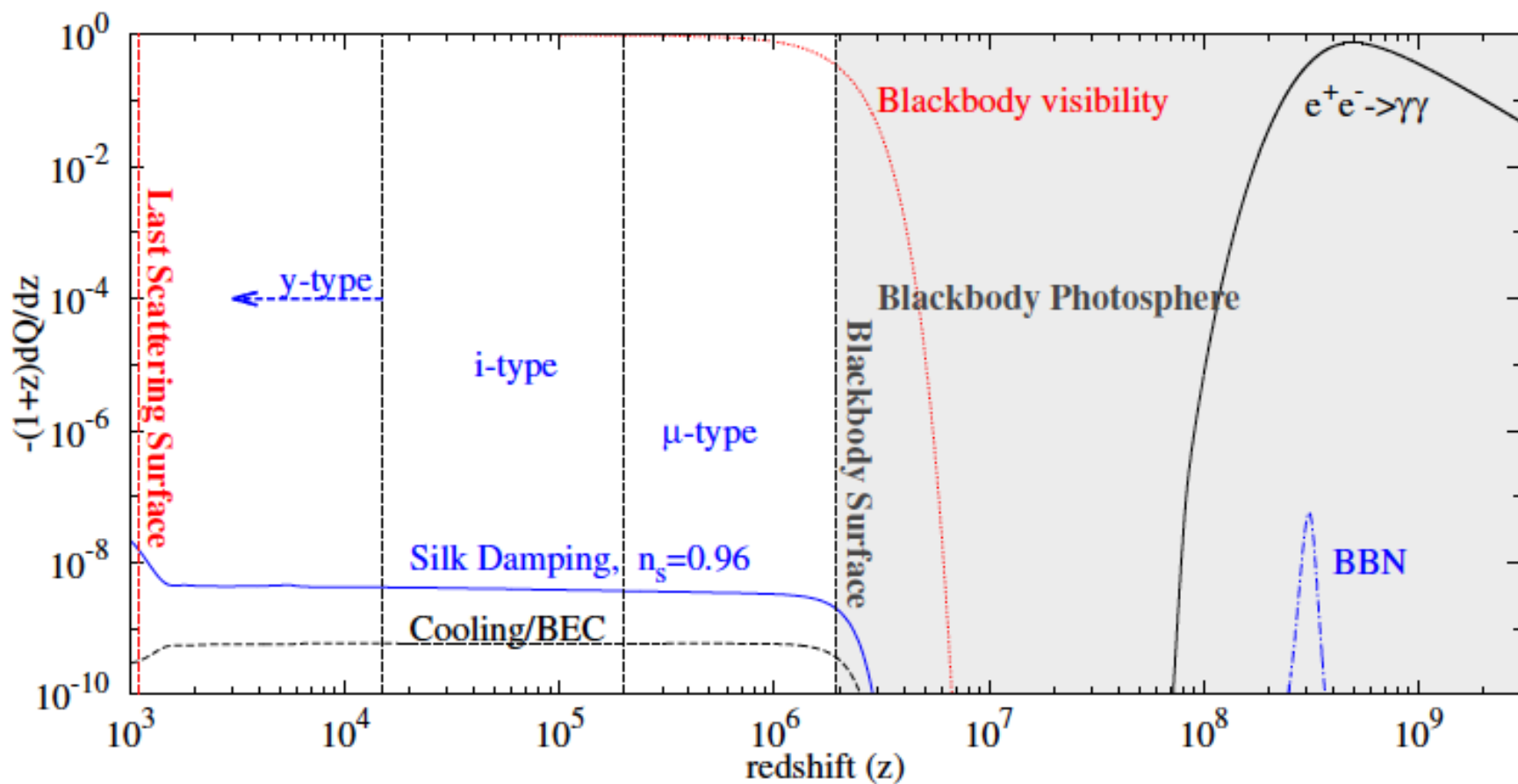
$$n(x) = \frac{1}{e^{x+\mu} - 1}$$

Given two constraints, energy density (E) and number density (N) of photons, T, μ uniquely determined.

Idea behind analytic solutions:

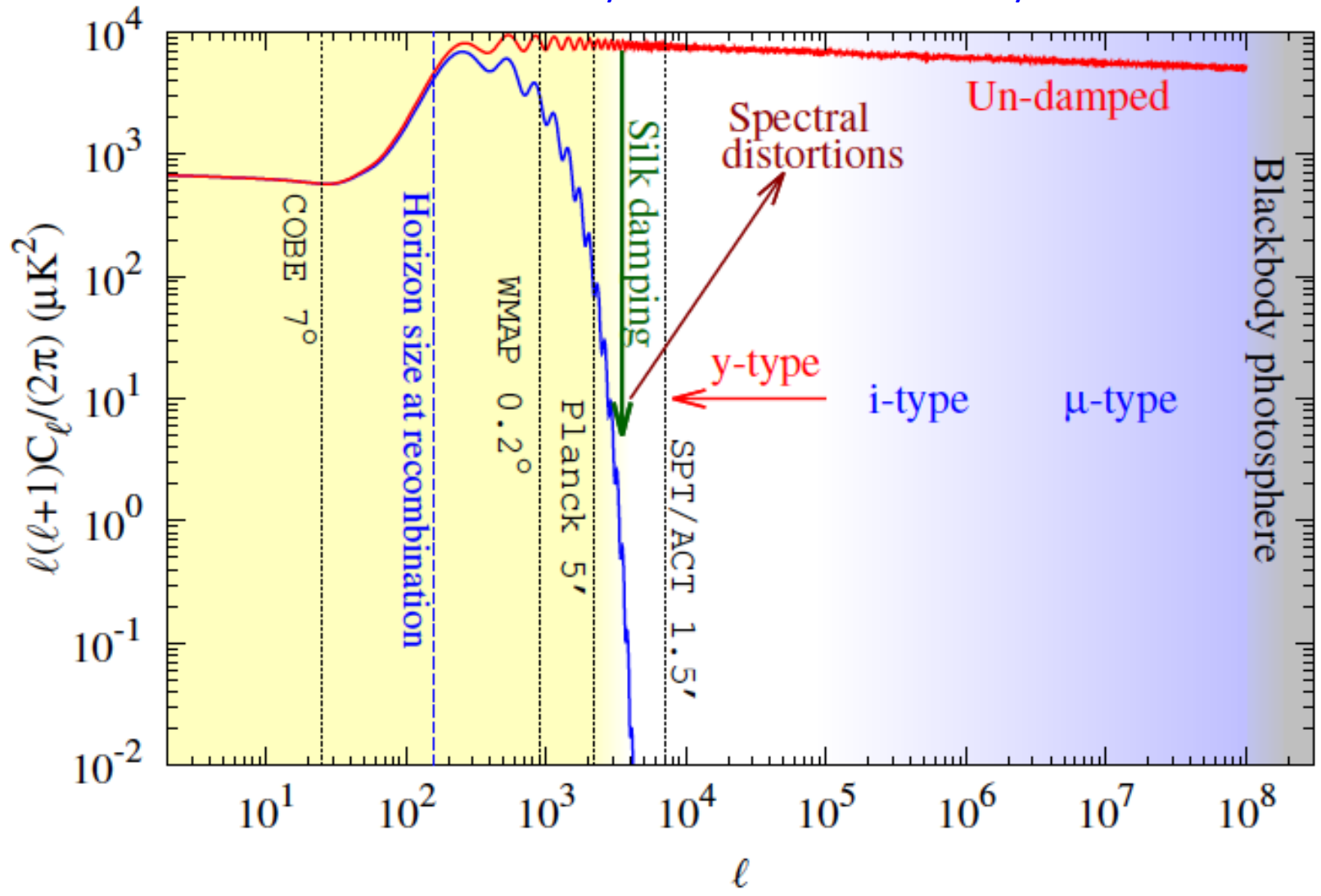
If we know rate of production of photons and energy injection rate, we can calculate the evolution/production of μ (and T)

The general picture

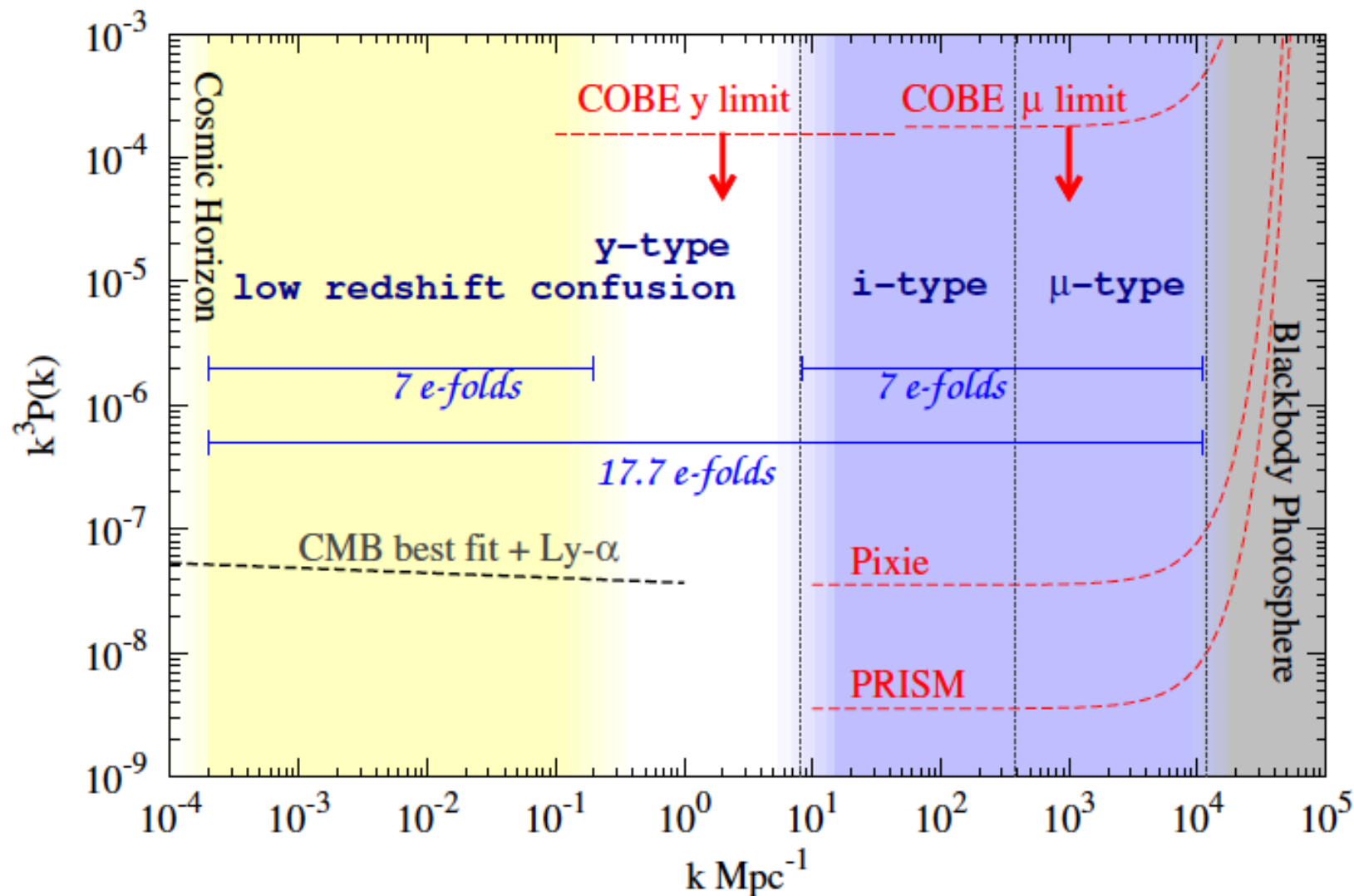


We have reached the resolution limit for CMB anisotropies

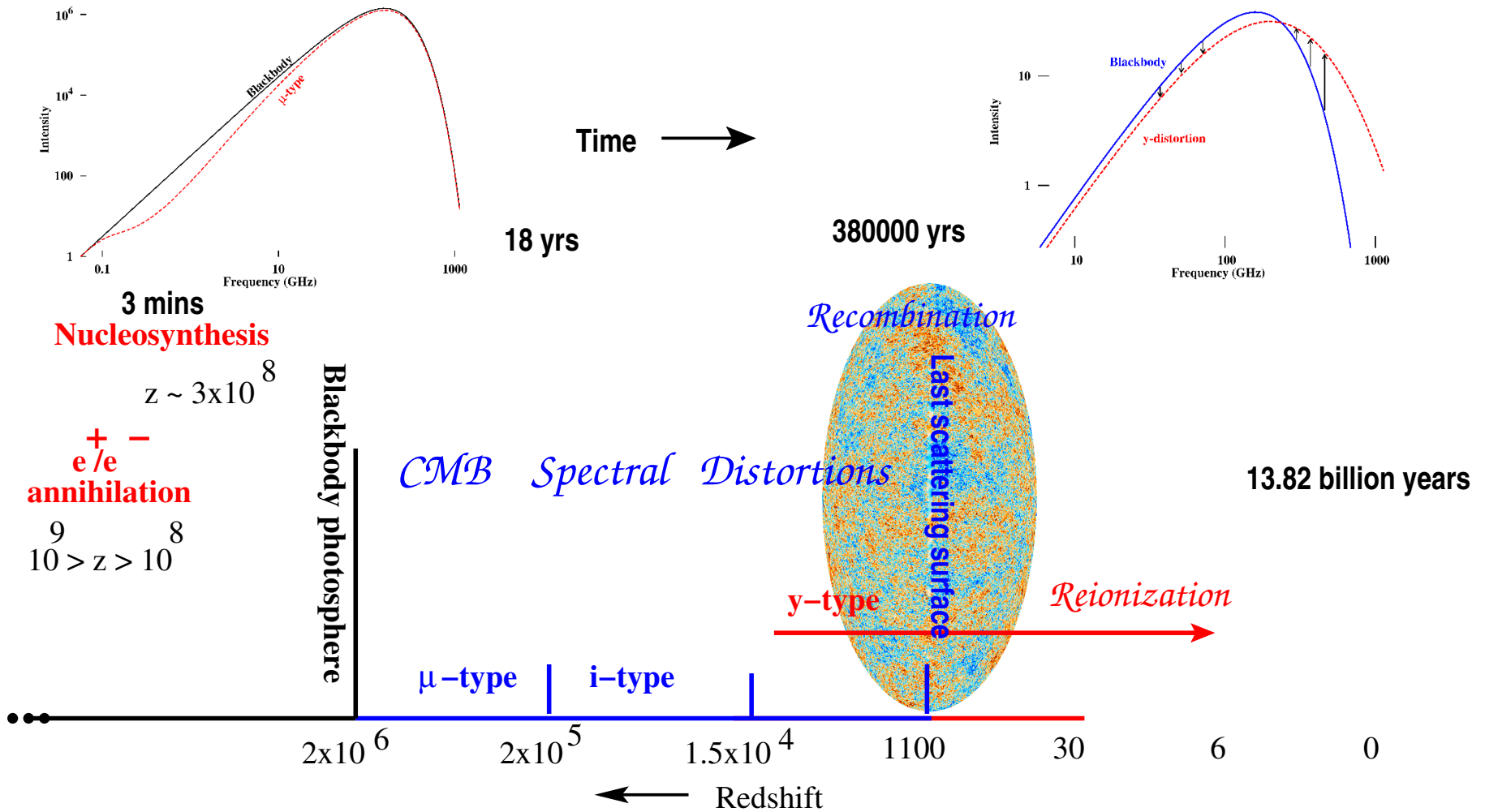
Silk damping of standing sound waves due to radiative viscosity and thermal conductivity

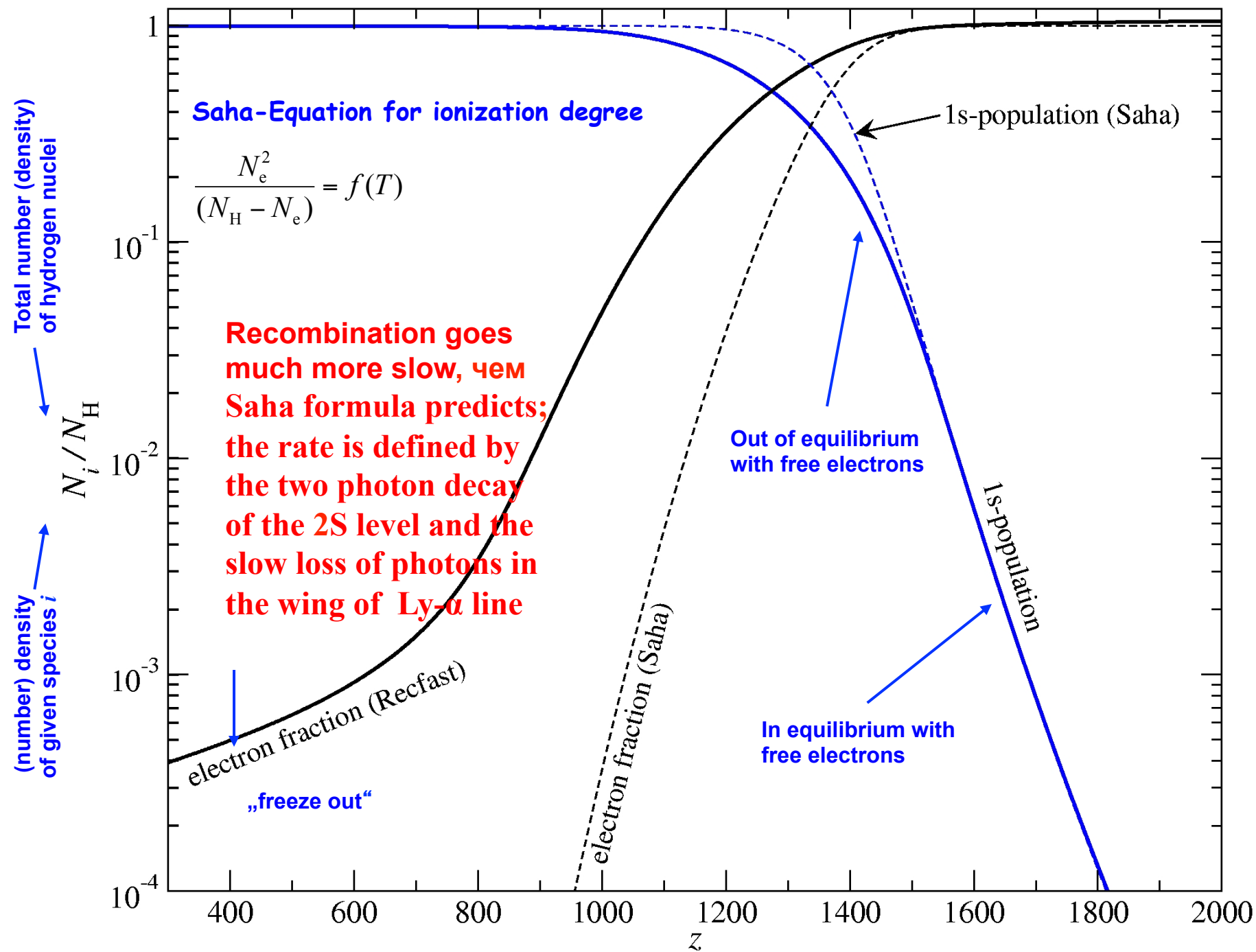


Going from 7 to 17 e-folds of inflation



*Two milestones in the life of the Universe:
Last Scattering Surface and
Black Body Photosphere*





from Chluba, Sunyaev, 2009

Zeldovich, Kurt, Sunyaev, 1968; Peebles, 1968

R. A. SUNYAEV and YA. B. ZELDOVICH

(Received 11 September, 1969)

Astrophysics and Space Science 7 (1970) 3

Visibility function

Last scattering surface

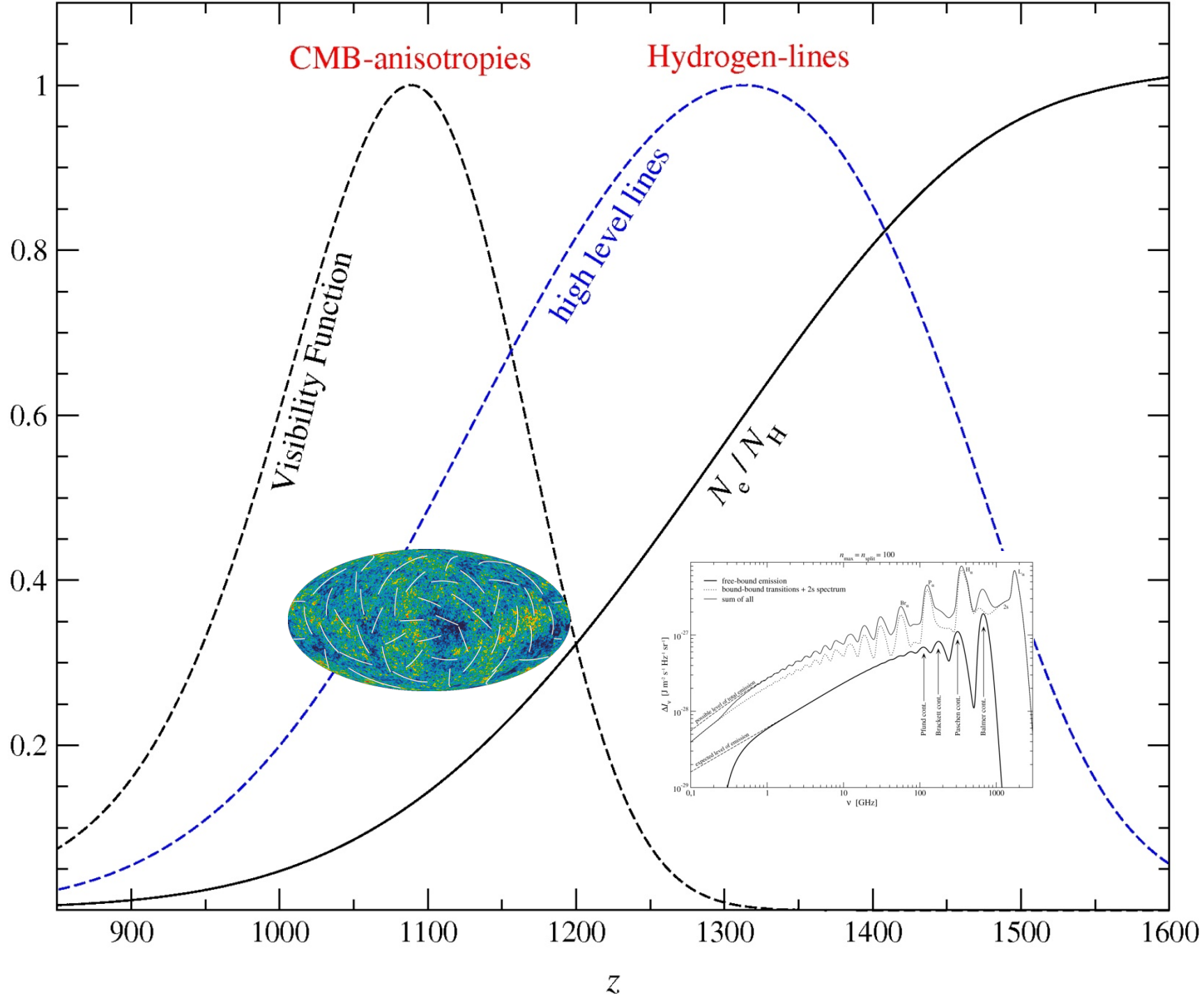
Below we will need the

function

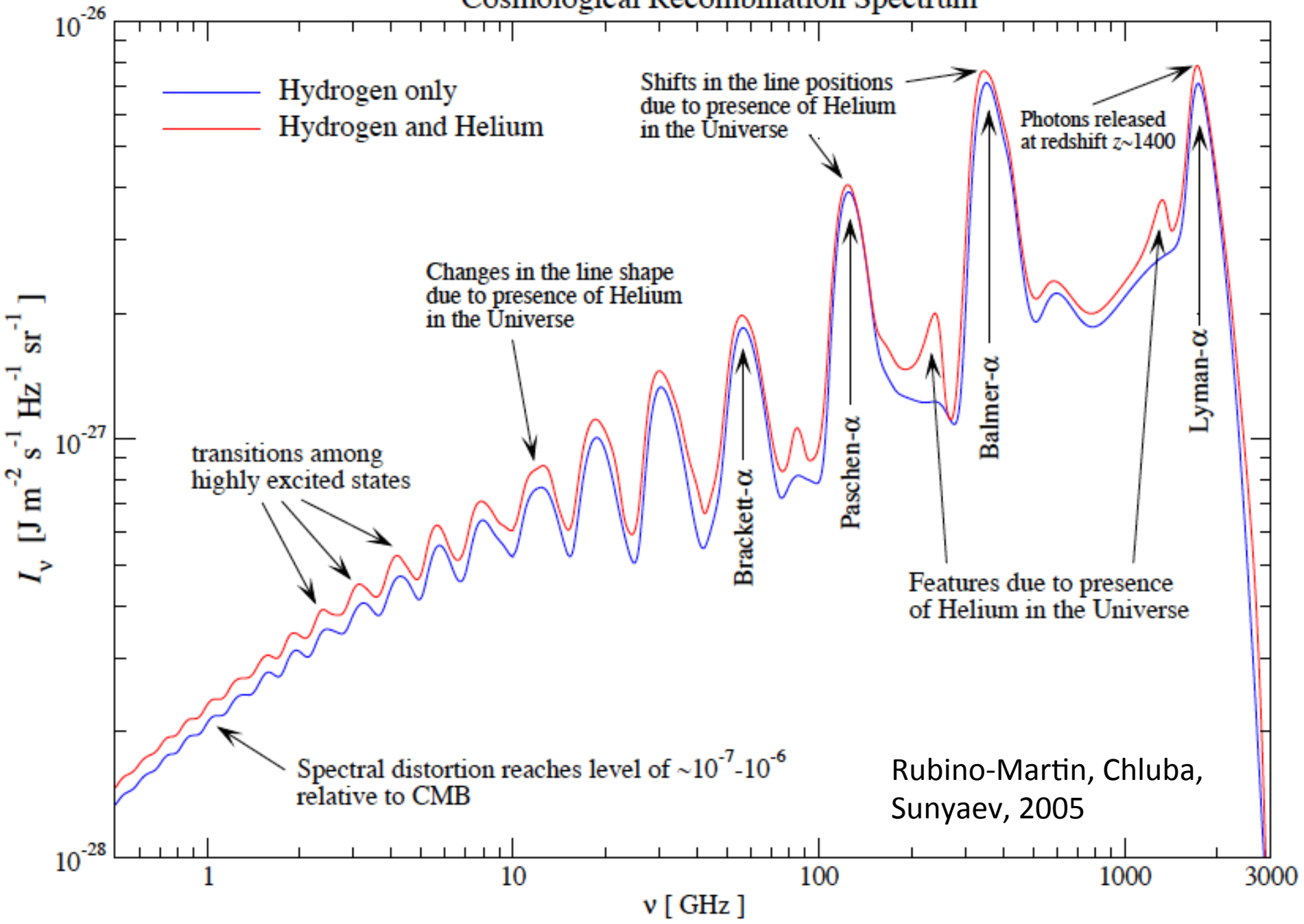
$$e^{-\tau} \frac{d\tau}{dz} = \sigma_T n_c c H_0^{-1} A z^{-1/2} \exp \left\{ - a z^{3/2} e^{-B/z} - \frac{B}{z} - \tau_0 \right\}, \quad (6)$$

which in agreement with (3) has a sharp maximum for $z_{\max} = 1055$ ($e^{-\tau} (d\tau/dz)_{z=z[\max]} = 3.32 \times 10^{-3}$) and exponentially decreases in both directions, the value of the function decreasing to half its maximum value for $z_3 = 960$ and $z_4 = 1135$. It will be convenient in what follows to approximate this function by a Gaussian function with dispersion $\sigma_z = 75$ whose integral equals 1.

The redshift and the width of this function were very well confirmed by WMAP and recently PLANCK

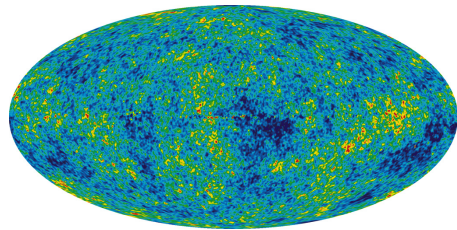


Cosmological Recombination Spectrum



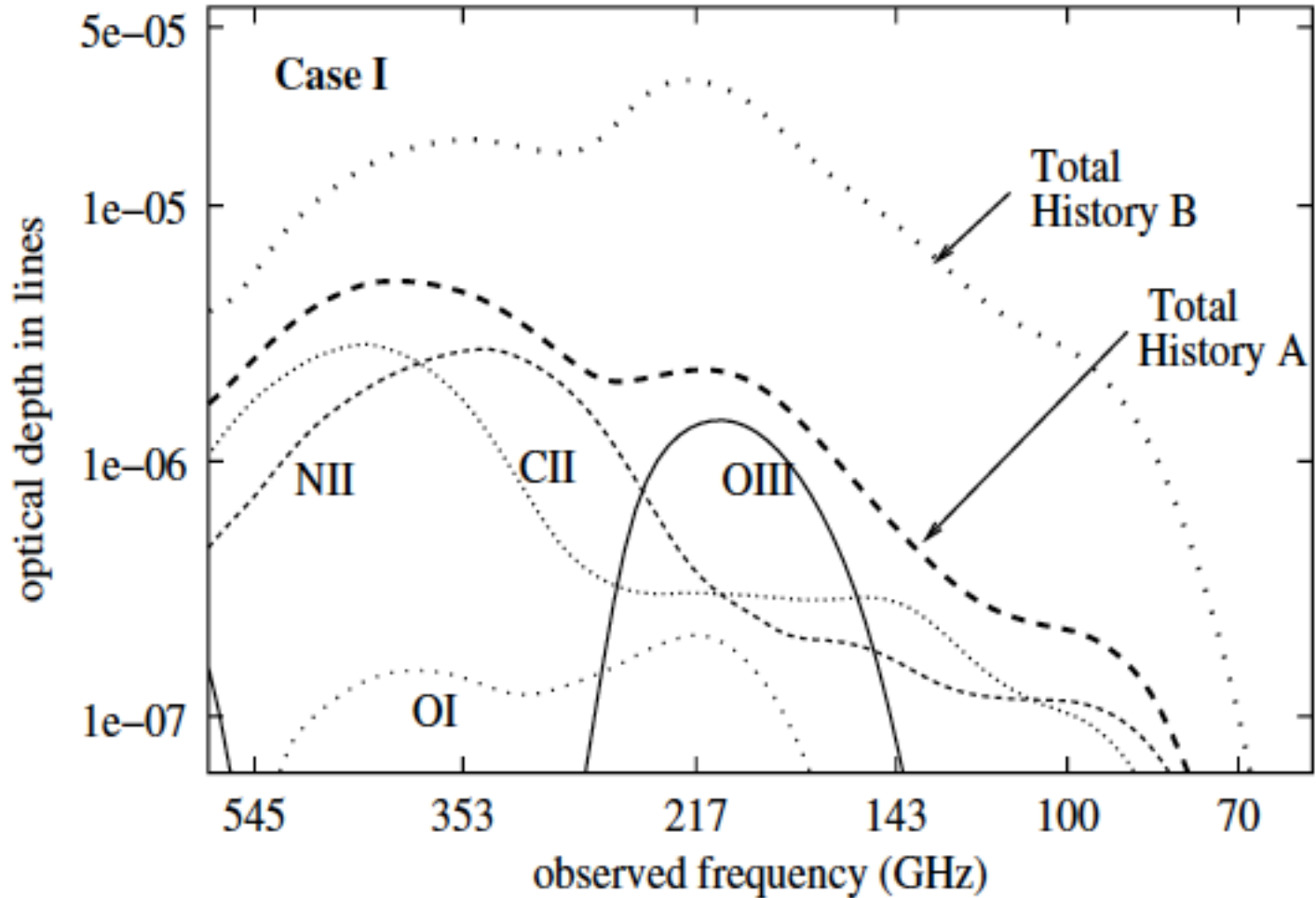
the blurring of primordial fluctuations. Thomson tau = 0.85 (WMAP)

full analogy with Gunn-Peterson effect, but τ inhomogeneities on the sky are playing the role of quasars and submm lines are used instead Ly-alpha.



Hot and cold spots

zero effect for monopole,
polarization from quadrupole



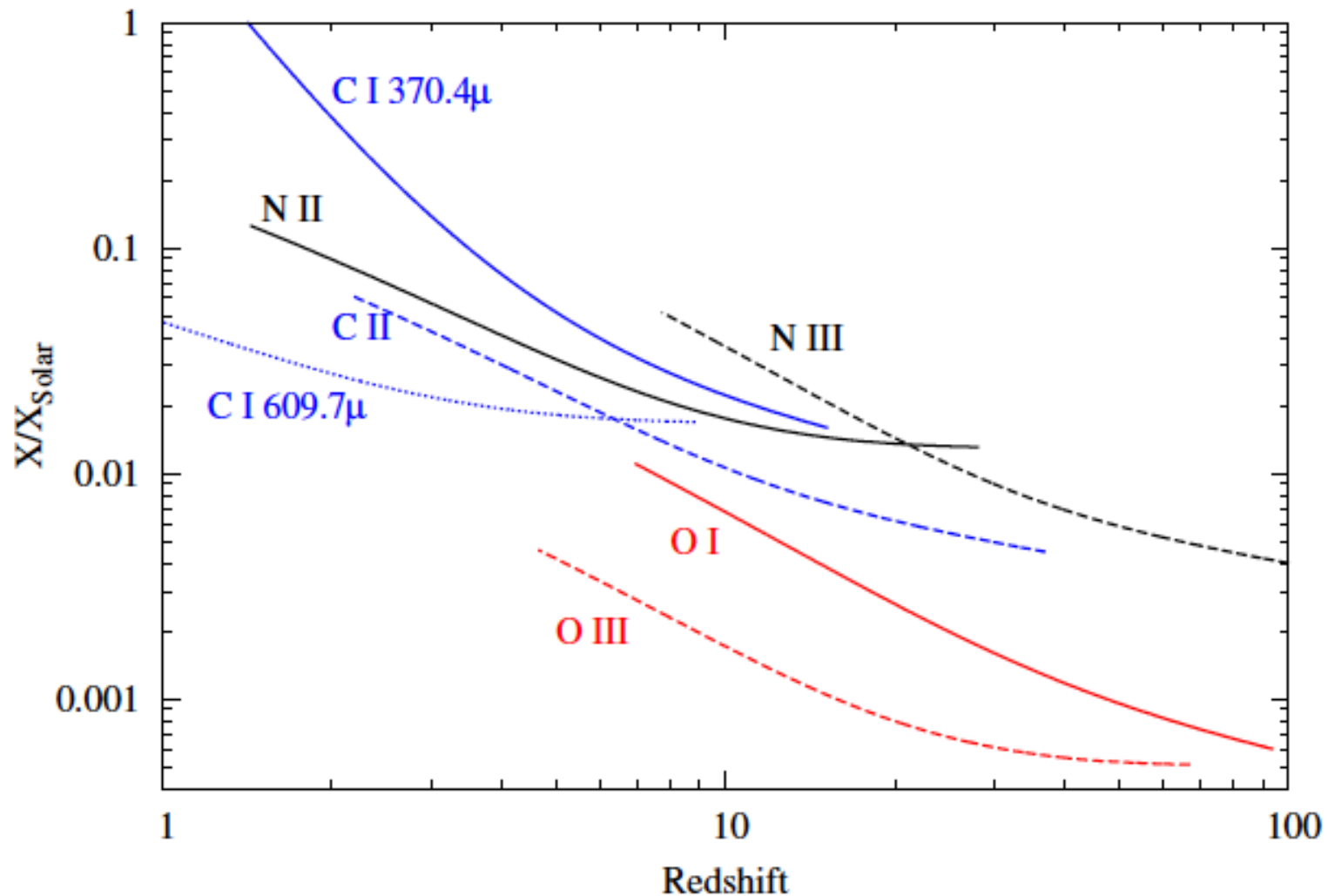
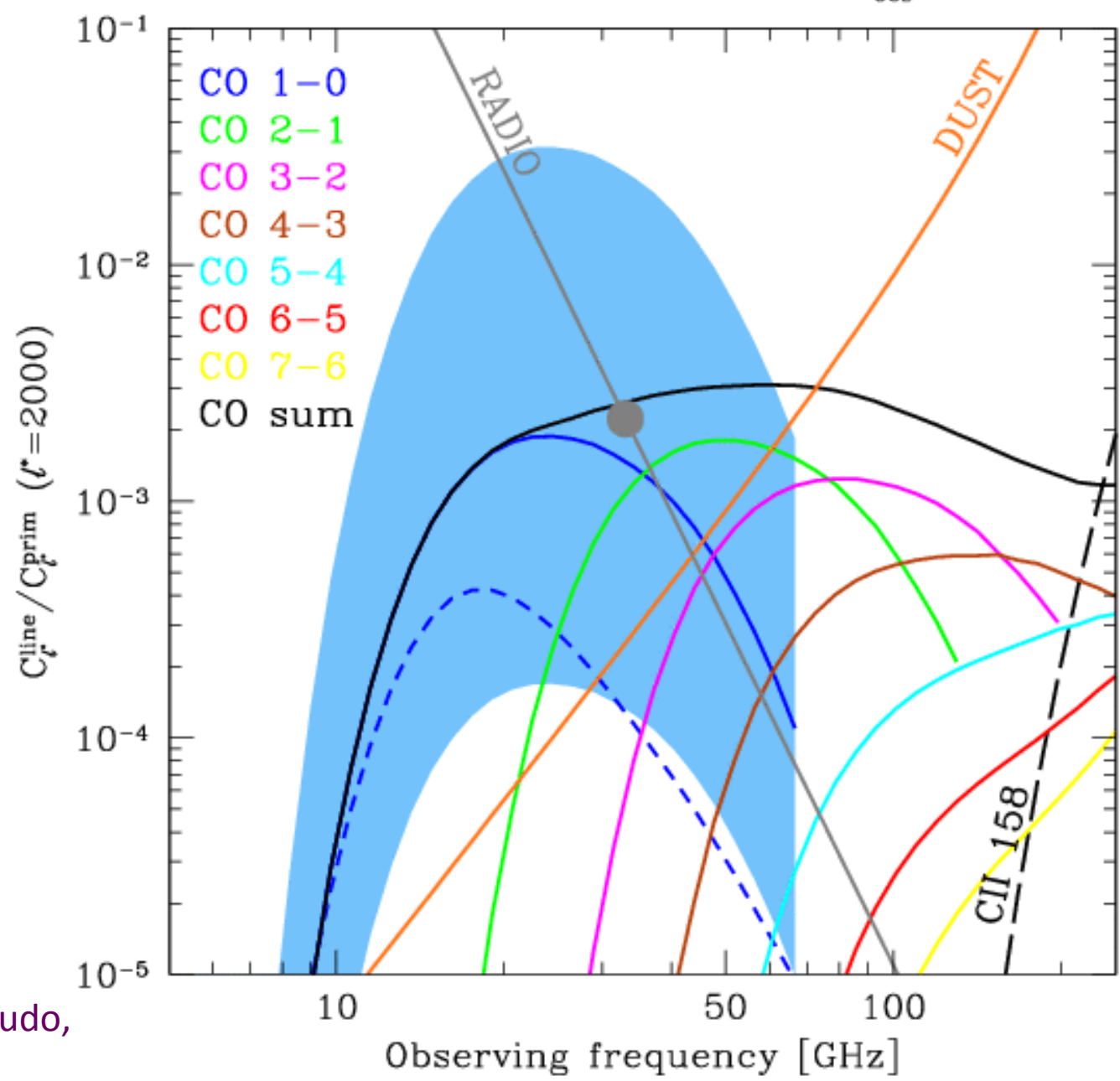


Figure 47. Projected constraints on abundance of C,N,O atoms and ions from 50-600 GHz channels of PRISM assuming it will have the inter-channel calibration accuracy of 0.001% to be able to measure the difference in the optical depth (to the last scattering surface) seen by different channels of $\tau_{\text{LSS}} = 10^{-5}$. The highest and lowest redshifts at the endpoints of each curve correspond to 50 GHz and 600 GHz observed frequency respectively. The constraints as a fraction of solar abundance are plotted, with the reference solar abundances taken to be photosphere abundances in [399].

Frequency dependence - $\Delta\nu/\nu_{\text{obs}}=10^{-3}$



Righi, Hernandez-Monteagudo,
Sunyaev, 2008

Experiments of the type of COBE/FIRAS are possible not much often than once in 25 years

The goal, theorists are dreaming:

a sensitivity necessary to detect

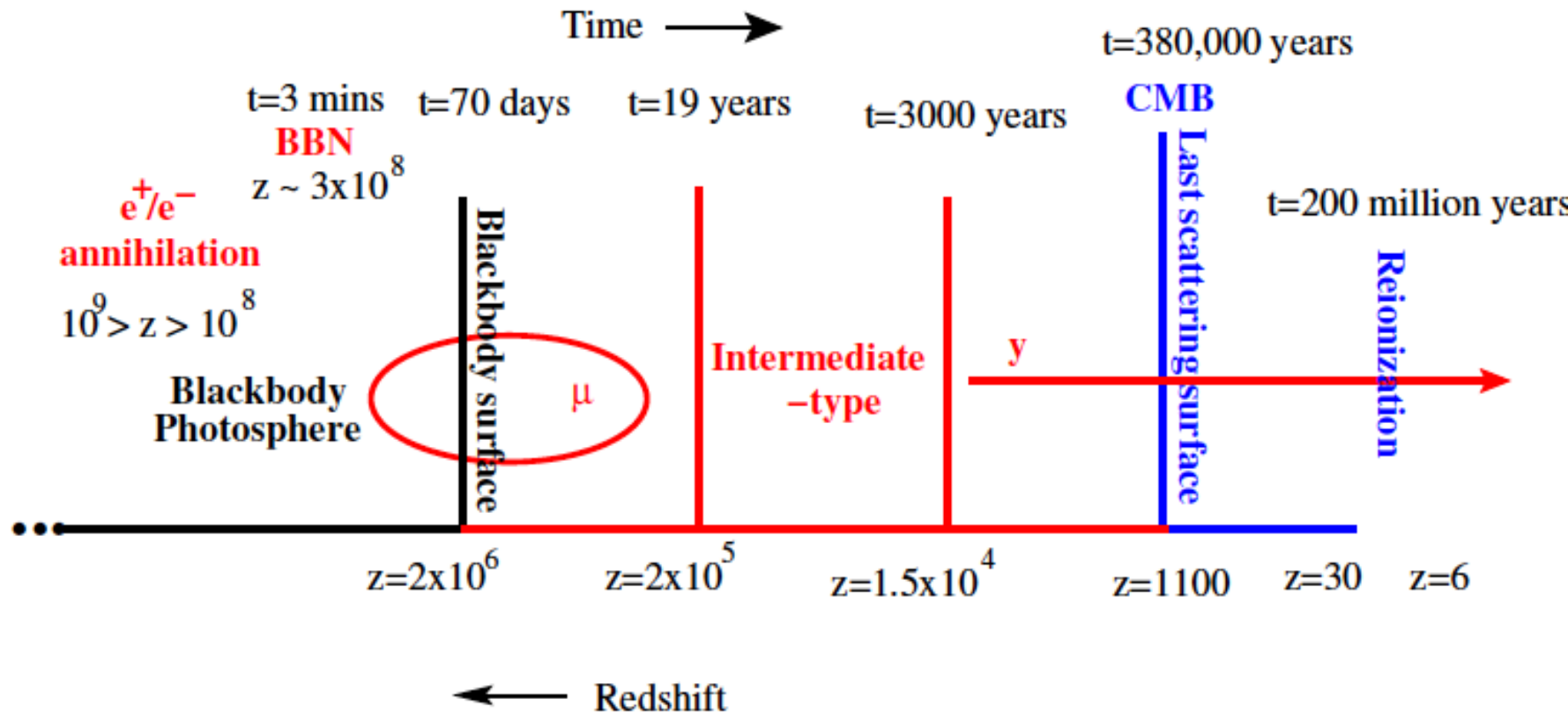
- a) μ -type distortions on the level of 10^{-9} (we do not expect signal below few times 10^{-9} , but who knows?). However any upper limit will be useful.
- b) such a sensitivity will permit to study recombinational lines of hydrogen and helium coming from redshifts ~ 1500 , 2400 and 6000
- c) It will be possible to separate γ distortions produced before recombination from generated much later (they will distort the recombinational spectrum)

Summary

- ▶ The shape of the μ and intermediate type distortions is rich in information
- ▶ With spectral distortions we can extend our 'view' of inflation from 6-7 e-folds at present to 17 e-folds
- ▶ Spectral distortions take us a little nearer to the end of inflation
- ▶ μ -type and intermediate type distortions can be calculated very fast using analytic and pre-calculated cosmology-independent high precision numerical solutions (Green's functions). This allows us to explore the rich multidimensional parameter space
- ▶ i -type distortions are quite powerful in removing degeneracies between power spectrum parameters. The extra information comes from the shape of the i -type distortion

THANK YOU !!!

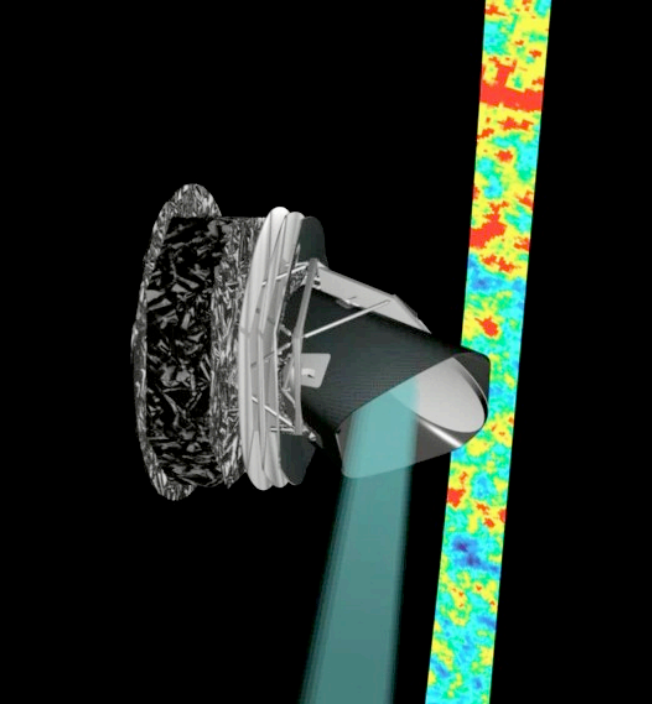
μ -type distortions



Compton + double Compton + bremsstrahlung

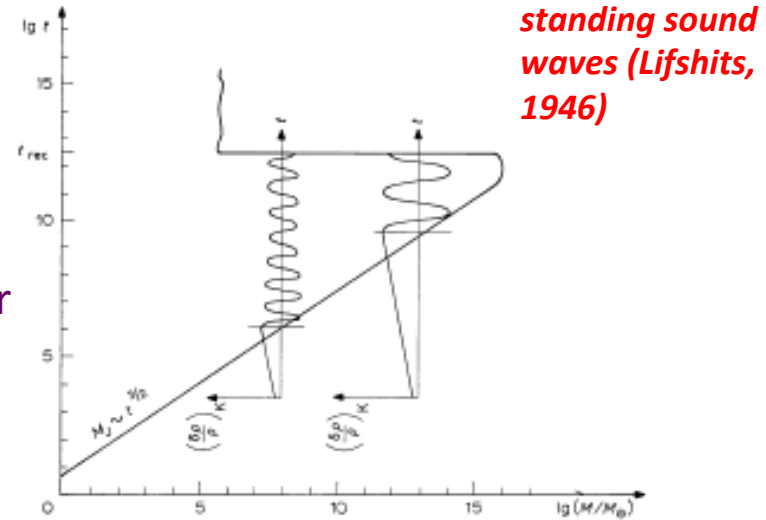
Analytic solution: $\mu = 1.4 \int \frac{dQ}{dz} e^{-\mathcal{I}(z)} dz$

(Sunyaev and Zeldovich 1970)



PLANCK spacecraft scans the sky

From paper Sunyaev, Zeldovich 1970



standing sound waves (Lifshits, 1946)

Fig. 1a. Diagram of gravitational instability in the 'big-bang' model. The region of instability is located to the right of the line $M_J(t)$; the region of stability to the left. The two additional lines of the graph demonstrate the temporal evolution of density perturbations of matter: growth until the moment when the considered mass is smaller than the Jeans mass and oscillations thereafter. It is apparent that at the moment of recombination perturbations corresponding to different masses correspond to different phases.

Planck Collaboration: The *Planck* mission

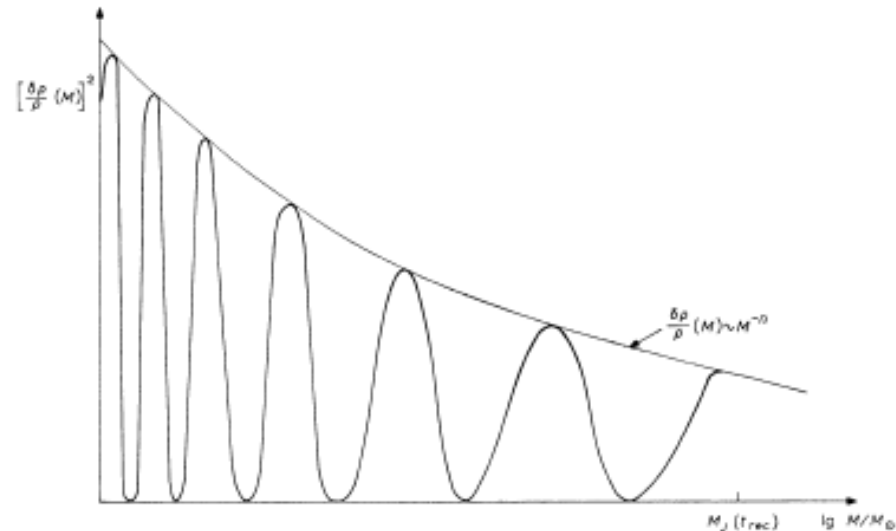
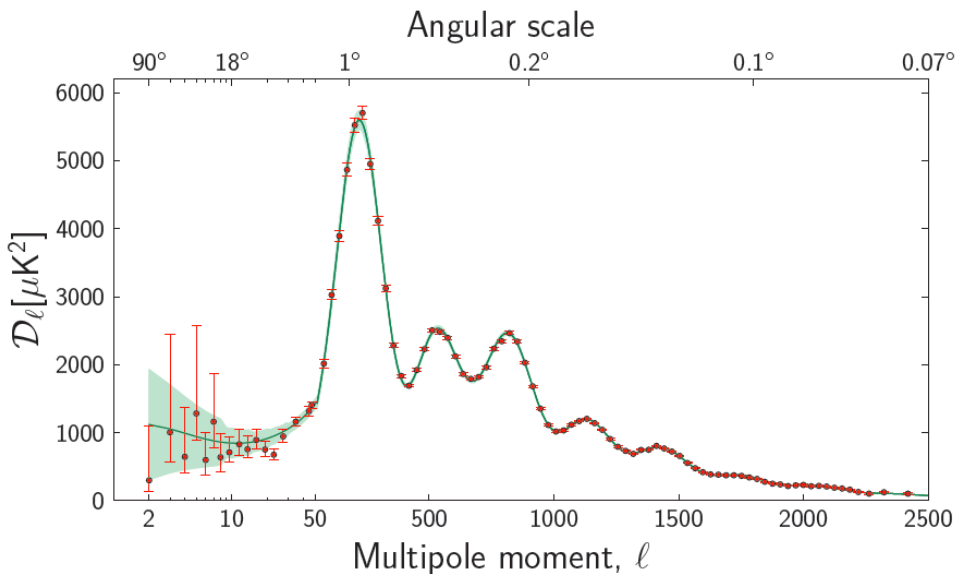
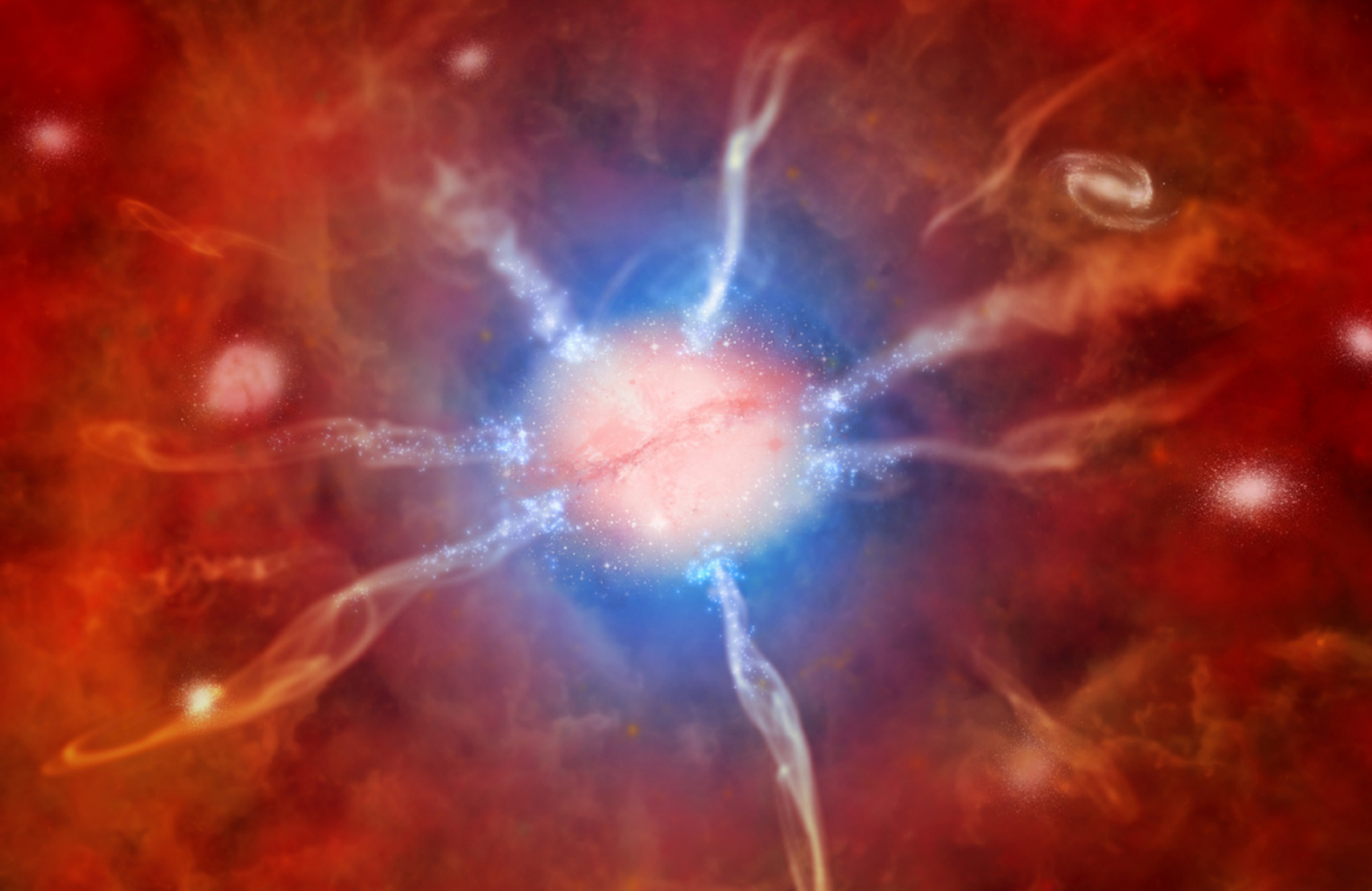


Fig. 1b. The dependence of the square of the amplitude of density perturbations of matter on scale. The fine line designates the usually assumed dependence $(\delta\rho/\rho)_{ar} \sim M^{-2}$. It is apparent that fluctuations of relic radiation should depend on scale in a similar manner.



Fenix cluster of galaxies discovered by SPT at $z=0.596$ and observed by CHANDRA, GALEX and Magellan: star burst – 800 solar masses a year, luminosity 8×10^{45} erg/s, cooling flow ~ 3000 Solar masses a year. Black hole in the center accretes 60 solar masses a year.

Summary continued

With intermediate-type distortions we can distinguish between different mechanisms of energy injection which have different redshift dependence

There is more....

- ▶ Cosmological recombination spectrum gives measurement of primordial helium
Kurt,Zeldovich,Sunyaev,Peebles,Dubrovich,Chluba,Rubino-Martin
- ▶ Resonant scattering on C,N,O and other ions during and after **reionization** makes the optical depth to the last scattering surface frequency dependent

Basu, Hernandez-Monteagudo, and Sunyaev 2004

- ▶ Sunyaev-Zeldovich effect from hot electrons during reionization/WHIM can give a measurement of average electron temperature, **find missing baryons**

Zeldovich & Sunyaev 1969, Hu, Scott, Silk 1994, Cen and Ostriker 1999,2006,

- ▶ Primordial non-gaussianity on extremely small scales

Pajer and Zaldarriaga 2012, Ganc and Komatsu 2012

Summary continued

- ▶ Silk damping: $\frac{dQ}{dz} \propto (1+z)^{(3n_s-5)/2}$
(Chluba, Khatri and Sunyaev 2012, Khatri, Sunyaev and Chluba 2012)
- ▶ Adiabatic cooling: Opposite sign to Silk damping with $n_s = 1$
(Chluba and Sunyaev 2012, Khatri, Sunyaev and Chluba 2012b)
- ▶ Particle decay: $\frac{dQ}{dz} \propto \frac{e^{-\left(\frac{1+z_{\text{decay}}}{1+z}\right)^2}}{(1+z)^4}$
(Hu and Silk 1993, Chluba and Sunyaev 2012, Khatri and Sunyaev 2012a, 2012b)
- ▶ Cosmic strings: $\frac{dQ}{dz} \propto \text{constant}$
Tashiro, Sabancilar, Vachaspati 2012
- ▶ Primordial magnetic fields : $\propto (1+z)^{(3n+7)/2}$, n is the spectral index of magnetic field power spectrum *(Jedamzik, Katalinic, and Olinto 2000)*
- ▶ Black holes: Depends on the mass function
Tashiro and Sugiyama 2008, Carr et al. 2010
- ▶ Quantum wave function collapse: $\frac{dQ}{dz} \propto (1+z)^{-4}$
Lochan, Das and Bassi 2012

There is still a long road ahead for CMB cosmology

CMB spectrum is very rich in information about the early Universe,
late time Universe and fundamental physics

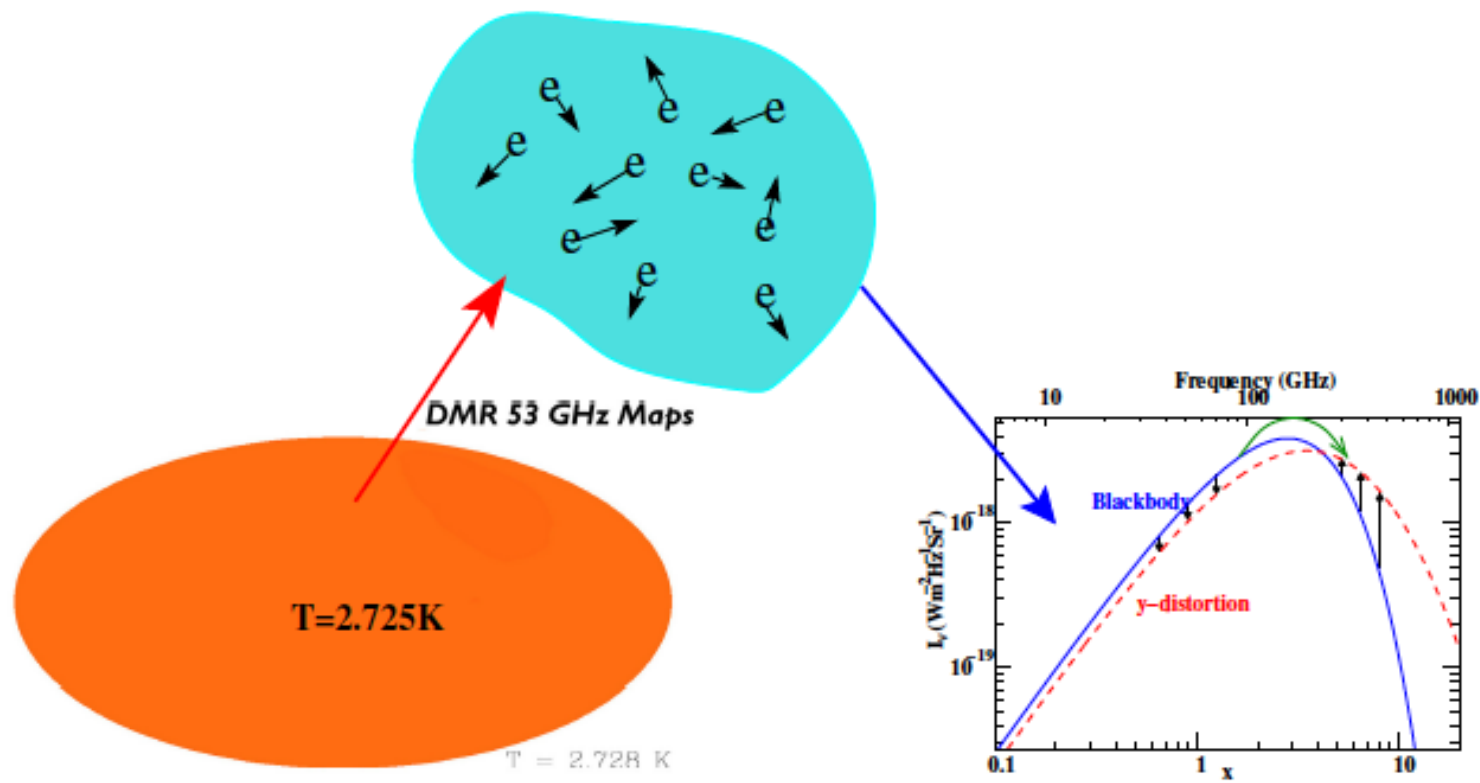
This information is accessible and within reach of experiments in not
too far future: Pixie, PRISM

Thank you !!!

clusters/reionization

$$y_\gamma \ll 1, T_e \sim 10^4$$

$$y = (\tau_{\text{reionization}}) \frac{k_B T_e}{m_e c^2} \sim (0.1)(1.6 \times 10^{-6}) \sim 10^{-7}$$



Efficiency of energy exchange between electrons and photons

Recoil:

$$y_\gamma = \int dt c \sigma_T n_e \frac{k_B T_\gamma}{m_e c^2}, \quad T_\gamma = 2.725(1+z)$$

No. of scatterings

Energy transfer per scattering

Doppler effect:

$$y_e = \int dt c \sigma_T n_e \frac{k_B T_e}{m_e c^2}$$

In early Universe $y_\gamma \approx y_e$

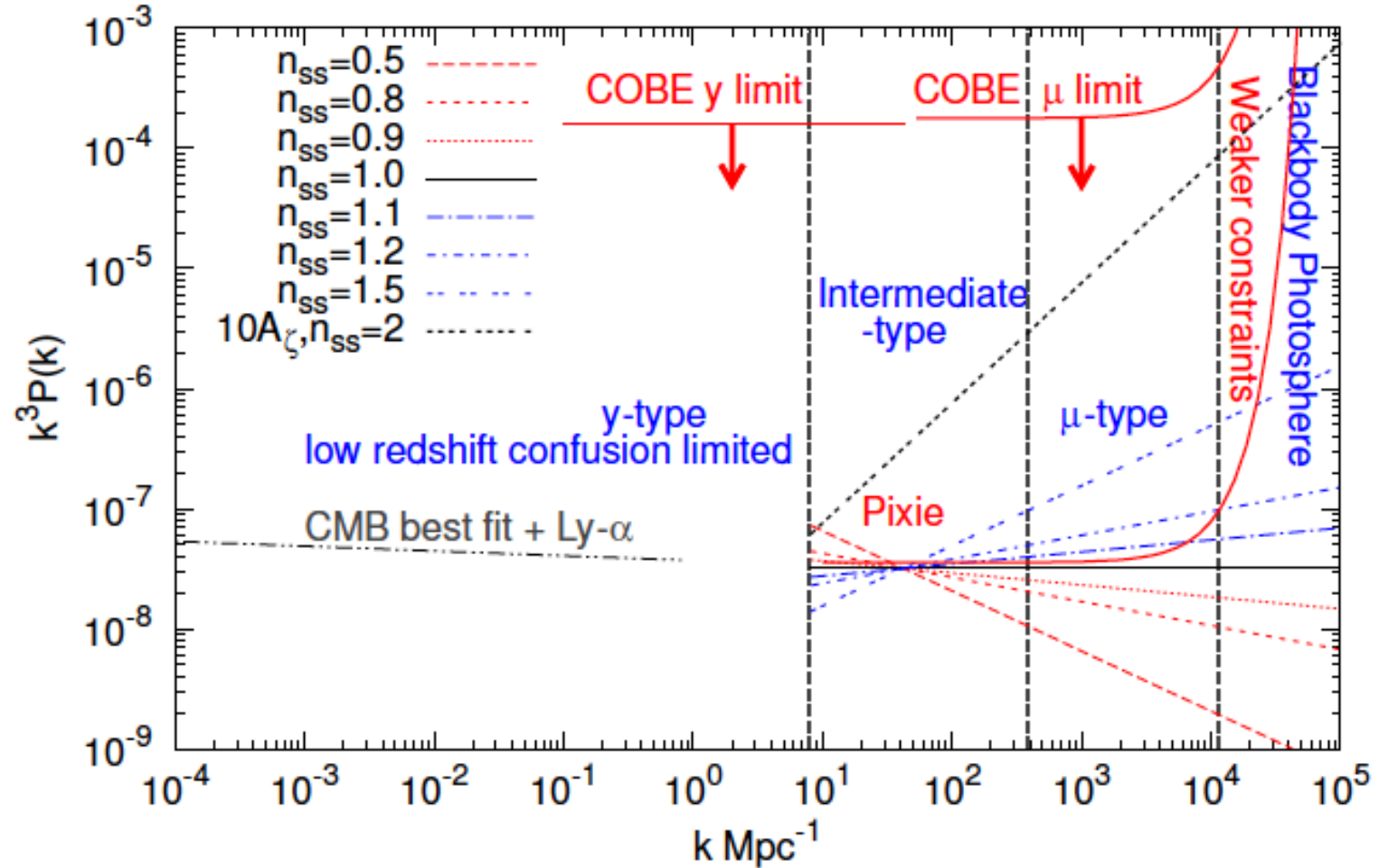
y : Amplitude of distortion

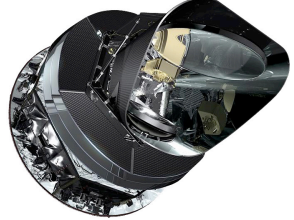
$$y = \int dt c \sigma_T n_e \frac{k_B (T_e - T_\gamma)}{m_e c^2}$$

Pivot point $k_0 = 42 \text{ Mpc}^{-1}$

Power spectrum of initial density perturbations

$$P_\zeta = (A_\zeta 2\pi^2 / k^3) (k/k_0)^{n_s - 1 + \frac{1}{2} dn_s / d \ln k (\ln k / k_0)}$$



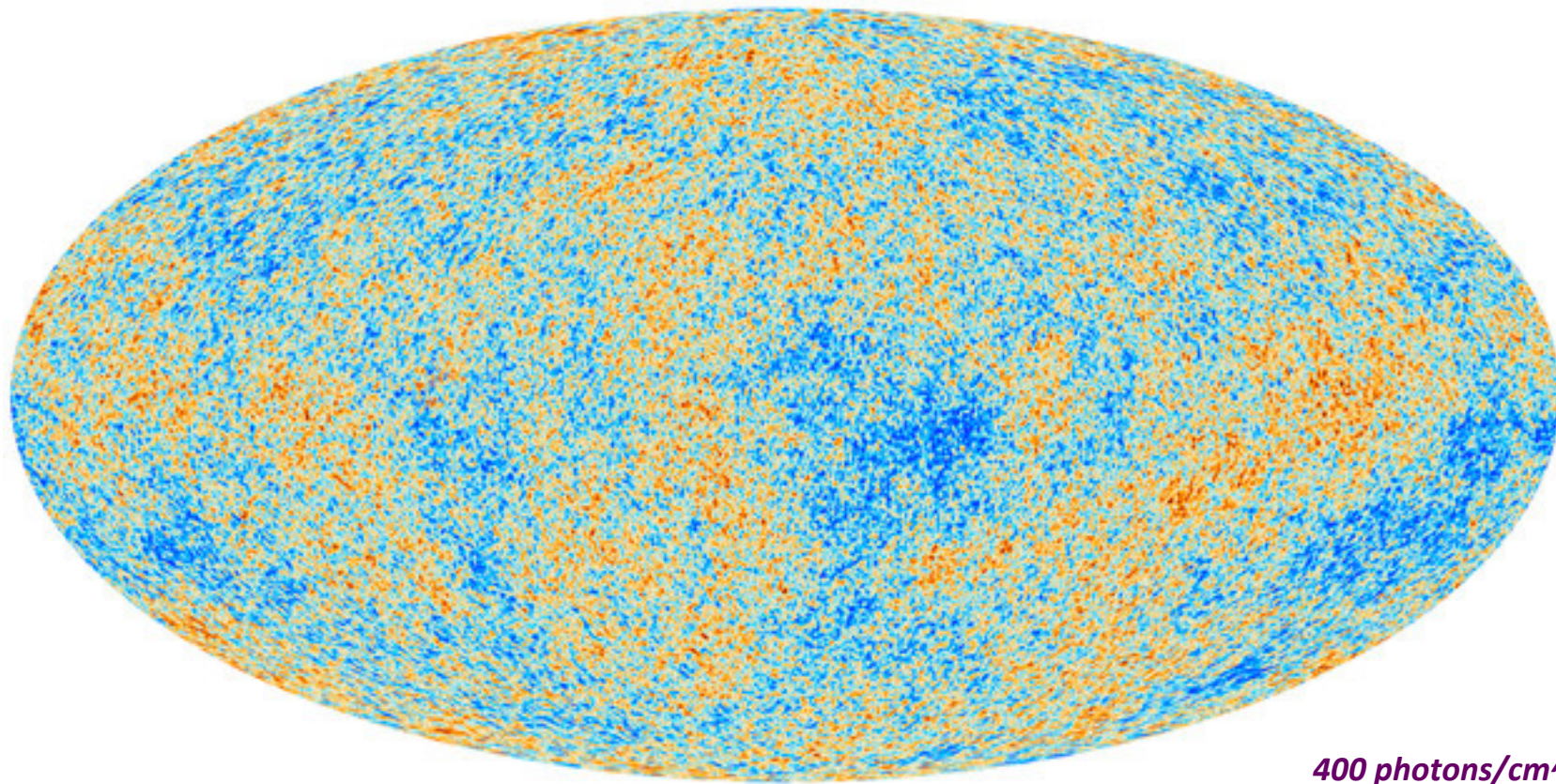
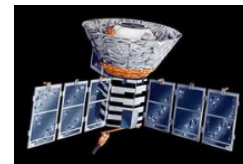


black body spectrum

$$T_r = 2.725 (1+z)K$$

practically isotropic

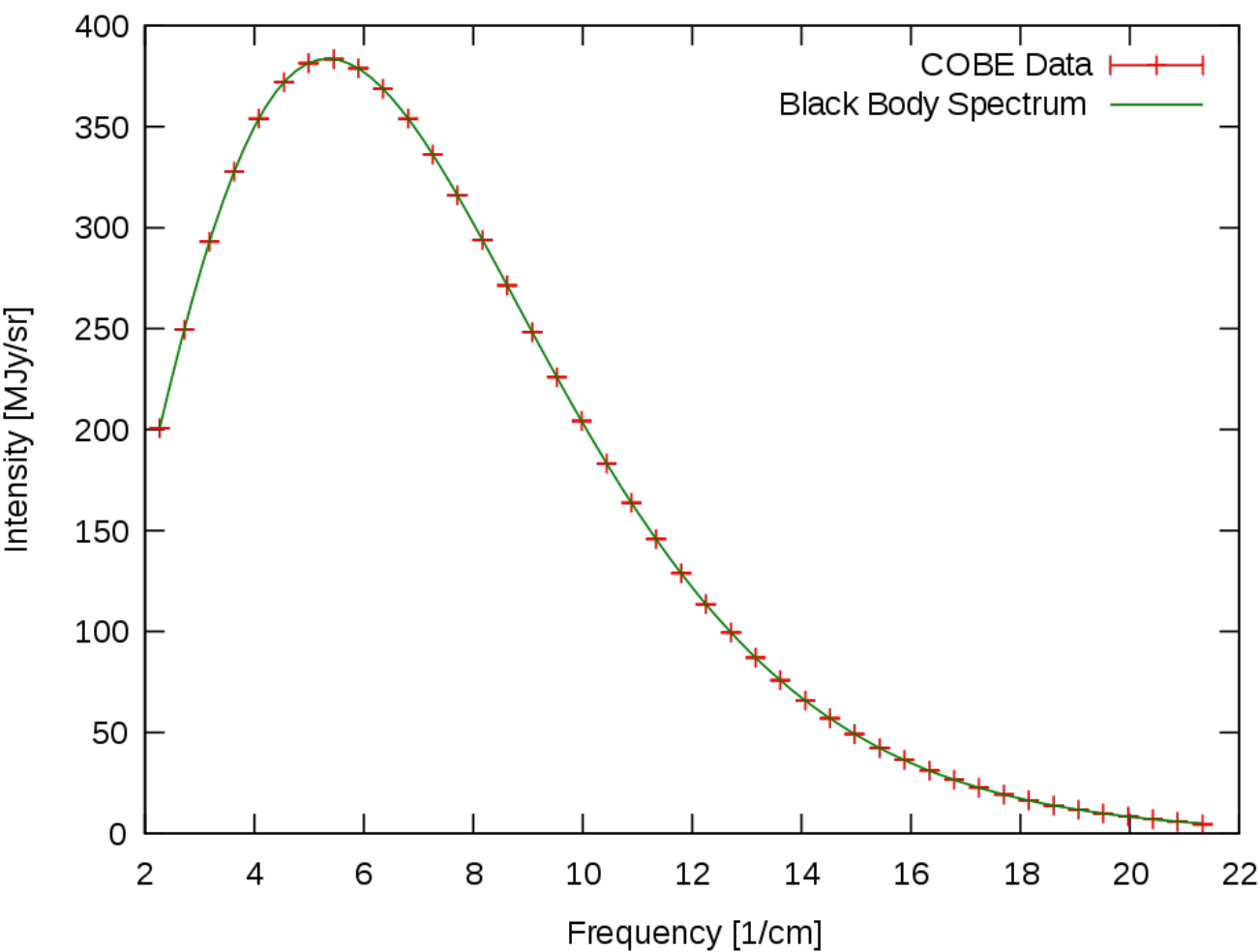
COBE-Firas:



400 photons/cm³

dark blue - 200 microK

red +200 microK



Max Planck 1858-1947



Cosmic Microwave Background (CMB): The most precise black body known: $T = 2.725K \pm 1mK$

No spectral deviations are detected !!!

Energy density of Planck spectrum

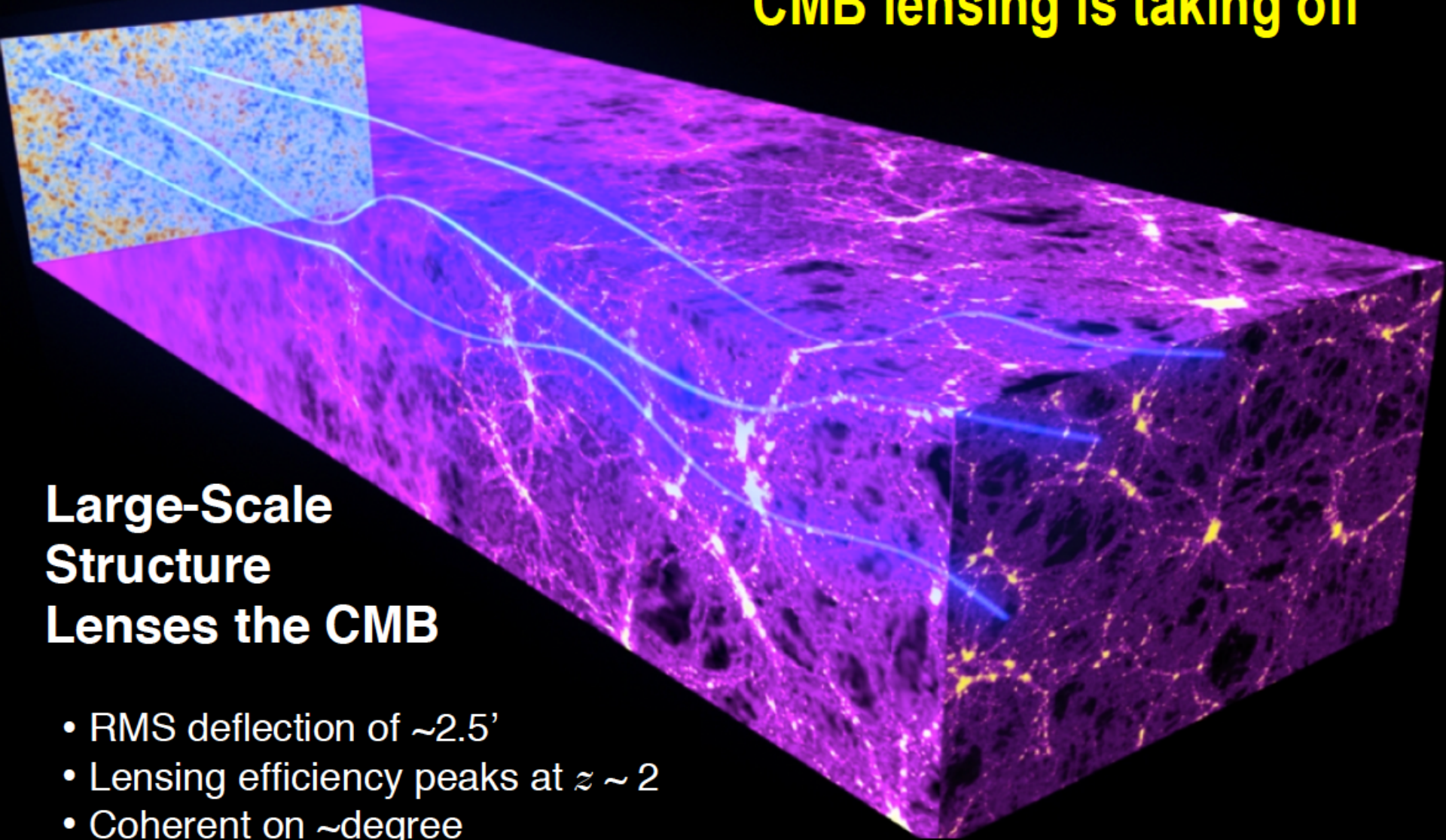
$$E_\nu = \frac{8\pi h\nu^3}{c^3} \frac{1}{e^{\frac{h\nu}{kT}} - 1}$$

$$E = a_R T^4$$

CMB lensing is taking off

Large-Scale Structure Lenses the CMB

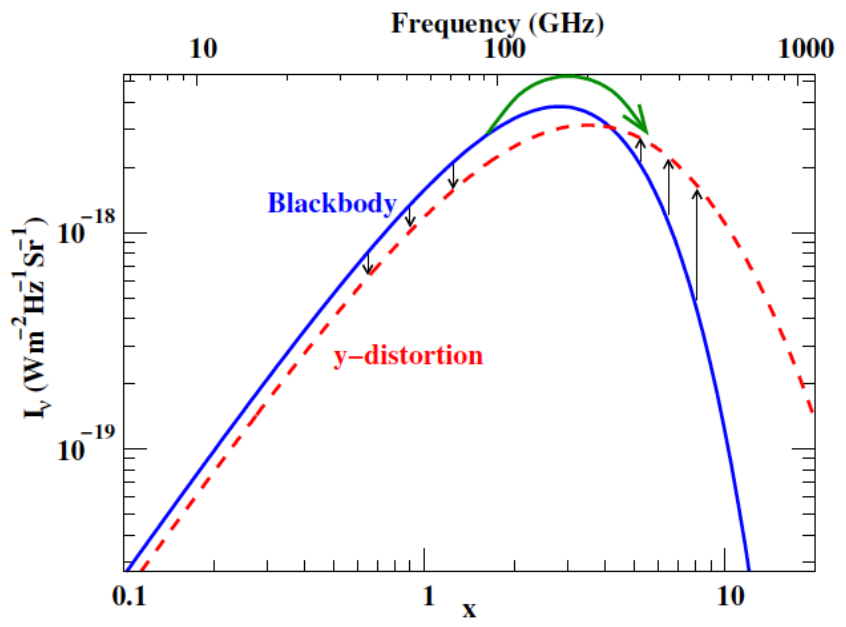
- RMS deflection of $\sim 2.5'$
- Lensing efficiency peaks at $z \sim 2$
- Coherent on \sim degree (~ 300 Mpc) scales



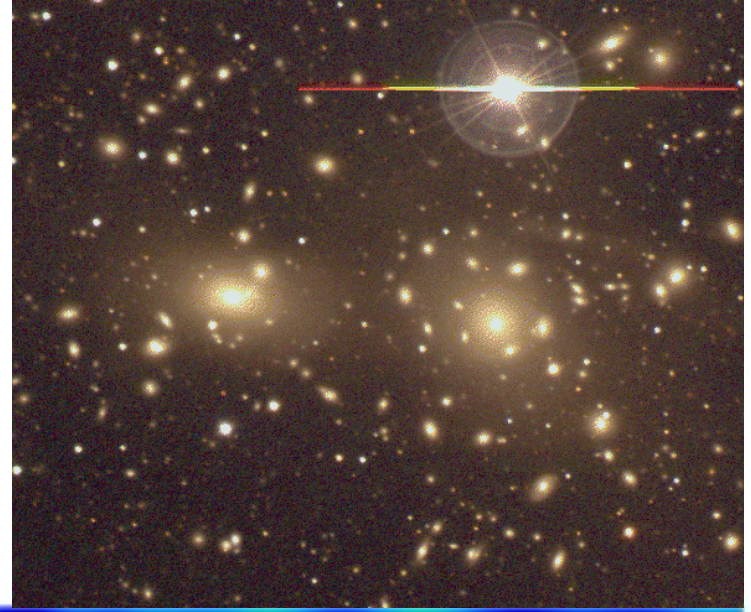
$$n_{SZ} = y T^4 \frac{\partial}{\partial T} \frac{1}{T^2} \frac{\partial n_{Pl}}{\partial T}$$
$$= y \frac{x e^x}{(e^x - 1)^2} \left(x \frac{e^x + 1}{e^x - 1} - 4 \right)$$

$$\Delta I_{sz} = I_{sz} - I_{planck} = \frac{2h\nu^3}{c^2} n_{sz}$$

(Zeldovich and Sunyaev 1969)
 COBE-FIRAS limit (95%): $y \lesssim 1.5 \times 10^{-5}$ (Fixsen et al. 1996)



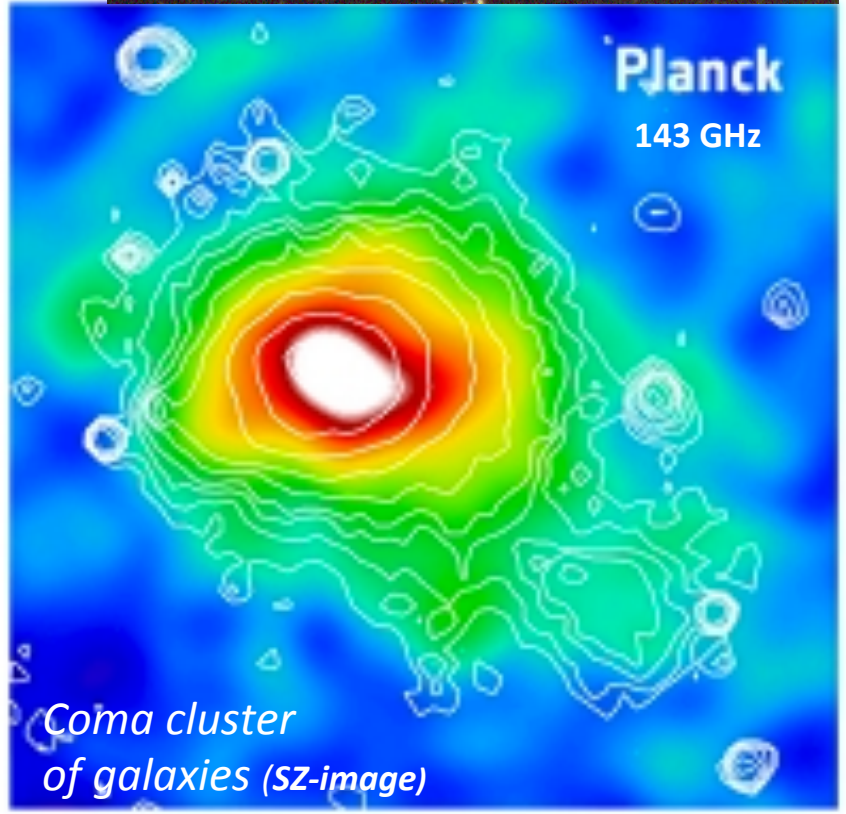
Coma,
 optical
 image,
 central
 part



$$n_{SZ} = y T^4 \frac{\partial}{\partial T} \frac{1}{T^2} \frac{\partial n_{Pl}}{\partial T}$$

$$= y \frac{x e^x}{(e^x - 1)^2} \left(x \frac{e^x + 1}{e^x - 1} - 4 \right)$$

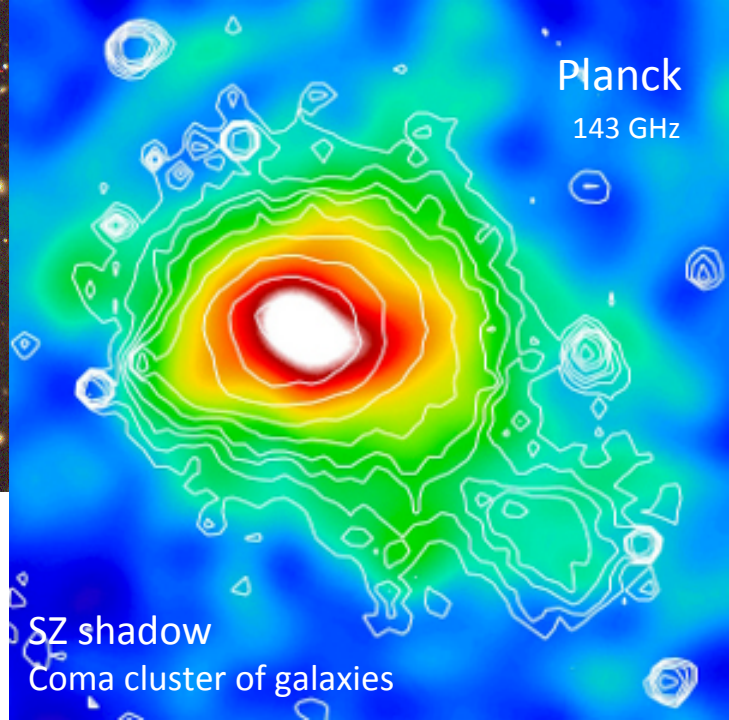
$$\Delta I_{SZ} = I_{SZ} - I_{planck} = \frac{2 h \nu^3}{c^2} n_{SZ}$$



PLANCK/HFI



*Coma, optical image
central part*

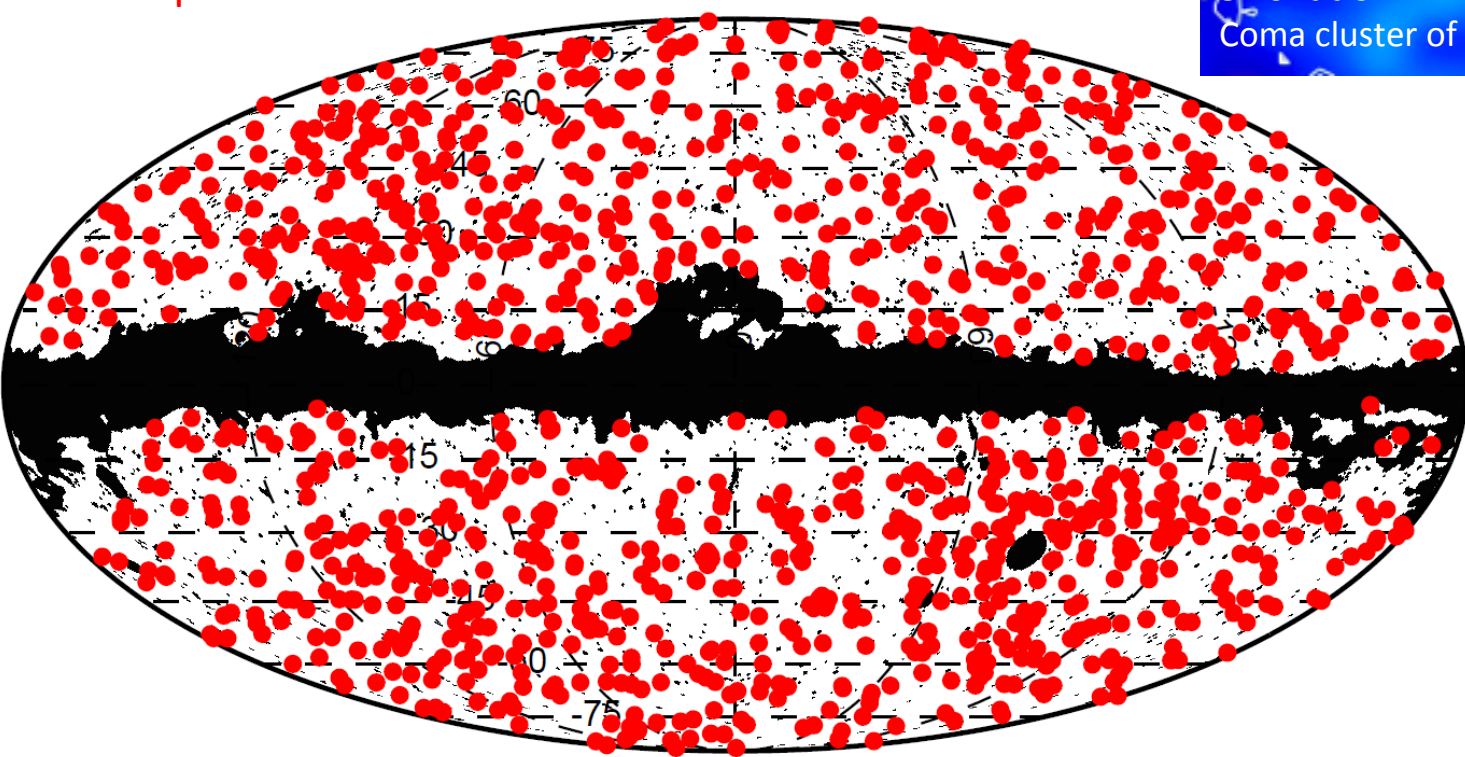


Planck

143 GHz

SZ shadow
Coma cluster of galaxies

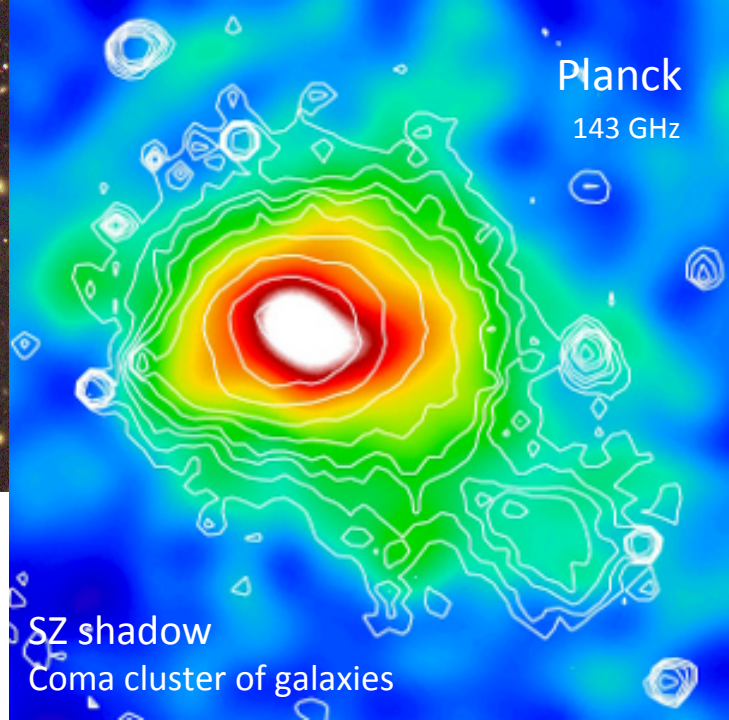
~ 900 clusters confirmed by X-Ray
or optical observations



PLANCK/HFI



*Coma, optical image
central part*

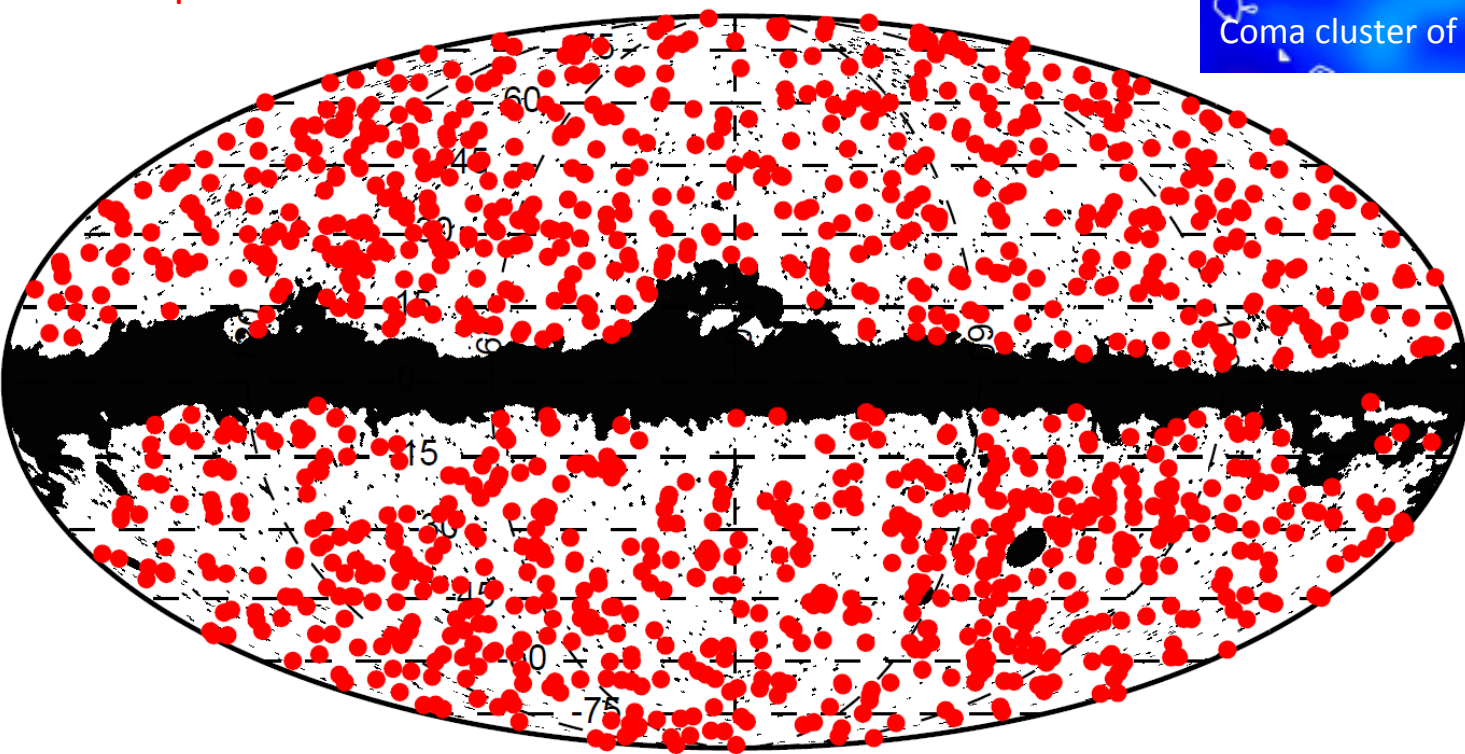


Planck

143 GHz

SZ shadow
Coma cluster of galaxies

~ 900 clusters confirmed by X-Ray
or optical observations



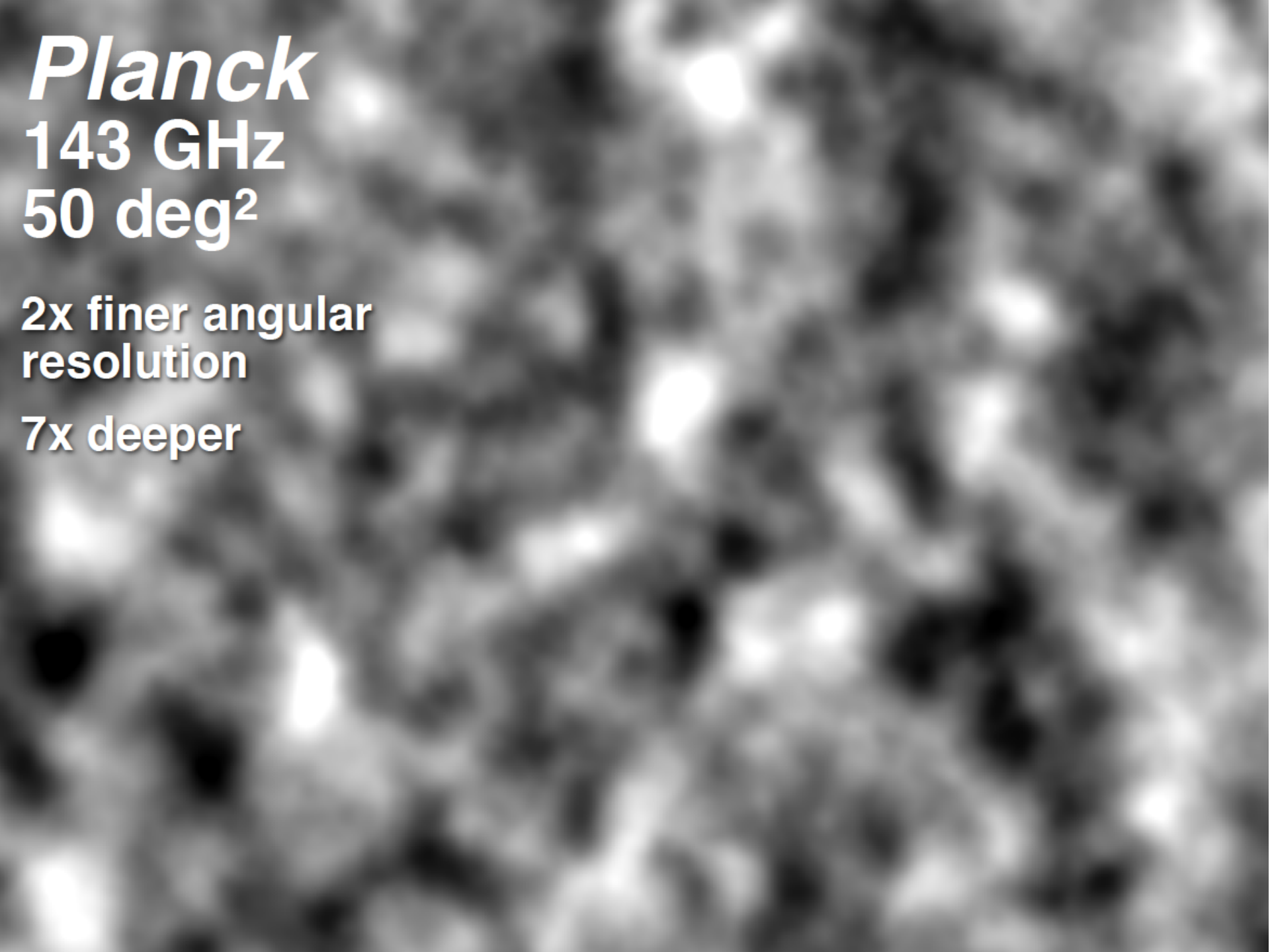
Planck

143 GHz

50 deg²

**2x finer angular
resolution**

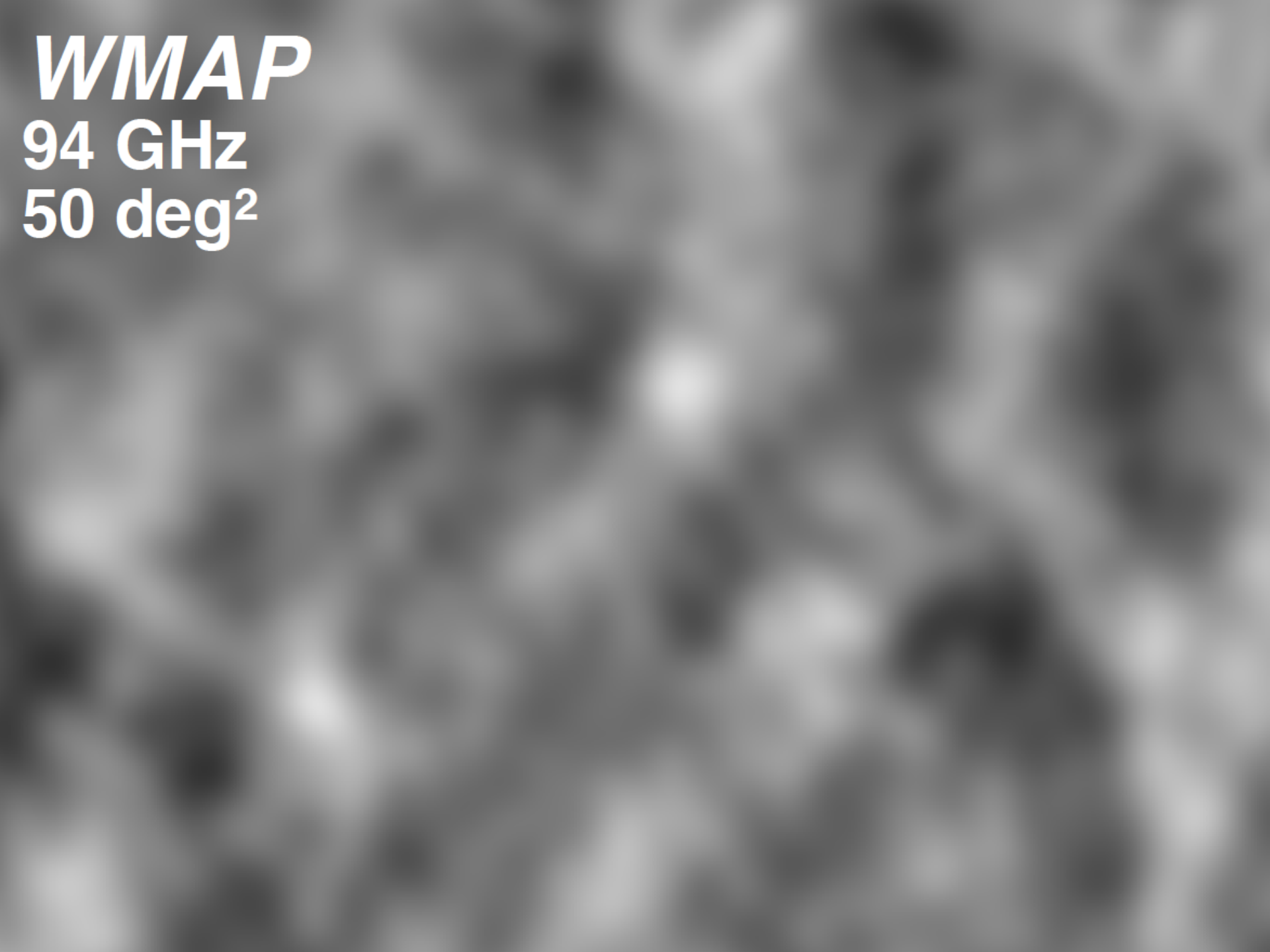
7x deeper



WMAP

94 GHz

50 deg²



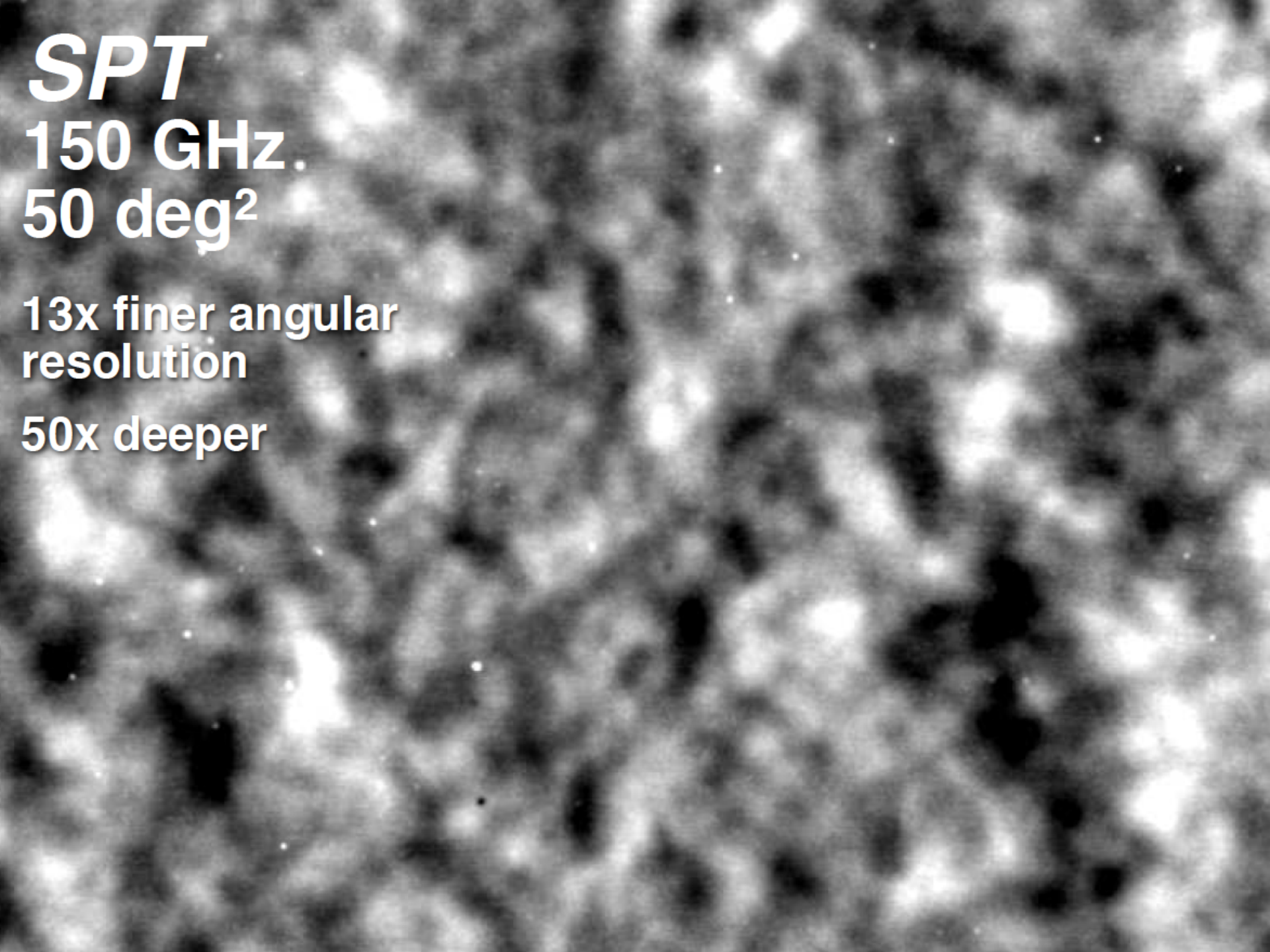
SPT

150 GHz.

50 deg²

**13x finer angular
resolution**

50x deeper

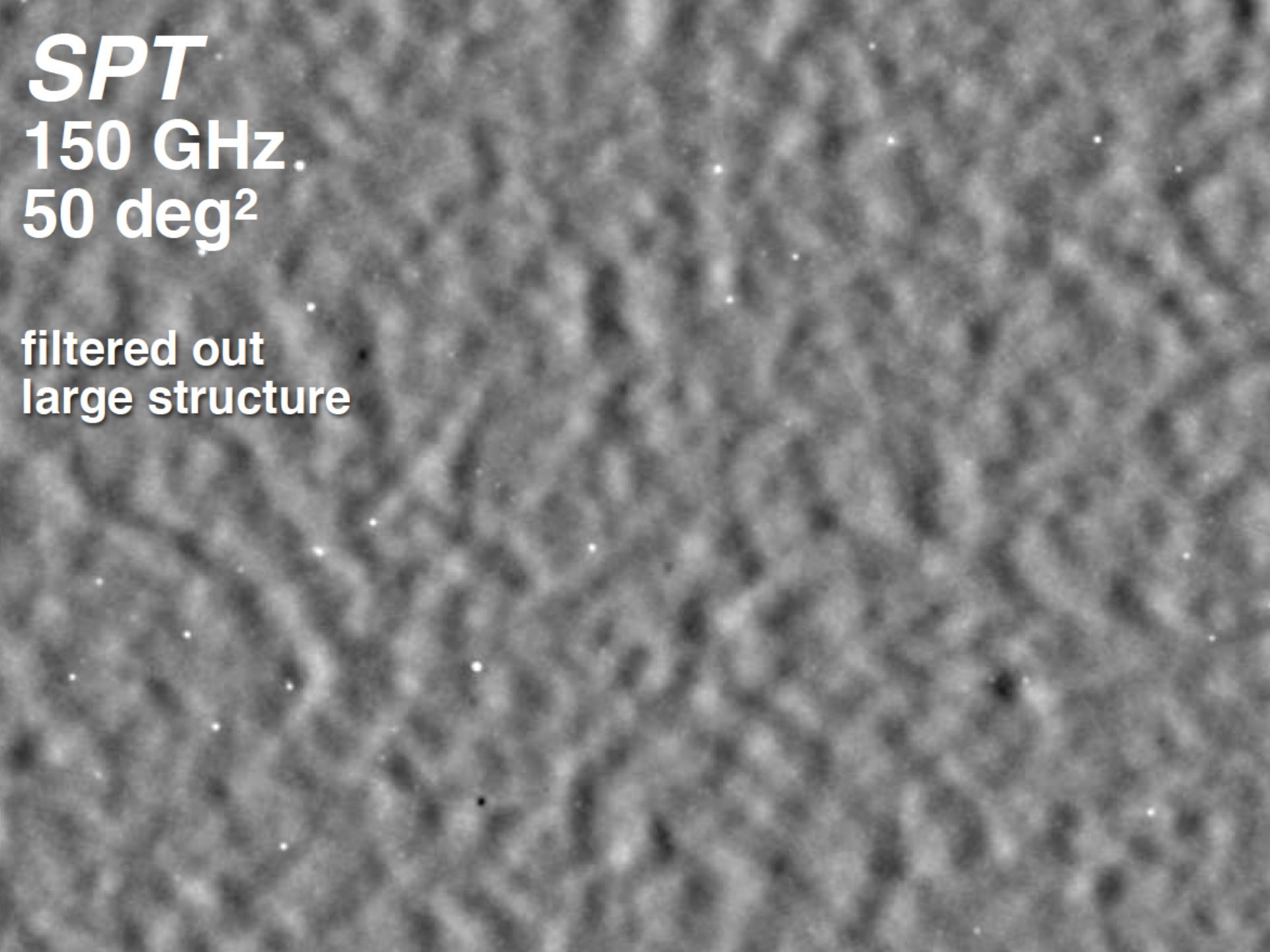


SPT

150 GHz.

50 deg²

**filtered out
large structure**



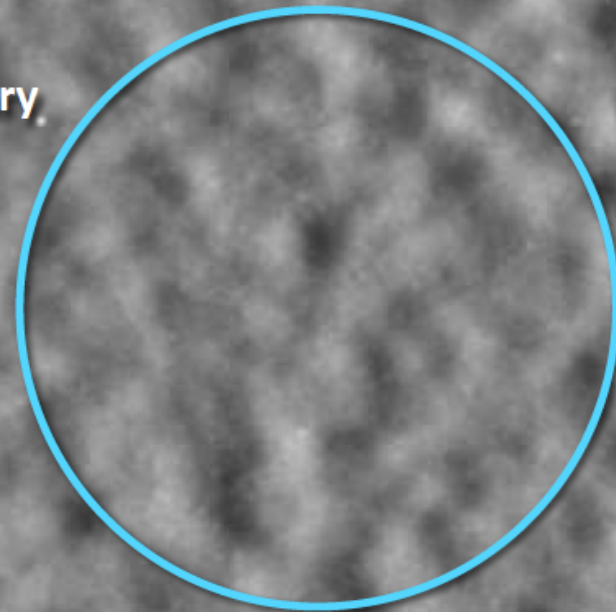
SPT

150 GHz.

50 deg²

CMB Anisotropy

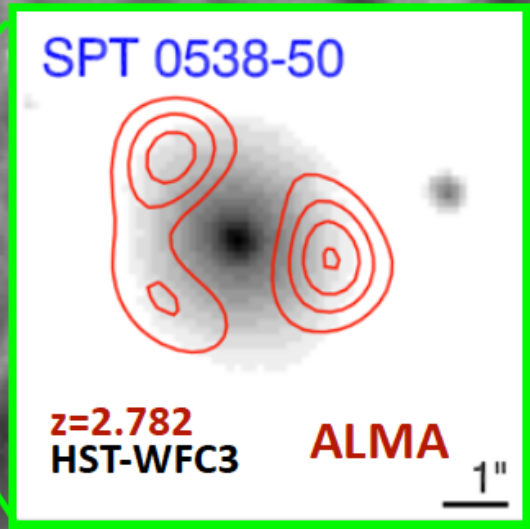
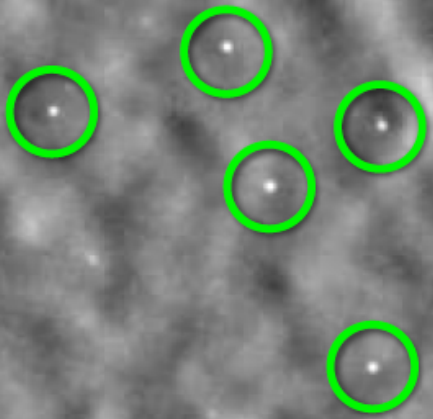
Primordial and secondary
anisotropy in the CMB



SPT
150 GHz
50 deg²

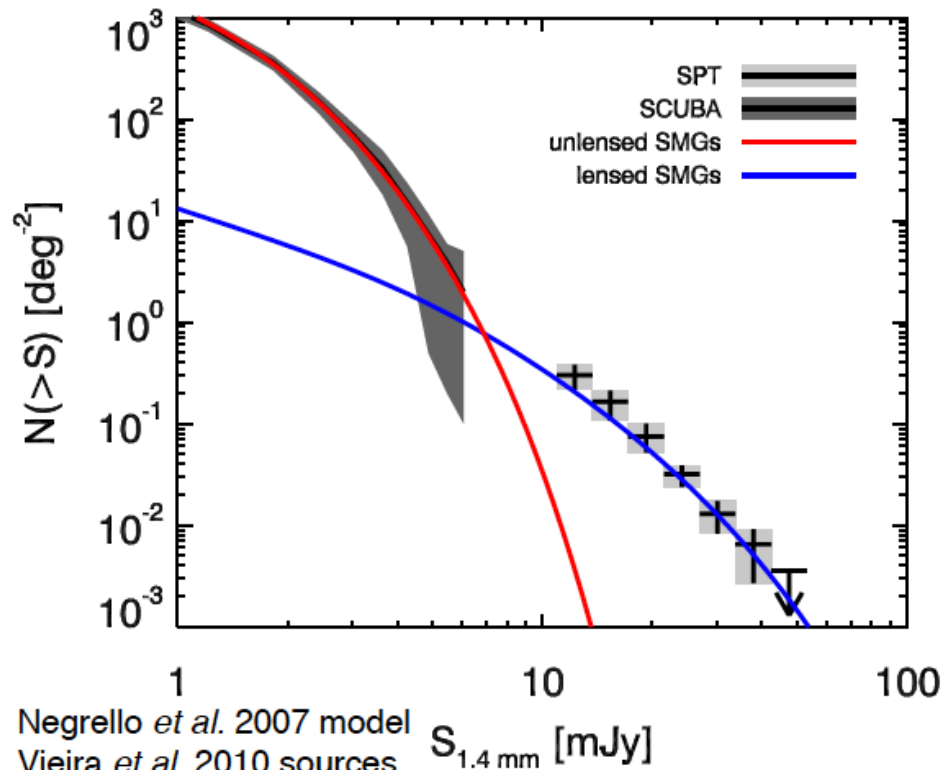
Point Sources

Active galactic nuclei, and the most distant, star-forming galaxies

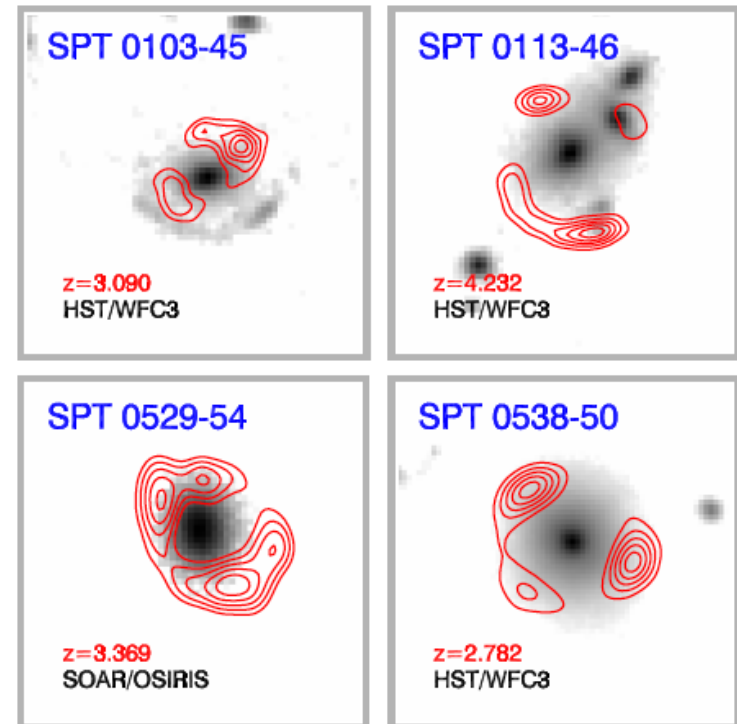


SPT-SZ: *Lensed Sources in SPT-SZ Survey*

mm-wavelength Source Number Counts



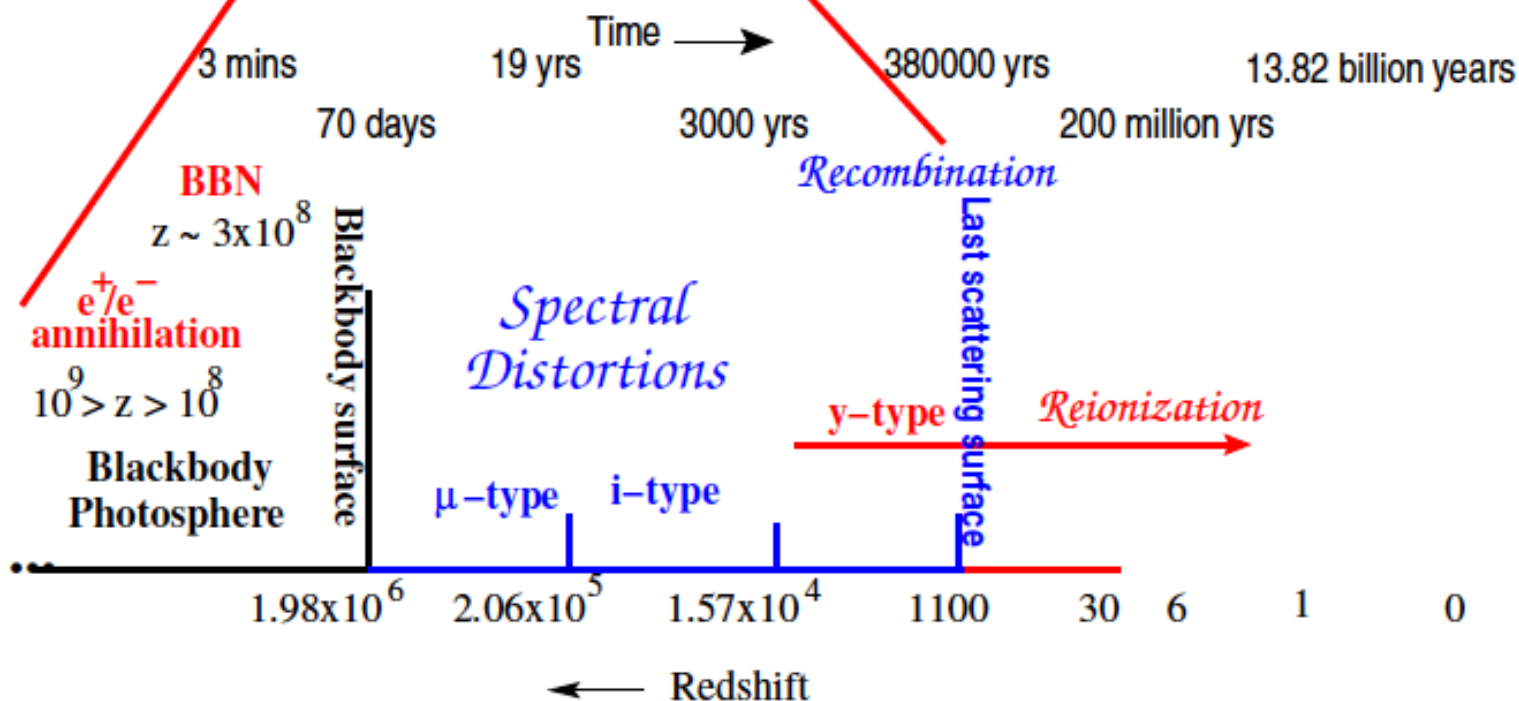
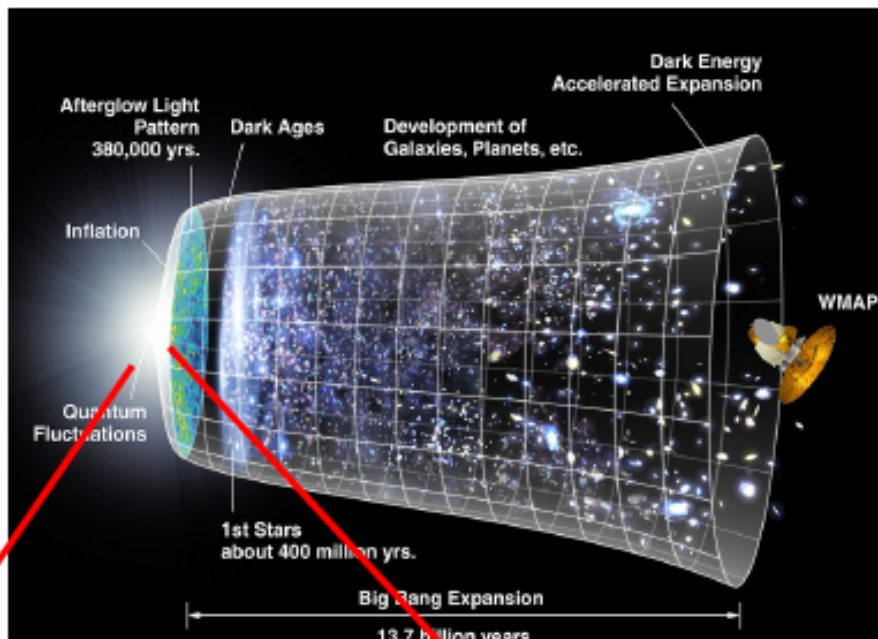
SPT lensed high- z ($2 < z < 6$) galaxies resolved by ALMA



Vieira *et al.* 2013 Nature
Hezevah *et al.* 2013

**Next use exquisite resolution and sensitive of ALMA
ALMA to image dark matter subhalos of the lens**

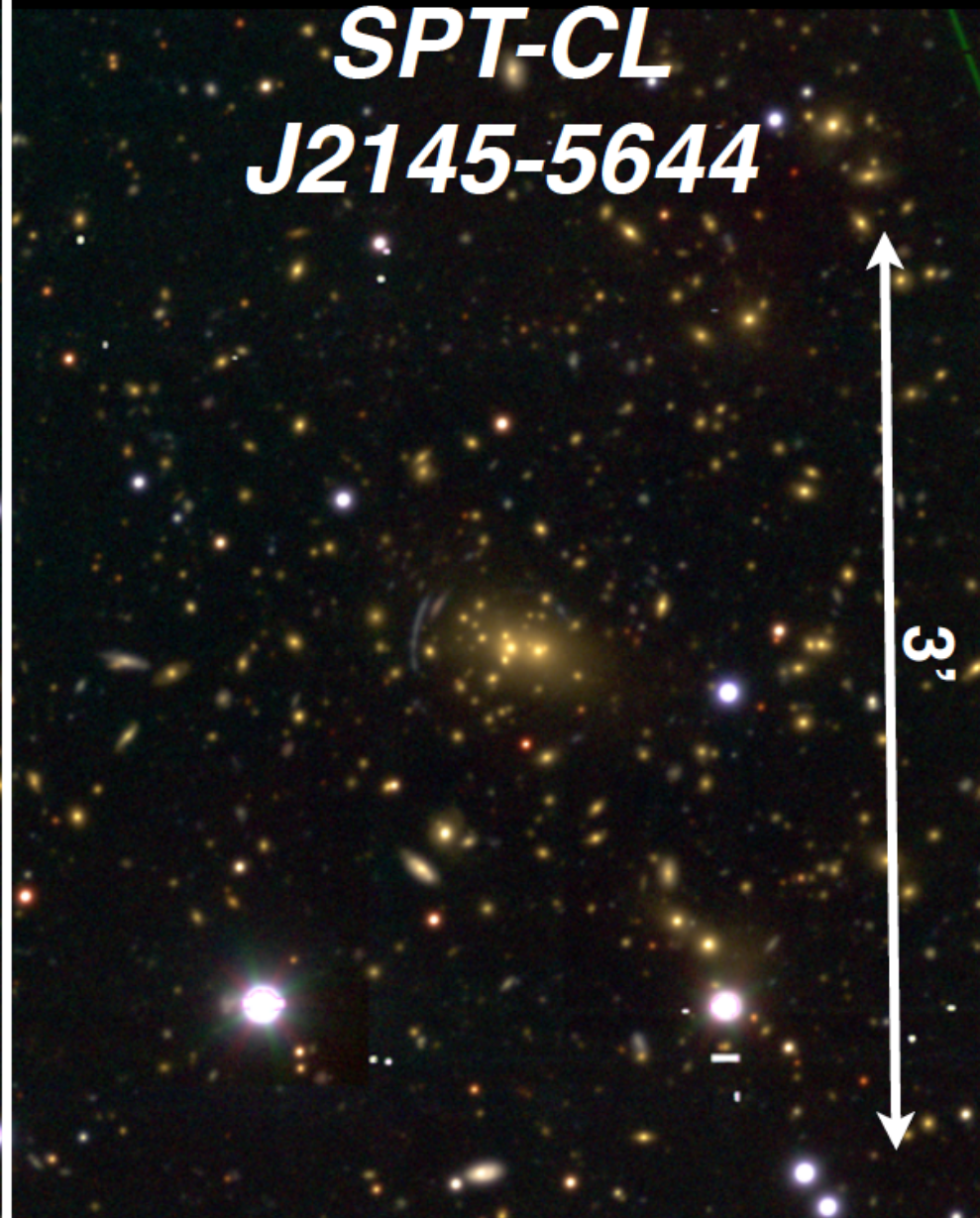
Brief history



**SPT-CL
J2138-6008**



**SPT-CL
J2145-5644**



Optical follow-up; redshifts, lensing, dynamical masses

Entropy is conserved in thermodynamic equilibrium

Entropy per baryon of radiation + baryons

$$\sigma = \frac{4a_R T^3}{3n_B} + Nk_B \ln \left(\frac{T^{3/2}}{n_B C} \right)$$

baryon density

$$n_B \propto (1 + z)^3$$

Constant entropy

$$T_{\text{radiation}} \propto 1 + z$$

$$T_{\text{baryons}} \propto (1 + z)^2$$

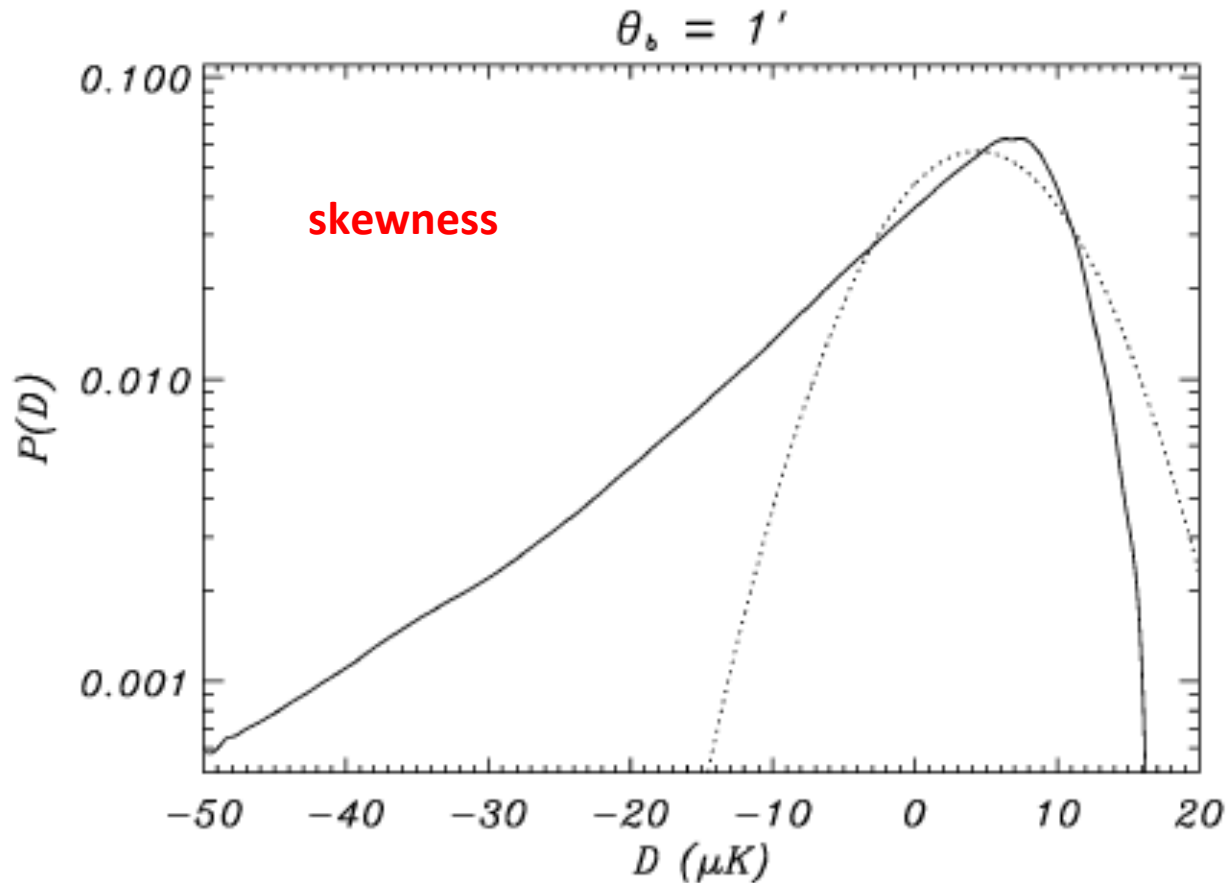
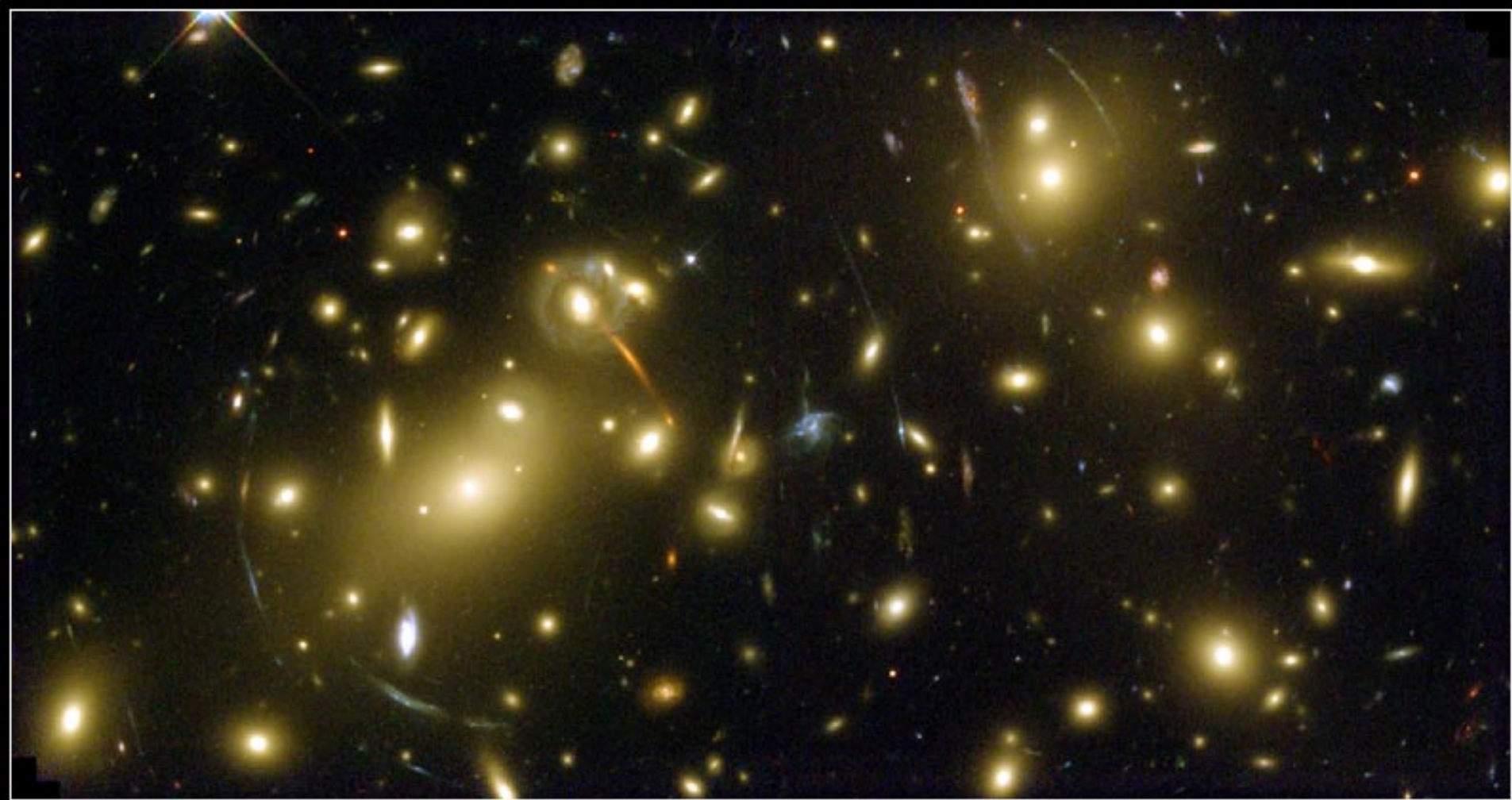


Figure 2. Example of the strong non-Gaussianity of the $P(D)$ function for SZ clusters. We present the $P(D)$ function for a SZ map in the Rayleigh–Jeans region of the spectrum, where clusters are ‘negative’ sources. For comparison, we also show the best Gaussian fit to this $P(D)$ curve ($\sigma = 6.1 \mu\text{K}$). This curve will be explained in detail in Section 7.



Galaxy Cluster Abell 2218

HST • WFPC2

NASA, A. Fruchter and the ERO Team (STScI) • STScI-PRC00-08

Thousands of galaxies with $v \sim 1000$ km/s

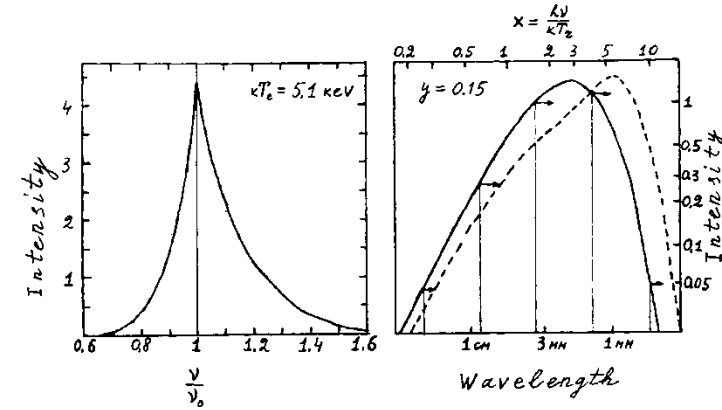
Hot intergalactic gas with $T_e \sim 3 - 10$ KeV

Gravitational potential defined by
invisible *dark matter*

Distant galaxies are gravitationally *lensed* by A 2218

There are three effects which make cloud visible:

1. **Thermal effect (change of the CMB spectrum in the direction to the cloud with hot gas)**



2. **Kinetic effect (moving cloud changes the spectrum of scattered CMB photons due to Doppler effect)**

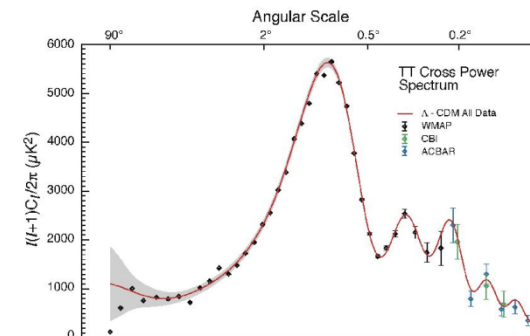
$$\frac{\Delta T}{T_r} = - \frac{v_r}{c} \tau_T$$

Full analogy with the origin of the Dipole Component in the CMB angular distribution arising due to our motion relative to the reference frame where CMB is isotropic.

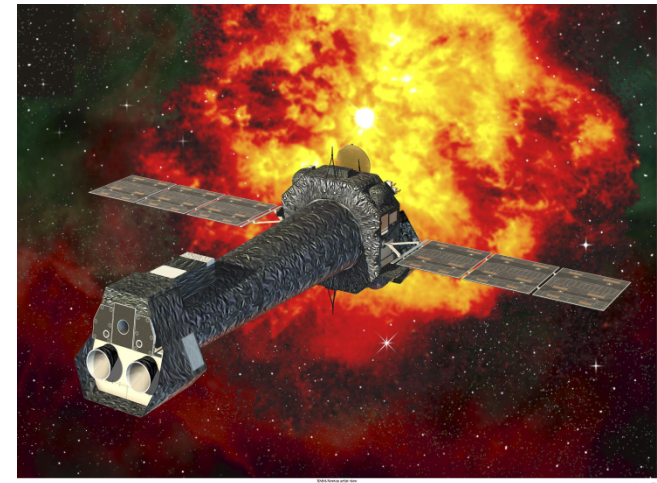
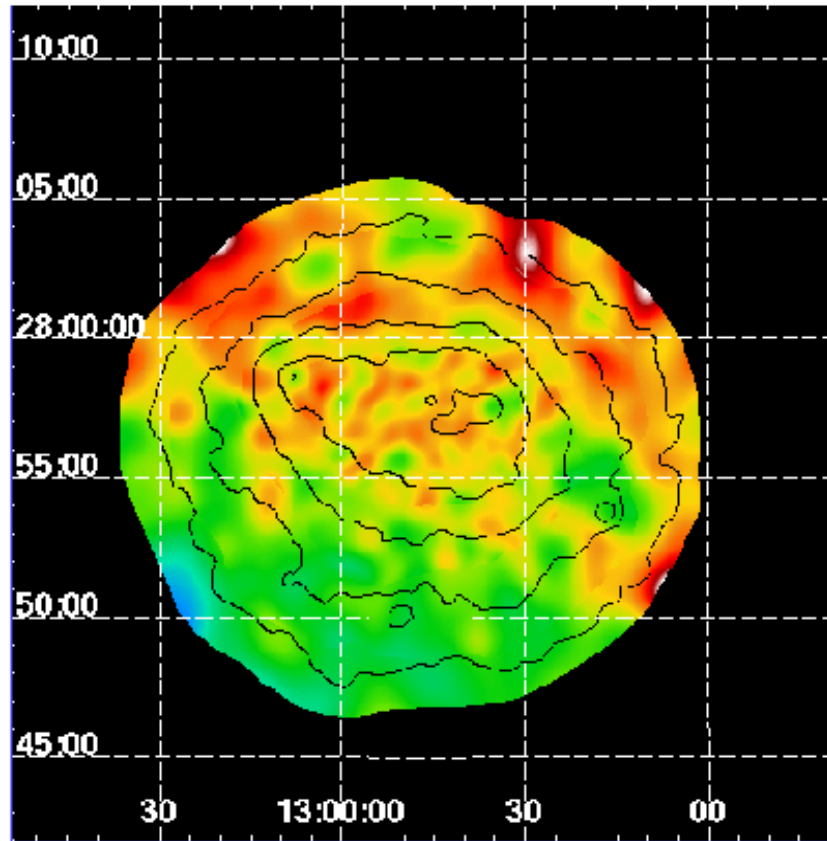
3. **Blurring effect (CMB in reality is not isotropic. There are angular fluctuations. Scattering in the cloud removes all anisotropies in the direction to the cloud except 10% of quadrupole at the position of a cloud)**

$$\frac{\Delta I}{I_0} = \frac{I_1(\mu) - I(\mu)}{I_0} = - \tau_T \times \left[a\mu + 0.9b(\mu^2 - \frac{1}{3}) + \sum_{n=3}^{\infty} C_n P_n(\mu) \right]$$

(see Sunyaev, Zeldovich, 1981)



X-RAY EMISSION FROM CLUSTERS OF GALAXIES



Electron temperature ~ 9 KeV

Electron density $\sim 0.03 \text{ cm}^{-3}$

COMA CLUSTER TEMPERATURE MAP (XMM-Newton)
(Briel et al. 2001, image by Churazov)

**Dark matter mass –
up to $10^{15} M_{\text{sun}}$**

$M_{\text{sun}} = 2 \cdot 10^{33} \text{ g}$

Sound velocity of gas is close to velocities of galaxies

SOUTH POLE TELESCOPE

PI: J. Carlstrom



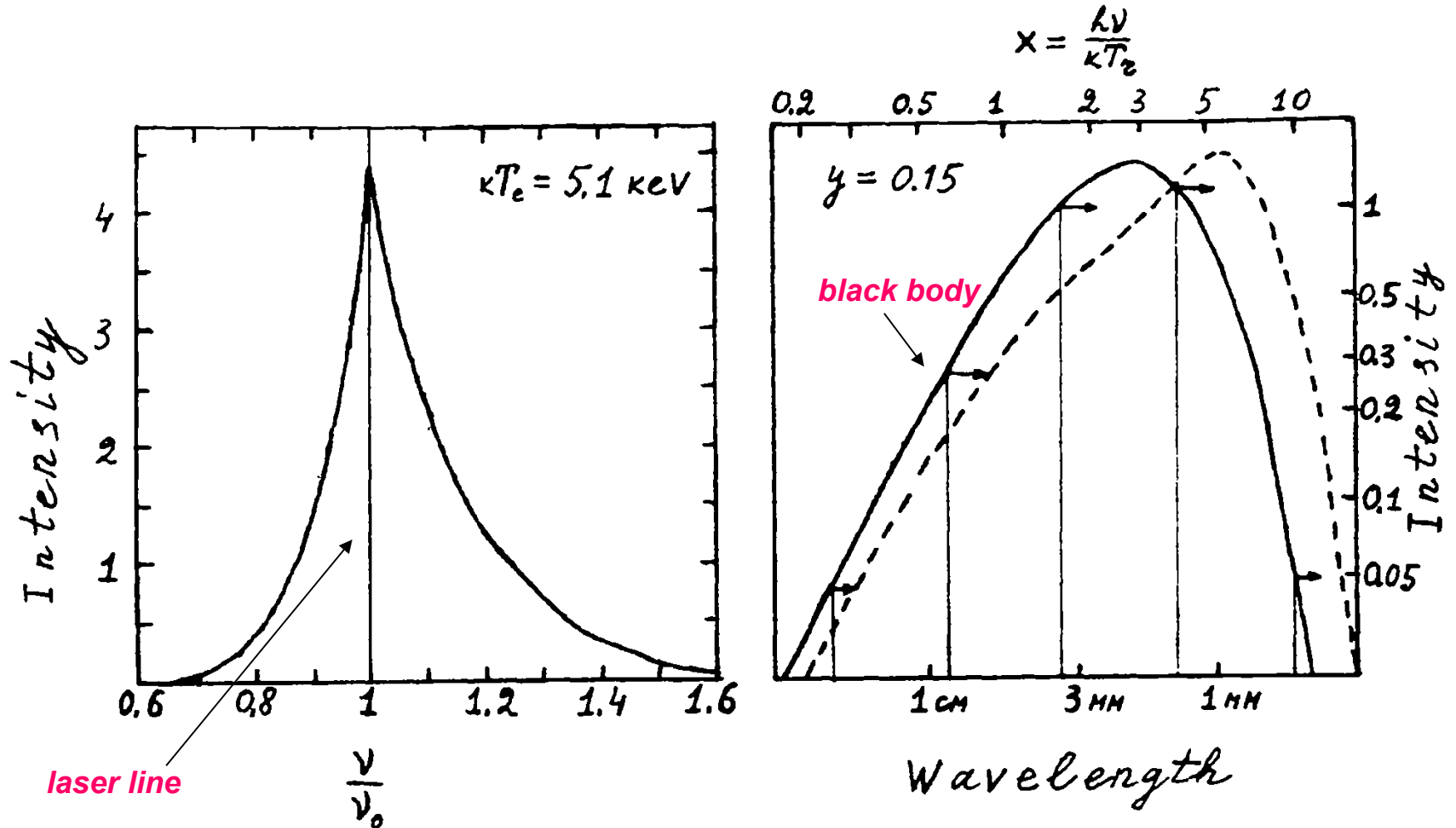
10m dish; 95, 150, 220 GHz
1'

Photograph by: Glenn Grant
National Science Foundation

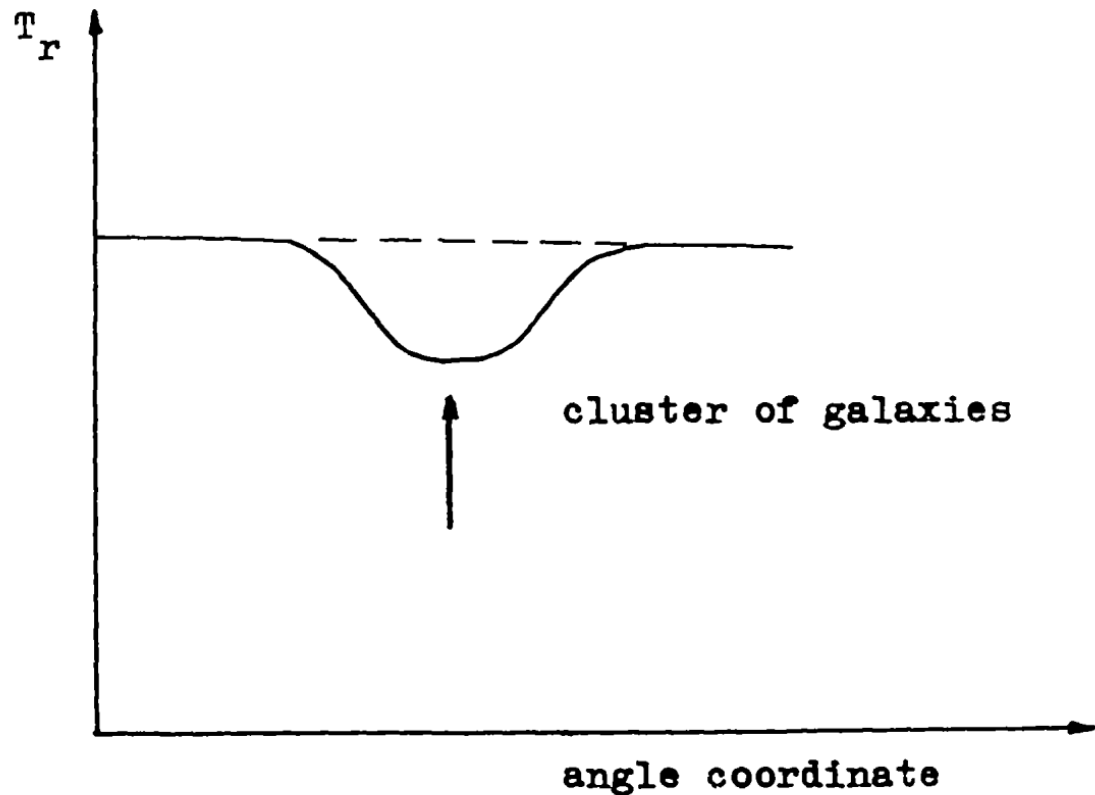
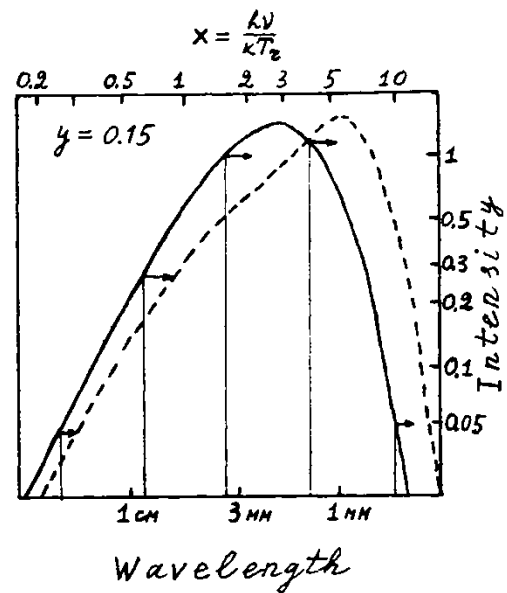


SCATTERING OF RADIATION BY HOT MAXWELLIAN ELECTRONS

spectral changes due to doppler-effect on moving electrons
with $kT_e \sim 5 \text{ KeV}$ and average velocity of the order of $1/7 c$



Line is broadened and effectively shifted toward higher frequencies due to second order effects in v/c



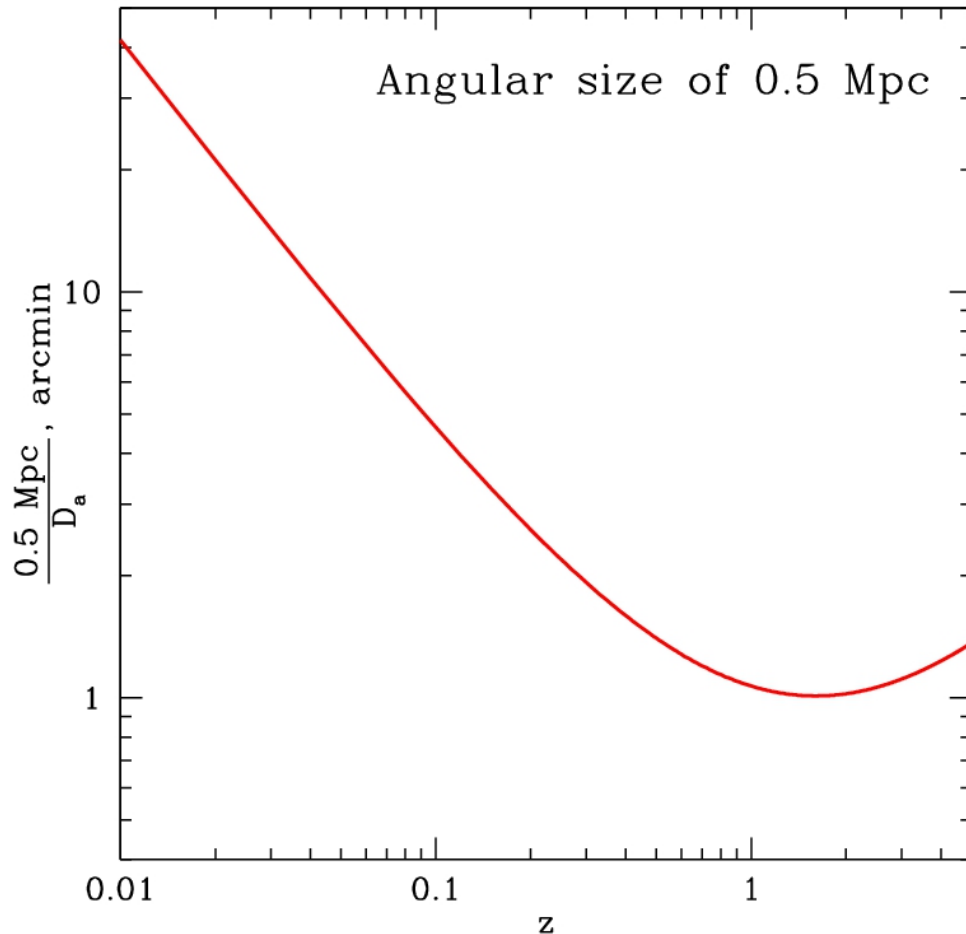
$$y = \int \frac{\sigma_T}{m_e c^2} P_e dl$$

$P_e = N_e k T_e$ – electron thermal pressure

*In centimeter and mm spectral bands clusters should be observed as a **holes** in the sky average brightness defined by CMB intensity*

the depth of this hole does not depend on the redshift of the cluster of galaxies
 It depends only on temperature of the electrons and optical depth of the cluster

Angular size as a function of z



For distant clusters
their angular size
does not depend
on redshift!

It is close to 1 arcmin

This means, that their total flux also does not depend on redshift for $0.5 < z < 2$
(for similar clusters at different redshifts)

because observed surface brightness also does not depend on the redshift

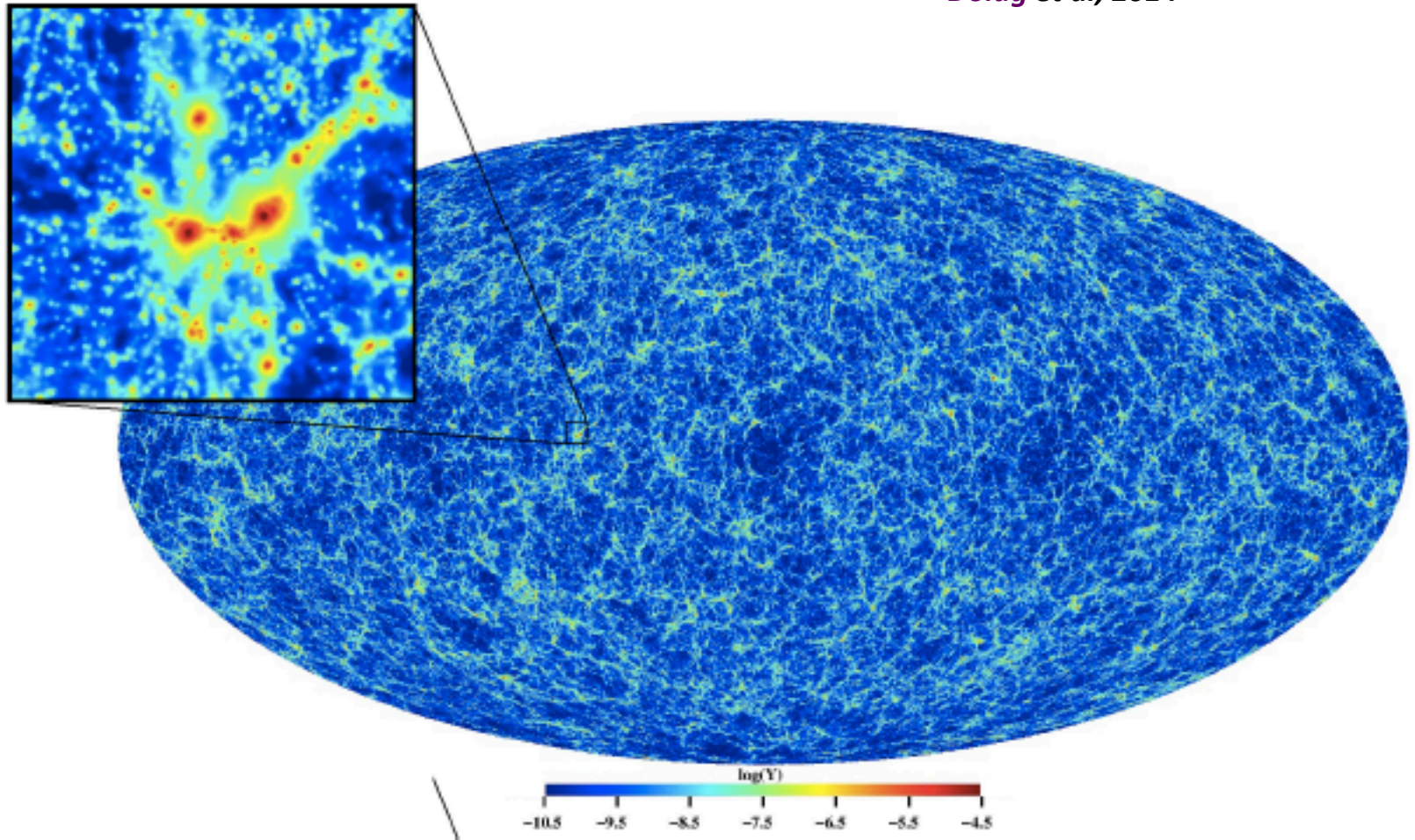


Figure 34. Map of simulated y -distortion taken from [207]. The y -type signal from the post-reionization epoch is dominated by the collapsed objects and filaments in the large scale structure.